



Università degli Studi di Ferrara

DOTTORATO DI RICERCA IN
BIOCHIMICA, BIOLOGIA MOLECOLARE E BIOTECNOLOGIE

CICLO XXVIII

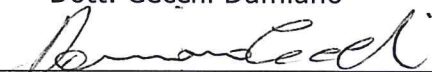
COORDINATORE Prof. Bernardi Francesco

**Herpes simplex virus type 1 and
neurodegenerative disorders: can viral
infection increase the risk of developing
Alzheimer's disease?**

Settore Scientifico Disciplinare MED/07

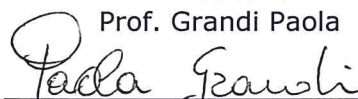
Dottorando

Dott. Cecchi Damiano


(firma)

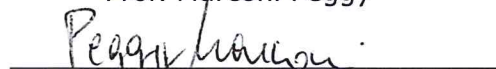
Tutore

Prof. Grandi Paola


(firma)

Co-Tutore

Prof. Marconi Peggy


(firma)

Co-Tutore

Prof. Manservigi Roberto


(firma)

Anni 2013/2015

To Giulia

Table of contents

Summary.....	4
1. General concepts on Alzheimer’s disease and Herpes simplex virus type1.....	7
1.1 Alzheimer’s disease.....	7
1.1.1 Macroscopic alterations.....	7
1.1.2 Pathogenesis.....	8
1.1.3 Amyloid cascade hypothesis.....	9
1.1.4 Hyperphosphorylated tau.....	11
1.1.5 Gliosis and chronic inflammation.....	12
1.1.6 Ca ²⁺ signalling dysregulation.....	13
1.1.7 Oxidative stress.....	14
1.1.8 Classification.....	14
1.1.9 Diagnosis and therapy.....	15
1.2 Herpes simplex virus type 1.....	17
1.2.1 Structure and genome of HSV-1.....	17
1.2.2 HSV-1 life cycle.....	18
1.2.3 Virus attachment and entry.....	19
1.2.4 Viral replication (lytic cycle).....	20
1.2.5 Latency and reactivation.....	21
1.2.6 HSV-1: a possible risk factor for AD.....	22
1.3 References.....	25
1.4 Aims of work: study of HSV-1 as a possible risk factor for AD.....	27
2. The role of US3 and UL13 viral kinases in hyperphosphorilation of Tau.....	27
2.1 Introduction.....	27
2.2 Material and methods.....	29
2.2.1 Cells.....	29
2.2.2 Plasmids.....	29
2.2.3 Transfection for transient expression of viral kinase.....	30
2.2.4 Viruses.....	30
2.2.5 Viral DNA purification.....	30

2.2.6	Calcium phosphate transfection.....	31
2.2.7	Limiting dilution.....	31
2.2.8	Southern blot.....	31
2.2.9	Viral stocks.....	32
2.2.10	Viral titration-plaque assay.....	32
2.2.11	Growth curve.....	33
2.2.12	Western blot.....	33
2.2.13	Immunofluorescence.....	34
2.3	Results.....	35
2.3.1	Construction of mutant viruses HSV-1 F Δ UL13 and F Δ US3 Δ UL13.....	35
2.3.2	Evaluation of replication activity of mutant viruses.....	38
2.3.3	Characterization of plasmid vectors expressing GFP-US3 and RFP-UL13.....	40
2.3.4	Analysis of US3 UL13 direct involvement in tau phosphorylation.....	42
2.4	Discussion.....	45
2.5	References.....	46
3.	HSV-1 and Nuclear Tau.....	47
3.1	Introduction.....	47
3.2	Material and methods.....	49
3.2.1	Cells.....	49
3.2.2	Animals and neuronal cultures.....	49
3.2.3	Infection.....	49
3.2.4	Transfections.....	50
3.2.5	Drugs.....	50
3.2.6	Immunofluorescence.....	51
3.2.7	Western Blot.....	51
3.3	Results.....	52
3.3.1	HSV-1 increases and relocalizes nuclear tau in epithelial and neuroblastoma cells.....	52
3.3.2	The nucleolar viral protein US11 does not cause the redistribution of nuclear tau outside the nucleolus.....	55
3.3.3	Alterations in nuclear tau doesn't seem to be related to viral replication.....	58
3.3.4	HSV-1 increases Tau-1 staining in Alzheimer's disease mouse model neurons.....	61
3.4	Discussion.....	64
3.5	References.....	67

4. HSV-1 and Ca²⁺ signalling.....	69
4.1 Introduction.....	69
4.2 Material and methods.....	72
4.2.1 Cells and viruses.....	72
4.2.2 gB purification.....	72
4.2.3 Transfection and Aequorin measurements.....	73
4.2.4 Fura-2/AM measurements.....	74
4.3 Results.....	75
4.3.1 A soluble recombinant gB is able to induce Ca ²⁺ release from intracellular stores of HRPE cells.....	75
4.3.2 Interaction of gB with HSPG down-regulate Ca ²⁺ signalling triggered by HSV-1.....	77
4.4 Discussion.....	79
4.5 References.....	80
5. An in vivo model to study the correlation between HSV-1 and neurodegeneration	
5.1 Introduction.....	81
5.2 Material and methods.....	82
5.2.1 Virus.....	82
5.2.2 Mice.....	82
5.2.3 Immunofluorescence.....	83
5.2.4 Antibodies.....	83
5.2.5 DNA extraction and PCR.....	83
5.3 Results.....	85
5.3.1 Route of HSV-1 in the nervous system of Ai6 mice.....	85
5.3.2 Validation of the system.....	86
5.3.3 Characterization of HSV-1 infection in Ai6 mice nervous system.....	87
5.3.4 HSV-1 activates inflammatory cells.....	91
5.3.5 HSV-1 doesn't increase the amount of beta amyloid and phospho tau in Ai6 mice.....	98
5.4 Discussion.....	101
5.5 References.....	104
6. Conclusion.....	105
Aknowledgements.....	106

Summary

Herpes simplex virus type 1 (HSV-1) is a human neurotropic virus whose lifecycle is based on a long-term dual interaction with the infected host, being able to establish both lytic and latent infections. After initial infection and lytic multiplication at the body periphery the virus enters the sensory neurons that innervate the infected epithelia and, following retrograde transport, establishes a lifelong latent infection in sensory ganglia. Increasing evidences indicate that periodic sub-clinical reactivations in the CNS and peripheral nervous system may occur, with subsequent immune response and neurodegeneration, suggesting that HSV-1 is a risk factor in the pathogenesis of Alzheimer's disease (AD). AD is a neurodegenerative disorder characterized by progressive decline in cognitive functions leading to memory loss and dementia. The main pathological hallmarks of the disease are: chronic inflammation, calcium dyshomeostasis and the presence of the aberrant highly insoluble protein aggregates neurofibrillary tangles (NFT) and senile plaques (SP), respectively composed by the amyloid- β peptide (A β) and the hyperphosphorylated protein tau (P-tau).

This work is focused on different aspects of the possible involvement of HSV in the pathogenesis of AD.

In the first part, the molecular mechanisms that might induce pathological alterations, with a particular emphasis on protein tau and Ca^{2+} signalling, were investigated, *in vitro*, in several cell lines such as epithelial, neuroblastoma and primary neuronal cells derived from newborn 3xTG mouse AD model.

Several studies have investigated the link between HSV-1 and phosphorylation of tau protein. To evaluate if the two viral kinases US3 and UL13 are involved in tau hyperphosphorylation, as suggested by the literature, mutant viruses lacking these genes and plasmid vectors for their expression in mammalian cells were generated. The phosphorylation status of tau, was evaluated by immunofluorescence and immunoblot analysis. Antibodies directed against 2 out of the 85 possible phosphorylation sites failed to detect significant events of hyperphosphorylation, making impossible to establish a possible direct role of these two viral genes in this process.

However, using the antibody Tau-1, directed against nuclear Tau, we have revealed strong differences between infected and uninfected cells. This antibody detects a nucleolar highly insoluble form of tau that is increased and redistributed throughout the whole nucleus after viral infection. Further analysis suggested us that these alterations could be related to a

modification on chromatin status that favours viral reactivation. The increase of this particular insoluble form of tau can contribute to the formation of NFT.

Alterations of intracellular Ca^{2+} homeostasis and signalling have also been implicated in AD pathogenesis. In fact, it is well known that intracellular Ca^{2+} , besides playing an essential role in neuronal functions, is a key element of neuronal survival and death. Several studies have reported that HSV-1 binding to neuronal membrane induced membrane depolarization leading to increased neuronal excitability and triggering action potentials. Since, the binding of HSV virions to the cell membrane is mainly mediated by the viral envelope glycoprotein B (gB) we have studied the role of this protein in Ca^{2+} release. The attachment of gB to the cell surface is mediated by a first binding to heparin sulfate proteoglycan (HSPG), an ubiquitous cell membrane molecule, followed by the recognition of a receptor that can be different depending on the cell type. Similarly, it has been reported that $\text{A}\beta$ can bind HSPG and the two proteins show a certain grade of homology. To evaluate if gB and/or HSPG binding site are involved in changes of the intracellular levels of Ca^{2+} we have utilized different cellular models and two Ca^{2+} -sensitive probes. Analysis with Aequorin revealed that a soluble recombinant form of gB can induce Ca^{2+} release from intracellular stores, while FURA-2 showed that an HSV-1 mutant expressing a gB deleted for the HSPG binding site increases intracellular Ca^{2+} uptake, compared to wild type virus. . These data demonstrate that gB is involved in the intracellular Ca^{2+} influx and that is negatively regulated by the binding of the protein to HSPG. We can speculated that in pathological conditions HSV-1 causes functional changes Ca^{2+} dependent, in cortical neurons, that promote APP processing and $\text{A}\beta$ production and excess of $\text{A}\beta$ can compete with gB to bind to HSPG, thus resulting in a movement of Ca^{2+} higher than in normal infection.

The second part of this work is focus on *in vivo* studies, using a reporter transgenic mouse model system, in order to have a wider comprehension of the correlation between HSV-1 and AD. This, *in vivo*, system utilizes a recombinant virus expressing CRE recombinase and the CRE reporter mouse strain Ai6. CRE recombinase mediates the permanent marking of infected cells, by the expression of the reporter gene. Trigeminal ganglia (TG) and brain slices of infected or uninfected adult Ai6 mice were analyzed by immunofluorescence assay until 126 days post-infection. Number of studies have revealed that HSV infection or reactivation was associated to neuroinflammation and to the appearance of AD several markers of neurodegeneration including APP and Tau hyperphosphorylation. Therefore, the pathological hallmarks analyzed in this system were the presence of neuroinflammation, SP and NFT. The results obtained in our studies have showed, in the areas affected by the virus infection, a

strong activation of macrophages and microglia, cells of the innate immunity that orchestrate inflammation in the nervous system. On the other hand nor SP nor NFT formations were detected, suggesting that their outcome may require more time, different events of reactivation and/or other predisposing elements.

The data presented in this work support the hypothesis that HSV-1 interferes with several cellular and systemic processes that in physiological conditions may be restored after acute phase of viral infection/reactivation. However these findings suggest that the alterations induced by the virus combined with ageing and other risk factors, can worsen a yet pathological situation, supporting the idea that HSV-1 is a relevant, although not essential, agent for the development of AD at different levels.

1. General concepts on Alzheimer's Disease and Herpes simplex virus type 1

1.1 Alzheimer's disease

Alzheimer's disease (AD) is the most common neurodegenerative disorder in the Western world, characterized by progressive degeneration and loss of specific subsets of neurons that lead to a decline in brain functions such as cognition and memory. Nowadays, AD is considered the most common form of dementia affecting 24,3 million people worldwide [1] and, because of the progressive demographic ageing, this number is estimated to increase in the next years together with its already high socio-economical costs. Ageing is considered the major risk factor related to the incidence of AD, indeed, the disease is extremely rare under the age of 65, the number of sufferers increase in older people being markedly high over the age of 85 years [2].

It was first described at the beginning of the XX century by the German psychiatrist and neuropathologist Alois Alzheimer, in a 51 years old woman suffering from early-onset dementia [3].

AD is often anticipated by a slight decrease in several cognitive functions mainly related to memory, perception and language. This condition is named mild cognitive impairment (MCI), it is an intermediate situation between normal ageing and dementia but doesn't necessarily progress to AD [4].

The course of the disease may be different for every single patient, anyway there are some symptomatic characteristic shared by all affected people that goes from progressive decline of cognitive functions in early and moderate phases to behavioural and psychiatric problems in advanced stages.

1.1.1 Macroscopic alterations

The main macroscopic characteristic in AD brains is the marked cortical atrophy that results in enhanced wideness of cerebral sulci, particularly evident in frontal, temporal and parietal lobe (Fig. 1.1). This morphological modification is balanced by the enlargement of ventricular cavities [5].

During late stages of the pathology, the cerebral areas interested are those of the medial temporal lobe, in particular hippocampus, amygdala, entorhinal cortex, the posterior cingulate, precuneus and the tempo-parietal neocortex [6].

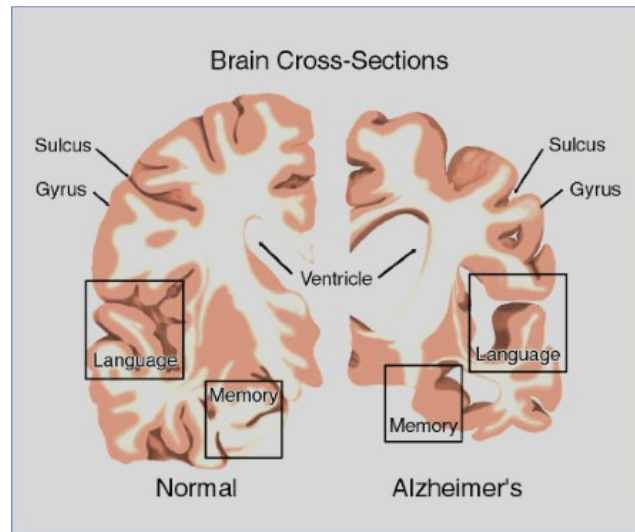


Fig. 1.1. Schematic comparison between frontal section from health (left) and AD (right) brains. AD brain presents cortex atrophy and enlargement of ventricular cavities

1.1.2 Pathogenesis

The classical microscopic alterations present in AD brain tissue are the two aberrant highly insoluble protein aggregates senile plaques (SPs) and neurofibrillary tangles (NFTs), respectively composed by the amyloid- β peptide ($A\beta$) and the hyperphosphorylated protein tau (Fig. 1.2).

Both NFTs and SPs, however, have been detected also in brains of cognitively unimpaired individuals. Further investigations revealed other pathological irregularities that accompany the progression of the disease. These include: gliosis and chronic inflammation, oxidative stress and Ca^{2+} dysregulation.

At present researchers have not fully elucidated the mechanisms that lead to neuronal death, synaptic loss and finally to the symptoms of AD. The pathological hallmarks cited above seems to interact with each other at several stages of the disease, anyway the most widely accepted hypothesis states a key role for $A\beta$.

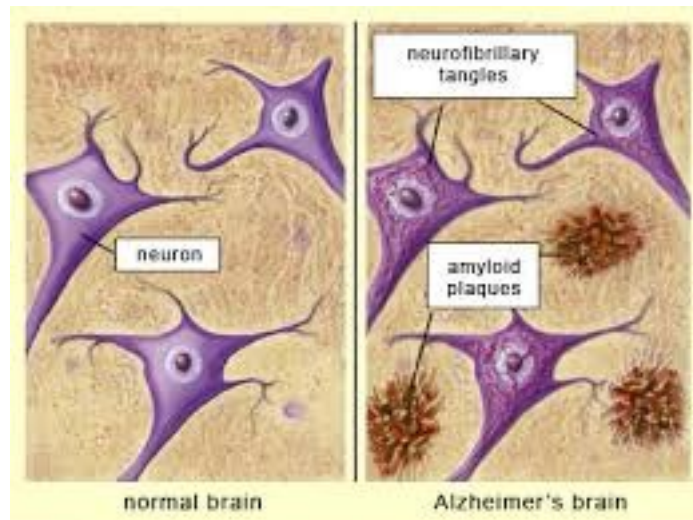


Fig. 1.2. Schematic representation of NFT and SP in AD brain (right)

1.1.3 Amyloid cascade hypothesis

SPs are round structures with a diameter of 20-200 μm located in extracellular space. The core of these aggregates is composed of numerous proteins, among which the most represented is amyloid- β peptide ($A\beta$). This central part is surrounded by neuronal debris and in the neighbouring areas there are often glial activated cells.

$A\beta$ derives from the cleavage of the ubiquitous membrane protein amyloid precursor protein (APP) that in central nervous system (CNS) is expressed by neurons, astrocytes and microglia. This protein is present in 8 different isoforms, the 3 major of which differ in size containing 695, 751 or 770 aminoacids, with APP₆₉₅ being the most represented isoform in neurons. Its primary physiological function is not known, but it seems to be involved in neuronal survival, synaptic plasticity and cell adhesion [7].

The processing of APP involves 3 groups of proteolytic enzymes: α -, β - and γ -secretases (Fig. 1.3). α -secretase activity is performed by members of the family of disintegrin and metalloproteinase domain proteins (ADAM), beta-site APP cleaving enzyme 1 (BACE1) represent the principal β -secretase and γ -secretase function requires a complex of at least four proteins: presenilin (PS) 1 or 2, nicastrin (nct), presenilin enhancer 2 (Pen2) and anterior pharynx defective 1 (Aph-1). Mature APP is transported to cell membrane where it is cleaved. APP can be alternatively cleaved by α - or β - secretases in 2 fragments. The N-terminal end is called secreted APP (sAPP) α or β respectively, while the C-terminal fragments (CTF) are referred to as CTF83 and CTF99 respectively. The cleavage of CTF by γ -secretases results in the generation of APP intracellular domain (AICD) at the carboxy-terminus, while at the amino-terminus in p3 or $A\beta$, respectively for CTF83 or CTF99 [8].

In healthy individuals APP cleavage is mainly mediated by α -secretase, while in AD patients β pathway is more enhanced resulting in overproduction of $A\beta$.

$A\beta$ might contain 40 or 42 aminoacids, depending on the γ -cleavage, both these peptides are produced during physiological metabolism, but in AD $A\beta_{42}$ is overproduced and is the first to deposit, subsequently $A\beta_{40}$ aggregates onto the initial deposit of $A\beta_{42}$ [9]. $A\beta$ is found in brain in different levels of aggregation such as monomers, dimers and high molecular weight oligomers. Further accumulation generates protofibrils and fibrils, which are the basis of SP [10].

According to amyloid cascade hypothesis, aberrant $A\beta$ aggregates may damage neurons by direct or indirect mechanisms. In the first case $A\beta$ physically interacts with cellular components inducing a toxic effect that lead to neuronal loss. The main indirect mechanism is the activation of microglia and the subsequent inflammatory process that lead to neuronal death by apoptosis or necrosis.

The idea of $A\beta$ as the primary trigger is supported by several facts. First plaque formation is found to appear relatively early in AD brain. Second all known mutations in familial cases of AD concern APP processing [11]. Third APP gene is located on chromosome 21 and Down's syndrome patients tend to develop early onset AD [12].

On the other hand there are also evidence that $A\beta$ alone is not sufficient to promote the onset of the disease. For example transgenic mouse models expressing familiar AD mutations doesn't harbour significant increase in the pathological hallmark, and $A\beta$ in vivo failed to show a toxic effect [13]. Therefore the etiology of AD cannot be attributed only to $A\beta$.

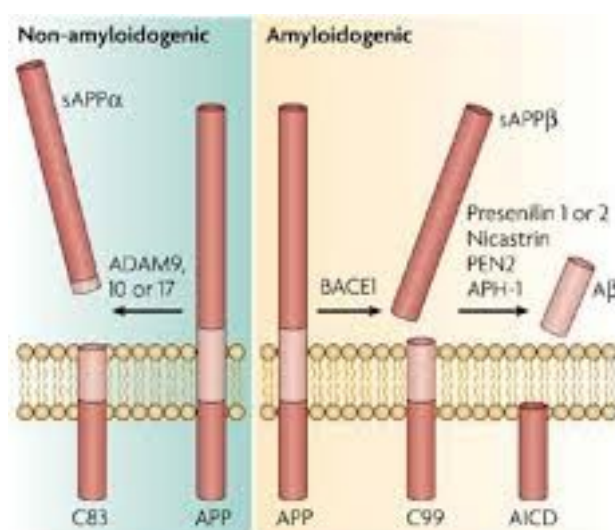


Fig. 1.3 Schematic representation of the $A\beta$ cleavage

1.1.4 Hyperphosphorylated tau

The fundamental component of NFT is the hyperphosphorylated protein tau.

Tau is a microtubule-associated protein (MAP) that is localized mainly, but not only, to the axons of neurons.

In human brain tissue tau protein is present in 6 isoforms resulting from alternative splicing of a unique transcript. These 6 isoforms differ for the number of the repeats of two sequences of the protein, one on the amino terminal region that can span from 0 to 2 and the other one, the microtubule-binding region placed at the carboxy-terminus, that can be 3 or 4. The shortest isoform is 352 amino acid long while the longest is 441 (Fig. 1.4.)

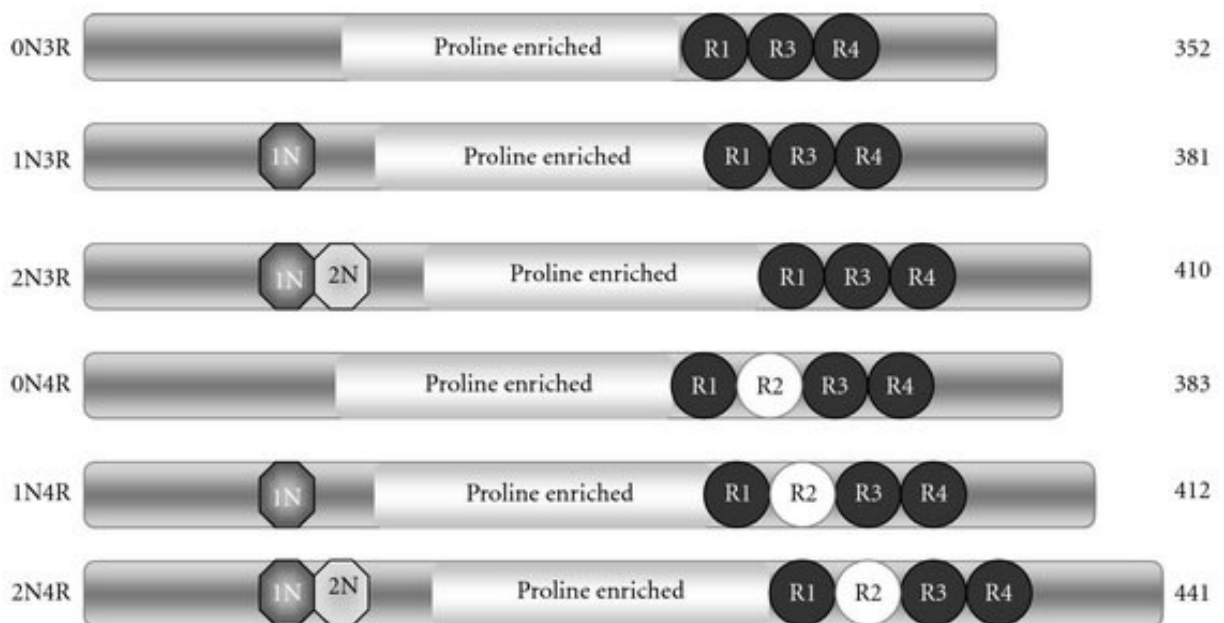


Fig.1.4. The 6 different isoforms of human tau

The main function of this protein is to stabilize microtubules, a process regulated by its phosphorylation (Fig.1.5). In AD tau is hyperphosphorylated aggregating in PHF and NFT and can no longer perform this role [14]. It has been proposed that this fact induces microtubules disintegrations dismantling cytoskeleton and thus neuronal transport [15]. This may first affect communications between neurons and finally lead to cell death [16].

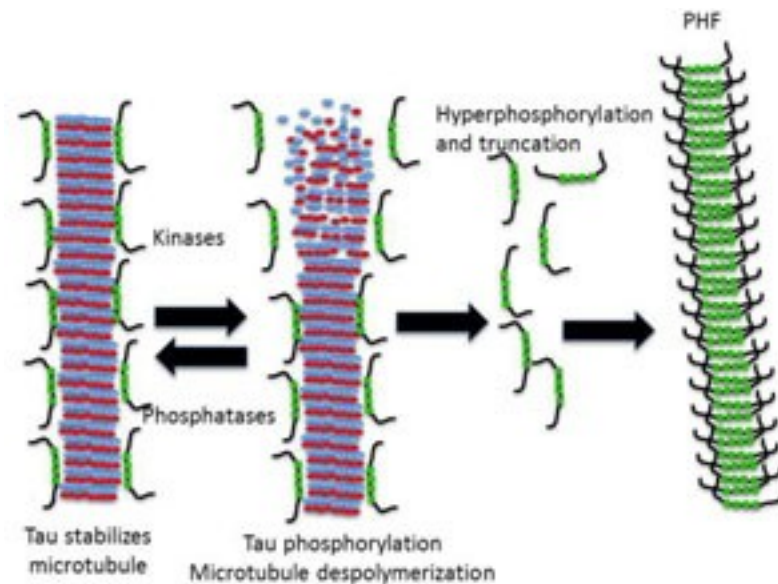


Fig. 1.5 Binding of tau to microtubules is regulated by phosphorylation

The potential sites of phosphorylation are 85 on the longest tau isoform, of these 36 have been described to be phosphorylated in the PHF [17].

Despite microtubules were the first site described for this protein, tau was also found to perform different functions in other cellular compartments, such as dendrites, ribosomes, plasma membrane and nucleus. Inside the nucleus tau seems to have a key role in chromatin organization and DNA protection from stress damage. Although nuclear form seems to be less phosphorylated, it is more insoluble than cytoplasmic tau and it has been suggested that under pathological conditions it may exit the nucleus and trigger the formation of PHF.

Therefore, NFTs are considered a secondary process in the pathogenesis of AD because of their correlation with severity of dementia [18] and since these alterations, referred as tauopathies, are shared by other diseases.

1.1.5 Gliosis and chronic inflammation

For a long time CNS was believed to be immunologically privileged. It is now evident that inflammation and consequent immune response are present in this organ, mediated mainly by glial cells, in particular, microglia and astrocytes [19]. Microglia is actually composed by resident microglia and infiltrated macrophages. Since most techniques are not able to distinguish the two populations they are described as a unique group, albeit the two populations have different properties and functions, contributing to the immune response in CNS. The general agreement is that the microglia acts like the “sentinel” of the nervous system it is the first cell population that responds to any kind of injury in brain. Once

activated, microglia shows phagocytic and scavenger activities and also starts the inflammatory response by producing several molecules, like chemokines, cytokines, prostaglandins, free radicals, cyclooxygenase-2 (COX-2) and inducible nitric oxide synthase (iNOS). Inflammatory mediators, like interleukin (IL) 1 and 6, activate astrocytes, which increase in size and/or number and overexpress the glial fibrillary acidic protein (GFAP) participating in the innate immune response. Macrophages in addition to a phagocytic role have also the function of antigen presenting cells to T lymphocytes that have been activated in the periphery [20].

Inflammation in neurodegenerative disorders have a controversial function because it might be both neuroprotective and neurotoxic. The protective action might turn in toxic when inflammatory response remains chronically activated. In AD, microglia and astrocytes were found around SP and it has been shown that A β can activate microglia, recruiting astrocytes in the sites of A β deposits [21, 22]. In physiological conditions glial cells are able to remove these deposits, however aging promote deregulation of immune response, in particular microglia shows an hypersensitive phenotype that results in a excessive activation of these cells [23]. Therefore inflammatory response stays on for a long time and the subsequent increased oxidative stress and neuropathological changes contribute to neurodegeneration.

1.1.6 Ca²⁺ signalling dysregulation

Intracellular Ca²⁺ signalling has several functions that are fundamental for neuronal physiology and viability. For this reason perturbations in Ca²⁺ homeostasis are implicated in several pathological processes and have become a factor of great interest in multifactorial neurodegenerative disorders such as AD. The most crucial disturbance is considered to be the excessive concentration of cytosolic Ca²⁺. Under resting conditions, cytosol contains a low nanomolar Ca²⁺ concentration and its trafficking is finely regulated by transport mechanisms that involves pumps and other ions, i. e. K⁺ and Na⁺. Ca²⁺ entry in cytosol originates from extracellular space and/or intracellular stores such as endoplasmic reticulum (ER) and mitochondria. The overload of intracytoplasmatic Ca²⁺ may be due to several causes. Excitotoxicity, a phenomenon triggered by over stimulation of glutamate receptor, is one of them. The binding of neurotransmitters to the receptor caused a transient increase of intracellular Ca²⁺ that is immediately restored under physiological condition, the abnormal increased release or decreased uptake of excitatory aminoacids results in a continuous increase in cytosolic Ca²⁺ concentration, that results toxic for the cell [24]. Another element involved in Ca²⁺ dysregulation derives from a stress condition of the main intracellular Ca²⁺

store, ER [25]. Moreover intracellular Ca^{2+} increase affects also mitochondria, which over produce reactive oxygen species (ROS), decrease energy metabolism, release cytochrome c and eventually induce apoptosis [26].

In AD Ca^{2+} dyshomeostasis have been linked to $\text{A}\beta$ formation and tau phosphorylation. Notably altered Ca^{2+} signalling and $\text{A}\beta$ generation are two parallel phenomena and one affects the other: Ca^{2+} dysregulation accelerates $\text{A}\beta$ formation, while $\text{A}\beta$ peptides induce Ca^{2+} alterations [27].

1.1.7 Oxidative stress

Oxidative damage of biological systems is due to an overcome of the cell's antioxidant capacity by the production of oxygen radicals and ROS. The excess of these products have a toxic effect that finally results in cell death. According to the free radical theory of aging, first proposed by Harman in 1956, ageing can be considered a progressive and inevitable process in part linked to accumulation of oxidative injury into biomolecules [28]. In addition to ageing, as discussed above, there are other factors that induce the formation of oxidative species, such as inflammation and mitochondria dysfunction. Therefore, oxidative stress has recently aroused a great interest in the study of AD and has been included in the list of the disease hallmarks [29].

1.1.8 Classification

Clinical forms of AD are classified according to the age of onset and they can be divided into 2 groups: early onset-familial (EOFAD) and sporadic or late onset (LOAD).

EOFAD

Approximately 5% of AD cases belong to this class, characterized by an early onset, usually between late 40s and early 50s. These forms of AD are mainly caused by mutations in 3 genes: APP on chromosome 21, PSEN1 on chromosome 14 and PSEN2 on chromosome 1, coding respectively for APP, PS1 and PS2 [11].

LOAD

The other 95% of the cases are defined by the age at onset, which is at least 65 years. Contrarily to EOFAD, characterized by autosomal-dominant inheritance, LOAD is the outcome of the combination of more complex genetic elements and environmental factors.

The inheritance of the apolipoprotein E (APOE) $\epsilon 4$ allele is the most influential genetic risk factor. This gene, located on chromosome 19, has three alleles $\epsilon 2$, $\epsilon 3$ and $\epsilon 4$ combined in

three different genotype of which $\epsilon 4/\epsilon 4$ increases AD risk about 12-fold, while $\epsilon 3/\epsilon 4$ 3-fold when compared with $\epsilon 3/\epsilon 3$. On the other hand, the $\epsilon 2$ allele seems to have a protective effect. The function of this protein in the nervous system is linked to the transport of cholesterol. The pathological mechanisms operated by the $\epsilon 4$ allele seem to be related to $A\beta$, however they remain to be elucidated [30].

Environmental risk factors for the sporadic forms of AD in addition to age, that is the most relevant one, are: head trauma, heart failure and infectious agents.

In the last decades, infectious agents are taking an increasingly important role in neurodegenerative disorders, this is mainly due to a general decline of the host immune defence, occurring with ageing, and in particular CNS may become more accessible to the infections because of a weakening in the blood-brain barrier (BBB). A growing body of evidence suggest that the most relevant pathogens possibly linked to AD are Chlamydia Pneumoniae and Herpes simplex virus type-1 (HSV-1) [31].

More than 20 years ago HSV-1 DNA has been detected in these cerebral areas in AD and normal brains [32, 33]. In addition viral DNA was detected more frequently in old people and poorly in young adults [34], this fact suggests that ageing promote the entry of the virus in the CNS, strengthening the idea that HSV-1 may be involved in late onset forms of AD.

Another evidence is the detection of antibodies against HSV-1 in the CSF of AD sufferers, indicating that one or more reactivation events occurred in brains.

Interestingly the presence of both the APOE- $\epsilon 4$ allele and HSV-1 induces a higher risk of developing AD compared to the presence of only one of these factors and it has been observed that this allele promotes viral infection [35].

1.1.9 Diagnosis and therapy

There is no cure for AD, the disorder lead to progressive decline of cerebral functions until death. Neurodegeneration may start as early as 20-30 years before the onset of the symptoms [36]. Caregivers can ameliorate everyday life of patients and available drugs can only delay symptoms progression [37]. Treatment should be started as soon as possible to achieve the best beneficial effects but, unfortunately, early diagnosis of AD remains difficult accomplish.

At present there are not laboratory tests for the diagnosis of AD. The most commonly used criteria are based mainly on clinical and neuropsychological findings [38]. Cerebral imaging techniques, such as magnetic resonance imaging (MRI), positron emission tomography (PET), single photon emission computed tomography (SPECT) and computed tomography

(CT), help to exclude other possible form of dementia, by the identification of the AD specific pattern of cerebral atrophy [39, 40]. Another diagnostic tool that is reaching more importance is the reduction of A β 42 or the A β 42/40 ratio and an increase in total and phospho-tau in cerebrospinal fluid (CSF) [41].

In general current available tests are characterized by good specificity but insufficient sensitivity.

1.2 Herpes simplex virus type 1

HSV-1 is one of the most ubiquitous viruses affecting about 90% of the people worldwide. HSV-1 is a double stranded DNA virus belong to the family of Herpesviridae composed by 8 members, named human herpes virus (HHV) 1-8, divided in 3 subfamilies, i. e. α -, β - and γ -Herpesvirinae, according to genome structure, tissue tropism, cytopathology and site of infection.

α Herpes viruses comprise HHV-1, -2 and -3 named also respectively HSV-1, HSV-2 and Varicella Zoster virus (VZV). HSV-1 and HSV-2 can both cause orolabial and genital herpes, although HSV-1 is mainly associated with orolabial infections while HSV-2 with genital. VZV causes chickenpox usually in infants and shingles when the virus reactivates in adult people.

β subfamily includes HHV-5, -6 and -7. HHV-5 also known as cytomegalovirus (CMV) is involved in infectious mononucleosis and pneumonias. HHV-6 and -7 are reported to cause Roseola.

To γ -Herpesvirinae belong HHV-4 and -8. HHV-4, or Epstein-Barr virus (EBV) is mainly implied in infectious mononucleosis and Burkitt's lymphoma. HHV-8 causes Kaposi's sarcoma, a cancer commonly occurring in acquired immunodeficiency syndrome (AIDS), for that reason is also called Kaposi's sarcoma-associated virus.

All of these viruses share some common features: they express a large number of enzymes responsible for the synthesis of DNA and viral proteins; assembly of new viral particles occur in the nucleus; after primary infection they persist lifelong in latent state and can eventually reactivate.

1.2.1 Structure and genome of HSV-1

HSV-1 virions possess a round shape with a diameter of 120-200 nm and they are composed by 4 elements: the outer envelope, the tegument, the capsid and the core (Fig.1.6).

The envelope consists of a lipid bilayer in which are embedded 12 glycoproteins, responsible for the entry in host cell. The tegument is an unstructured layer composed by approximately 20 proteins including viral protein (VP) 16 responsible for the initial viral transcription, VP22 involved in virus transport along microtubules and the virion host shutoff (vhs) that blocks host cell protein synthesis.

Capsid is composed by 162 capsomers in an icosaedral structure. The core is the central structure containing the viral genome [42].

HSV-1 genome is a linear double stranded DNA long 152 kbp and can be divided into two unique sequences, designated as unique long (UL) and unique short (US), flanked by repeated sequences internal (IRL and IRS) and terminal (TRL and TRS) [43].

HSV-1 genome encodes approximately 90 unique transcriptional units, of these at least 84 encode proteins, of which about 40 are necessary for viral replication.

The nomenclature of these genes is based on their position along the genome. The 56 genes identified in the UL sequence are named from UL1 to UL56, while those in the US sequence are listed from US1 to US12. As discussed below viral genes are classified according to their kinetic of expression in three major groups: α , β and γ .

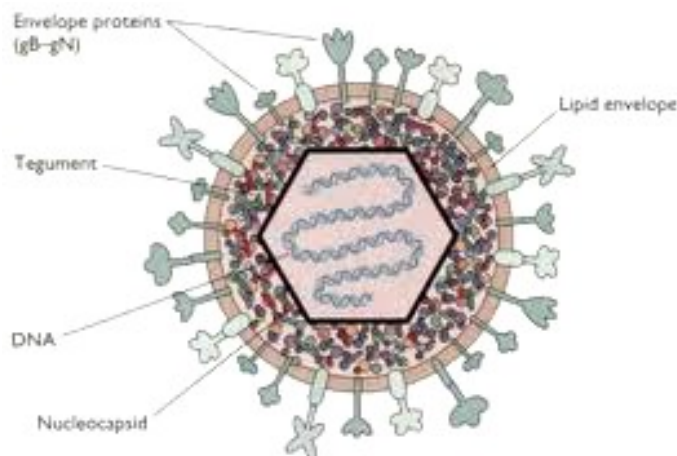


Fig. 1.6 HSV-1 structure

1.2.2 HSV-1 life cycle

After primary infection, occurring usually in the mucosal epithelium of the mouth the virus enters nerve endings of local sensory neurons and it is transported retrograde to the nucleus where it establishes latency (Fig. 1.7). In response to physical, hormonal or emotional stress, the virus can periodically reactivate and it is transported anterograde to or near the site of primary infection. Depending on several factors, including the host immune status, the reactivation may be asymptomatic or lead to a recurrent lesions [44].

Thus, when HSV-1 is inside a cell has two alternatives: its replication that ends with the lysis of host cell and the release of new viral progeny or establishes latency.

Both of these pathways anyway are preceded by the common event of the entry of the virus inside the cell.

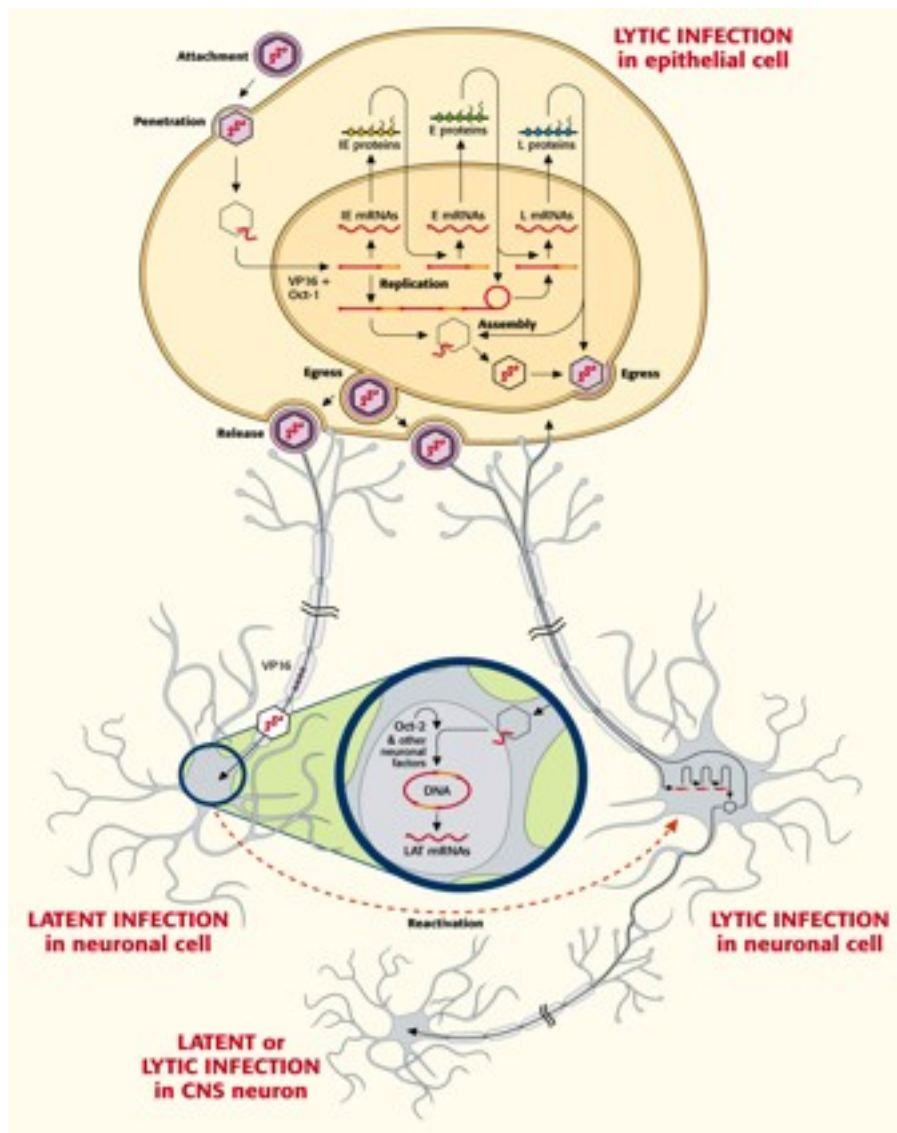


Fig. 1.7 HSV Life cycle.

1.2.3 Virus attachment and entry

The access of HSV-1 into cells requires the concerted activity of at least 4 envelope glycoproteins: gB, gD and heterooligomers of gH and gL [45]. This process is divided by subsequent stages (Fig. 1.8).

In the first step the virion must bind to the surface of the cell. This process is mainly mediated by the interaction with heparansulfate proteoglycans (HSPG) of the viral glycoprotein gC and gB. However the presence of HSPG and/or of gC is dispensable, although their interaction enhances infection.

Second gD interact with one or more cellular receptors, included a member of the tumor necrosis factor (TNF) family named herpes virus entry mediator (HVEM), members of the immunoglobulin superfamily such as nectin-1 and nectin-2 and 3-O-sulfated heparan sulfate. Finally envelope fuses with cellular membrane and viral particle is released inside the cytoplasm. The mechanisms underlying this final stage are not fully understood, it has been suggested that the binding of gD to cellular receptors induces a conformational change that activates gB or gH/gL or both to promote the fusion of viral and cellular phospholipidic bilayers (Fig. 1.8).

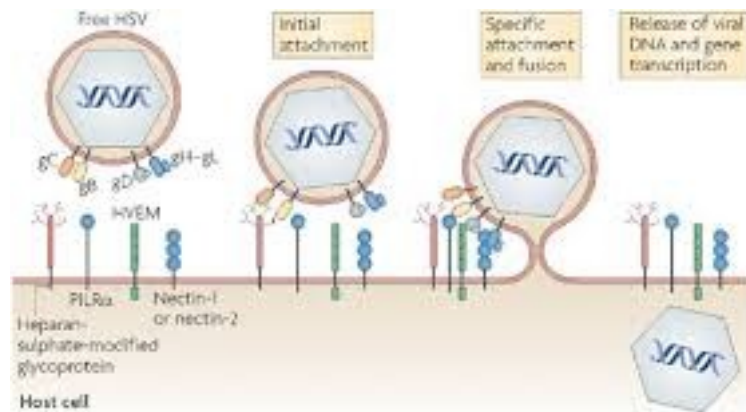


Fig. 1.8 Schematic representation of HSV-1 attachment and entry into the cell.

1.2.4 Viral replication (lytic cycle)

Once inside the cell, some tegument proteins remain in the cytoplasm while other are transported to the nucleus (VP16) or remain associated with the capsid that travel to the nucleus via microtubule network. As soon as the viral DNA enters the nucleus it is rapidly circularized and viral genes are expressed in a tightly regulated, interdependent temporal sequence [46].

α or immediate early (IE) genes, are first expressed, about 2-4 hours post-infection, by the combined action of the tegument protein VP16 with host cell elements. VP16 forms a complex with at least two cellular proteins, Oct-1 and HCF-1, that targets the TAATGARAT motif upstream of the IE promoters stimulating the transcription of these genes [47]. The IE gene products are 5 proteins: infected cell polypeptide (ICP) 0, 4, 22, 27 and 47. Except for ICP47 these proteins stimulate the expression of β genes.

Expression of β or early (E) genes requires at least the presence of functional ICP4 and reaches a peak at 4-8 hours post-infection. This class can be further divided in two groups: $\beta 1$ and $\beta 2$. $\beta 1$ are expressed immediately after or almost concurrently with the synthesis of α

proteins, while $\beta 2$ are expressed later. Several E genes are involved in viral DNA synthesis, event that starts after their expression.

γ or late (L) genes encode structural proteins, and they reach a peak in expression during late stages of infection after viral DNA synthesis has started. Also this group is organized in two subclasses: $\gamma 1$ or leaky-late and $\gamma 2$ or true-late. $\gamma 1$ genes are expressed relatively early during infection and they are stimulated a few fold by viral DNA synthesis. In contrast $\gamma 2$ gene expression is activated late in infection and it is prevented in the presence of inhibitors of viral DNA synthesis [48].

DNA synthesis occurs with the rolling-circle mechanism, resulting DNA concatamers are cleaved and single monomers are incorporated in the nucleocapsids [49]. Viral particles mature by budding through the nuclear membrane. Enveloped viral particles travel along endoplasmic reticulum and Golgi apparatus, where probably are further processed, to finally exit the host cell by exocytosis, that lead to lytic cell death [50].

In fully permissive tissue culture cells, the entire process of viral replication takes about 18 hours.

1.2.5 Latency and reactivation

As said above after the acute phase of infection, HSV-1 persists lifelong in a latent state in sensory neurons innervating the site of primary infection. In particular HSV-1 has been observed to establish latency in trigeminal ganglia (TG). During latency viral genome is tightly associated with cellular histones at episomal level, thus no gene expression is detected except for some mRNA, named latency associated transcripts (LATs) whose coding sequence are located in flanking regions of UL [51]. Their functions are not completely clear, but they have a fundamental role in maintaining the latency. Several stress stimuli may induce the reactivation of the virus that can be transported anterograde to the area of primary infection. In rare cases after reactivation the virus may be transported to CNS, where it can cause Herpesviral encephalitis (HSE), a severe disease that impair cerebral functions and if untreated can cause death [52].

1.3 References

1. Ferri, C.P., et al., *Global prevalence of dementia: a Delphi consensus study*. Lancet, 2005. **366**(9503): p. 2112-7.
2. Qiu, C., M. Kivipelto, and E. von Strauss, *Epidemiology of Alzheimer's disease: occurrence, determinants, and strategies toward intervention*. Dialogues Clin Neurosci, 2009. **11**(2): p. 111-28.
3. Berchtold, N.C. and C.W. Cotman, *Evolution in the conceptualization of dementia and Alzheimer's disease: Greco-Roman period to the 1960s*. Neurobiol Aging, 1998. **19**(3): p. 173-89.
4. DeCarli, C., *Mild cognitive impairment: prevalence, prognosis, aetiology, and treatment*. Lancet Neurol, 2003. **2**(1): p. 15-21.
5. Wenk, G.L., *Neuropathologic changes in Alzheimer's disease*. J Clin Psychiatry, 2003. **64 Suppl 9**: p. 7-10.
6. Whitwell, J.L., *Progression of atrophy in Alzheimer's disease and related disorders*. Neurotox Res. **18**(3-4): p. 339-46.
7. Mattson, M.P., *Pathways towards and away from Alzheimer's disease*. Nature, 2004. **430**(7000): p. 631-9.
8. Chow, V.W., et al., *An overview of APP processing enzymes and products*. Neuromolecular Med. **12**(1): p. 1-12.
9. Irie, K., et al., *Structure of beta-amyloid fibrils and its relevance to their neurotoxicity: implications for the pathogenesis of Alzheimer's disease*. J Biosci Bioeng, 2005. **99**(5): p. 437-47.
10. Klein, W.L., W.B. Stine, Jr., and D.B. Teplow, *Small assemblies of unmodified amyloid beta-protein are the proximate neurotoxin in Alzheimer's disease*. Neurobiol Aging, 2004. **25**(5): p. 569-80.
11. Tanzi, R.E., *The genetics of Alzheimer disease*. Cold Spring Harb Perspect Med. **2**(10).
12. Head, E., et al., *Aging in Down Syndrome and the Development of Alzheimer's Disease Neuropathology*. Curr Alzheimer Res. **13**(1): p. 18-29.
13. Suh, Y.H. and F. Checler, *Amyloid precursor protein, presenilins, and alpha-synuclein: molecular pathogenesis and pharmacological applications in Alzheimer's disease*. Pharmacol Rev, 2002. **54**(3): p. 469-525.
14. Spillantini, M.G. and M. Goedert, *Tau pathology and neurodegeneration*. Lancet Neurol. **12**(6): p. 609-22.
15. Iqbal, K., et al., *Tau pathology in Alzheimer disease and other tauopathies*. Biochim Biophys Acta, 2005. **1739**(2-3): p. 198-210.
16. Chun, W. and G.V. Johnson, *The role of tau phosphorylation and cleavage in neuronal cell death*. Front Biosci, 2007. **12**: p. 733-56.
17. Hanger, D.P., et al., *Novel phosphorylation sites in tau from Alzheimer brain support a role for casein kinase 1 in disease pathogenesis*. J Biol Chem, 2007. **282**(32): p. 23645-54.
18. Braak, H. and E. Braak, *Neuropathological staging of Alzheimer-related changes*. Acta Neuropathol, 1991. **82**(4): p. 239-59.
19. Tuppo, E.E. and H.R. Arias, *The role of inflammation in Alzheimer's disease*. Int J Biochem Cell Biol, 2005. **37**(2): p. 289-305.
20. Solito, E. and M. Sastre, *Microglia function in Alzheimer's disease*. Front Pharmacol. **3**: p. 14.
21. Eikelenboom, P. and W.A. van Gool, *Neuroinflammatory perspectives on the two faces of Alzheimer's disease*. J Neural Transm (Vienna), 2004. **111**(3): p. 281-94.
22. Eng, L.F., R.S. Ghirnikar, and Y.L. Lee, *Glial fibrillary acidic protein: GFAP-thirty-one years (1969-2000)*. Neurochem Res, 2000. **25**(9-10): p. 1439-51.

23. Godbout, J.P., et al., *Exaggerated neuroinflammation and sickness behavior in aged mice following activation of the peripheral innate immune system*. *FASEB J*, 2005. **19**(10): p. 1329-31.
24. Hynd, M.R., H.L. Scott, and P.R. Dodd, *Glutamate-mediated excitotoxicity and neurodegeneration in Alzheimer's disease*. *Neurochem Int*, 2004. **45**(5): p. 583-95.
25. Katayama, T., et al., *Induction of neuronal death by ER stress in Alzheimer's disease*. *J Chem Neuroanat*, 2004. **28**(1-2): p. 67-78.
26. Rego, A.C. and C.R. Oliveira, *Mitochondrial dysfunction and reactive oxygen species in excitotoxicity and apoptosis: implications for the pathogenesis of neurodegenerative diseases*. *Neurochem Res*, 2003. **28**(10): p. 1563-74.
27. Demuro, A., I. Parker, and G.E. Stutzmann, *Calcium signaling and amyloid toxicity in Alzheimer disease*. *J Biol Chem*. **285**(17): p. 12463-8.
28. Mariani, E., et al., *Oxidative stress in brain aging, neurodegenerative and vascular diseases: an overview*. *J Chromatogr B Analyt Technol Biomed Life Sci*, 2005. **827**(1): p. 65-75.
29. Sayre, L.M., et al., *Metal ions and oxidative protein modification in neurological disease*. *Ann Ist Super Sanita*, 2005. **41**(2): p. 143-64.
30. Koffie, R.M., et al., *Apolipoprotein E4 effects in Alzheimer's disease are mediated by synaptotoxic oligomeric amyloid-beta*. *Brain*. **135**(Pt 7): p. 2155-68.
31. De Chiara, G., et al., *Infectious agents and neurodegeneration*. *Mol Neurobiol*. **46**(3): p. 614-38.
32. Jamieson, G.A., et al., *Latent herpes simplex virus type 1 in normal and Alzheimer's disease brains*. *J Med Virol*, 1991. **33**(4): p. 224-7.
33. Jamieson, G.A., et al., *Herpes simplex virus type 1 DNA is present in specific regions of brain from aged people with and without senile dementia of the Alzheimer type*. *J Pathol*, 1992. **167**(4): p. 365-8.
34. Wozniak, M.A., et al., *Productive herpes simplex virus in brain of elderly normal subjects and Alzheimer's disease patients*. *J Med Virol*, 2005. **75**(2): p. 300-6.
35. Itzhaki, R.F., et al., *Herpes simplex virus type 1 in brain and risk of Alzheimer's disease*. *Lancet*, 1997. **349**(9047): p. 241-4.
36. DeKosky, S.T. and K. Marek, *Looking backward to move forward: early detection of neurodegenerative disorders*. *Science*, 2003. **302**(5646): p. 830-4.
37. Connell, C.M., M.R. Janevic, and M.P. Gallant, *The costs of caring: impact of dementia on family caregivers*. *J Geriatr Psychiatry Neurol*, 2001. **14**(4): p. 179-87.
38. Mendez, M.F., *The accurate diagnosis of early-onset dementia*. *Int J Psychiatry Med*, 2006. **36**(4): p. 401-12.
39. Schroeter, M.L., et al., *Neural correlates of Alzheimer's disease and mild cognitive impairment: a systematic and quantitative meta-analysis involving 1351 patients*. *Neuroimage*, 2009. **47**(4): p. 1196-206.
40. Waldemar, G., et al., *Recommendations for the diagnosis and management of Alzheimer's disease and other disorders associated with dementia: EFNS guideline*. *Eur J Neurol*, 2007. **14**(1): p. e1-26.
41. Herukka, S.K., et al., *CSF Aβ42 and tau or phosphorylated tau and prediction of progressive mild cognitive impairment*. *Neurology*, 2005. **64**(7): p. 1294-7.
42. Davison, A.J., *Overview of classification*. 2007.
43. Wadsworth, S., R.J. Jacob, and B. Roizman, *Anatomy of herpes simplex virus DNA. II. Size, composition, and arrangement of inverted terminal repetitions*. *J Virol*, 1975. **15**(6): p. 1487-97.
44. Perng, G.C. and C. Jones, *Towards an understanding of the herpes simplex virus type 1 latency-reactivation cycle*. *Interdiscip Perspect Infect Dis*. **2010**: p. 262415.
45. Akhtar, J. and D. Shukla, *Viral entry mechanisms: cellular and viral mediators of herpes simplex virus entry*. *FEBS J*, 2009. **276**(24): p. 7228-36.

46. Jones, P.C. and B. Roizman, *Regulation of herpesvirus macromolecular synthesis. VIII. The transcription program consists of three phases during which both extent of transcription and accumulation of RNA in the cytoplasm are regulated.* J Virol, 1979. **31**(2): p. 299-314.
47. Johnson, K.M., S.S. Mahajan, and A.C. Wilson, *Herpes simplex virus transactivator VP16 discriminates between HCF-1 and a novel family member, HCF-2.* J Virol, 1999. **73**(5): p. 3930-40.
48. Kibler, P.K., et al., *Regulation of herpes simplex virus true late gene expression: sequences downstream from the US11 TATA box inhibit expression from an unreplicated template.* J Virol, 1991. **65**(12): p. 6749-60.
49. Hay, J. and W.T. Ruyechan, *Alphaherpesvirus DNA replication.* 2007.
50. Baines, J.D., *Envelopment of herpes simplex virus nucleocapsids at the inner nuclear membrane.* 2007.
51. Stevens, J.G., et al., *Prominence of the herpes simplex virus latency-associated transcript in trigeminal ganglia from seropositive humans.* J Infect Dis, 1988. **158**(1): p. 117-23.
52. Banerjee, K. and B.T. Rouse, *Immunopathological aspects of HSV infection.* 2007.

1.4 Aims of work: study of HSV-1 as a possible risk factor for AD

Alzheimer's disease (AD), the most common form of dementia which generally develops in late life and the understanding of the complex processes that begin and contribute to the neurodegeneration remain an open challenge of basis research. Although certain genetic loci play a role in conferring susceptibility in some sporadic AD cases, probably other environmental potential risk factors concur in the development of the disease. The herpesviruses family is among the most probable pathogen candidates to central nervous system (CNS) neurodegeneration in old age, because of its well-known ability to escape peripheral immune responses by invading neurons. In particular recent evidences suggested a possible association between AD and herpes simplex virus type 1 (HSV-1) for its ability, within the sensory ganglia (trigeminal ganglia), to establish a latent infection that persists for the life of the individual. Previous studies on HSV-1 infection as possible risk factor for AD were limited to either epidemiological surveys or analysis of AD molecular hallmarks in infected neurons but, so far, no experimental evidence clearly demonstrated the pathophysiological role of HSV-1 in AD. In the last decades the very deep knowledge acquired on the genetics and molecular biology of HSV-1 has evidenced that viral infection causes hyperphosphorylation and caspase-3 mediated cleavage of the microtubule-associated tau protein, inducing tau aggregation. HSV-1 contributes to intracellular and extracellular accumulation of amyloid beta (A β) in neurons), causing also a persistent voltage-gated Ca²⁺ channel activation. Moreover an homology between amyloid peptide and HSV-1 glycoprotein B has been evidenced so also molecular mimicry can be one of the mechanisms that trigger the immune response. The understanding of immunologic control during latency and reactivation of HSV-1 in humans remains incomplete. Multiple evidences suggest an emerging role for T lymphocytes, as CD8⁺ T cell responses appear central to control of HSV-1 replication and prevention of recurrence. Moreover as the inflammatory component seems to play a key role in neurodegeneration and most notably in AD, a novel and important aspect to deepen is the interplay between different component of immunity (innate and adaptive) and the multiple viral reactivation generally occurring during the life.

The aim of this work was to dissect the hypothesis that HSV-1 infections, when spreading to the CNS, may damage brain functions thus eventually contributing to neurodegeneration.

To this purpose a series of in vitro and in vivo experiments were addressed to investigate a possible viral interference with some particular physiological processes provoking AD related alterations.

These evaluations concern 4 different aspects: phosphorylation of cytoplasmic tau, alterations in nuclear tau, Ca²⁺ dyshomeostasis and neuroinflammation.

For convenience these topics were treated separately in the following 4 sections of this thesis.

2. The role of US3 and UL13 viral kinases in hyperphosphorylation of Tau

2.1 Introduction

Tau was first discovered as a microtubule-associated protein (MAP) that, under physiological condition, stimulates tubulin assembly into microtubules in the brain, but when abnormally phosphorylated it loses this ability and tends to aggregate to structure the paired helical filaments (PHFs) of neurofibrillary tangles (NFTs), one of the principal AD hallmarks. The potential sites of phosphorylation of this protein are 85 of which 36 have been described to be phosphorylated in the PHF [1]. The normal level of tau phosphorylation is a consequence of dynamic regulation of tau kinases and tau phosphatases. Numerous studies have identified the major tau kinases and phosphatases in the brain that are: glycogen-synthase kinase-3 β (GSK-3 β), cyclin-dependent protein kinases (cdk), protein kinase A (PKA), and stress-activated protein kinases [2].

In the last decade, based on these studies, several authors have shown, in vitro neuroblastoma cells, that HSV-1 induces tau phosphorylation in various sites [3, 4]. The reasons why this happens remain unknown, but as detailed below, HSV-1 harbours some features that suggest it may mimic or interfere with the activity of these cellular enzymes supporting a possible involvement of the virus in the outcome of an AD-like cellular alteration. In order to elucidate the mechanisms underlying the viral-induced phosphorylation of tau, it is necessary to understand which are the cellular and viral factors involved in this event.

HSV-1 encodes at least three protein kinases, UL13, US3 and UL39 [5], two of which, US3 and UL13, seem to be linked with tau phosphorylation.

US3 is a serine-threonine protein kinase encoded by HSV-1 and the phosphorylation target site specificity of HSV-1 Us3 has been reported to be similar to that of PKA, a cellular cyclic AMP-dependent protein kinase reported to phosphorylate tau [6], and Akt/protein kinase B (Akt) suggesting that Us3 is a multifunctional protein that plays various roles in viral replication by phosphorylating a number of viral and cellular substrates.

UL13 also is a serine/threonine viral protein kinase and the amino acid sequence is one of those “conserved herpesviral protein kinases” (CHPKs) among all three herpesvirus subfamilies [7]. Ball et al. recently hypothesized a possible direct effect on tau phosphorylation from UL13 [8]. Their assumption stems from several functional overlapping between UL13 and cellular kinases. On one side the viral protein VP22 has been reported to be a phosphorylation target for both UL13 and human casein kinase 2 (CK2). CK2 phosphorylates also tau, and they observed a certain grade of homology between VP22 and tau. On the other side there is evidence that the cellular protein elongation factor 1 δ (EF1 δ), can be phosphorylated by both UL13 and humane kinase cell division cycle 2 (cdc2), another cellular protein known to phosphorylate tau. Therefore they speculate a possible cross-phosphorylation of tau mediated by UL13.

To investigate a possible role of the viral kinases US3 and UL13 in tau phosphorylation, mutant viruses lacking these genes and plasmid vectors for their expression in mammalian cells were generated. SH-SHSY5Y neuroblastoma cells were infected or transfected with these constructs and the phosphorylation of tau was evaluated by immunofluorescence and western blot in two particular sites: Ser202 and Ser214, respectively known target of cdc2 [9] and of PKA [10].

2.2 Material and methods

2.2.1 Cells

Vero cells were grown in Dulbecco's minimal essential medium (DMEM) containing 100 U/ml penicillin, 100 µg/ml streptomycin, 2mM L-glutamine and 10% heat-inactivated fetal calf serum (FCS), and were used to the preparation of viral stocks as described below.

SH-SH5Y cells were grown in a mixture 1:1 of Eagle's minimal essential medium and nutrient F12 Ham (EMEM-F12) supplemented with 100 U/ml penicillin, 100 µg/ml streptomycin, 2mM L-glutamine and 15% FCS. Cultures were maintained at 37°C in 5% CO₂ atmosphere. 24 hours prior to infection or transfection cells were seeded at a concentration of $2 \cdot 10^4$ cells per well in a 24-well plate for immunofluorescence assay and $5 \cdot 10^5$ per well in a 6-well plate for western blot.

2.2.2 Plasmids

All the restriction enzymes were purchased from New England BioLabs, Ipswich, MO, USA. To construct the plasmid pBSSK13, the sequence of HSV-1 genome located between nucleotides 25380 to 28630, that contains UL13 gene, was excised from the cosmid B of a library of 5 cosmids that cover the entire genome of the virus [11], by digestion with restriction enzymes BglII and KpnI, and inserted into pBlueScriptIISK- (PBSSK-, Invitrogen, Carlsbad, CA, USA).

To generate the plasmid pBSSK13-EGFP, the expression cassette of the enhanced green fluorescent protein (EGFP) reporter gene under CMV promoter was digested and excised, from pcDNA3.1Hygro(+)-EGFP plasmid, with NruI and SphI restriction enzymes and inserted inside the UL13 ORF, in pBSSK13 previously digested with EcoRV and SphI thus interrupting this sequence (Fig. 2.1).

pEGFP-US3 and pRFP-UL13 are plasmids expressing the viral kinases US3 and UL13 fused respectively to EGFP and mCherry, a red fluorescent protein. To create these constructs the sequences of the two viral genes were amplified by PCR from wild type HSV-1 DNA strain F, with the following primers:

US3 forward (5'-GGAAGATCTCGATGGCCTGTCGTAAGTTTTGTCG-3');

US3 reverse (5'-CGGAATTCTCATTCTGTTGAAACAGCGGCAAACAAAGC3-');

UL13 forward (5'-GGAAGATCTCGATGGATGAGTCCCGCAGACAGCGACCTGC-3');

UL13 reverse (5'-CGGAATTCTCACGACAGCGCGTGCCGCGCGCACG-3').

Both primers forward contain a restriction site for BglIII, while both reverse primers carry an EcoRI site, to allow digestion of the PCR products with these enzymes. US3 was then cloned into pEGFP-C2 (BD Biosciences, Franklin Lakes, NJ, USA) while UL13 into pmCherry-C2, a plasmid vector kindly provided by prof. S. Efsthathiou, where the ORF of EGFP in pEGFP-C2 was replaced with that of mCherry (Fig. 2.2).

2.2.3 Transfection for transient expression of viral kinase

SH-SY5Y cells were transfected with Lipofectamine® Reagent (Invitrogen, Carlsbad, CA, USA).

10µl of Lipofectamine reagent were added in 50µl of Optimem medium (Gibco, Thermofisher scientific, Waltham, USA) and 2µg of pEGFP-US3 or pRFP-UL13, were added in 50µl of Optimem medium. The two solutions were left separated 5 minutes at room temperature (RT) and then mixed. After 20 minutes, 100µl of the mix were added to cells. 24 hours post-transfection cells were subjected to western blot.

2.2.4 Viruses

The viruses used were a HSV-1 wild type strain F and R7041, an US3-negative mutant virus kindly provided by B. Roizman and previously described [12].

To generate the mutant viruses named FAUL13 and FAUS3ΔUL13, the UL13 deletion was inserted respectively in F and R7041 with the method of homologous recombination, by the co-transfection in Vero cells of viral DNA and the plasmid pBSSK13-EGFP, as detailed below.

The amount of virus used to infect cells, is indicated as molteplicity of infection (m.o.i.), and represent the number of plaque forming units (p.f.u.) per cell. Viral particles were diluted in culture medium and added to cell monolayer, after 1 hour at 37°C, the viral inoculum was removed and replaced with fresh medium.

2.2.5 Viral DNA purification

Vero cells, 10^7 for large preparative or $2 \cdot 10^5$ for mini stocks, were infected with a molteplicity of infection (m.o.i.) of 1 plaque forming unit (p.f.u.) per cell. 24 hours post-infection cells were collected in 15ml tubes and spinned at 1500 rpm for 15 minutes, resuspended in lysis buffer (10mM tris, 1mM EDTA, 0,6% SDS, 0,1mg/ml proteinase K) and shaken for 16 hours at 37°C.

The first step to purify viral DNA was the sequential centrifugation at 13000rpm for 3 minutes of cell lysates in two different solutions: phenol/chloroform/isoamyl alcohol 25:24:1 (Ambion, applied Biosystem) and chloroform/isoamyl alcohol 24:1 (Ambion, applied Biosystem, Thermofisher scientific). The aqueous phase obtained was diluted 1:3 in absolute ethanol and DNA was precipitated at -80°C for 30 minutes. Finally samples were spinned at 13000rpm for 15 minutes, washed with 75% ethanol and resuspended in water.

2.2.6 Calcium phosphate transfection

1µg of pBSSK13-EGFP, previously linearized with the restriction enzyme XbaI, and 5µg of viral DNA were diluted in 500µl of HEPES-buffered saline (HBS: 200mM HEPES, 135mM NaCl, 5mM KCl, 5mM dextrose and 0,7mM Na₂HPO₄, pH 7,05). 30µl of 2M CaCl₂ were mixed with DNA suspension and this solution was then added to Vero cell monolayer previously seeded to obtain a confluence of 80-90% in 6-well plates. 10 minutes later, DNA suspension was diluted in 3ml of culture medium and after 5 hours at 37°C the entry of DNA into the cells was helped by replacing medium with a solution of 15% glycerol in DMEM for 3 minutes. After that cells were left in culture medium and the presence of EGFP expressing viral plaques was checked in the following 72 hours with a fluorescent microscope Nikon Eclipse TE 2000-S.

2.2.7 Limiting dilution

EGFP expressing viral plaques were harvested and titrated to determine viral concentration (see below). In order to isolate recombined viruses from wild type, 2·10⁶ Vero were infected with 20 p.f.u. in 2ml of DMEM and shaken for 1 hour at 37°C. Then cellular and viral suspension was diluted in 10ml of medium and seeded in 96-well plates with a concentration of 100µl per well. 72 hours later, the wells containing a single EGFP expressing plaque were harvested and subjected to a new cycle of limiting dilution. For every virus 3 cycles of limiting dilution were performed. Finally the deletion of UL13 was checked by Southern blot.

2.2.8 Southern blot

Ministocks of viral DNA were prepared for each recombined HSV-1 collected from the fourth limiting dilution. These samples, DNA extracted from HSV-1 F and R7041, pBSSK13 and pBSSK13EGFP were digested with KpnI and subjected to electrophoresis at 25V for 16 hours on a 0,8% agarose gel containing 2µM ethidium bromide. The gel was then processed with

0,25N HCl for 8 minutes, then 30 minutes with 1,5M NaCl and further 30 minutes with 0,5N NaOH. Finally DNA was transferred, by capillary action, to a nitrocellulose membrane (NITRAN N, Whatman, GE Healthcare, Little Chalfont, UK). To permanently attach the transferred DNA to the membrane, this was then exposed to UV radiation. The detection of the band in the region of UL13 was performed using Amersham Gene Images AlkPhos Direct Labelling and Detection System (GE Healthcare) according to manufacturer's instructions.

2.2.9 Viral Stocks

In order to have a large quantity of recombined virus $6 \cdot 10^7$ Vero were infected with a m.o.i. of 0.01 p.f.u./cell. When 100% of cytopathic effect was observed cells were harvested and spun down at 1500rpm for 10 minutes. Supernatant was further centrifuged at 19000rpm for 30 minutes and then the viral pellet was collected. Cell pellet was subjected to 3 cycles of freeze/thaw, sonicated and centrifuged at 3000rpm for 10 minutes to discharge cellular debris. The supernatant collected after this centrifugation was mixed with viral pellet previously obtained and the mix was further centrifuged at 19000rpm for 30 minutes. Final viral pellet was resuspended in DMEM, sonicated and aliquoted.

Viral preparations were titrated and stock at -80°C .

2.2.10 Viral titration - Plaque assay

To determine viral titre, the number of viral particles per ml, every viral sample were serially diluted 1:10 in 1ml. Every dilution was added in a single well of a 6-well plate to a Vero cells monolayer previously seeded. After 1 hour at 37°C medium was replaced with medium containing 1% methyl cellulose (SIGMA-Aldrich, St. Louis, MO, USA).

72 hours later viral titre was determined by plaque assay.

Cells were washed twice with Tris-buffered saline (TBS: 50mM Tris, 150 mM NaCl, pH 7,6), fixed and stained with a solution of 50% methanol in water containing 1% of crystal violet for 30 minutes at RT.

Plates were washed with tap water and plaques were counted. Viral titre was determined by multiplying the number of the plaques times the dilution factor.

2.2.11 Growth curve

Recombined viruses were tested to observe if the mutation of UL13 may affect the ability to replicate. To this purpose it was created a growth curve, by infecting cells and collecting the virus at several time points: input (-1), 0, 4, 8, 12, 24, 32, 48, 56 and 72 hours post-infection. Vero cells were seeded in 6-well plates with a concentration of 10^6 cells/well and infected with a m.o.i. of 0,01 p.f.u./cell in 1ml. The first samples collected (input) were diluted immediately with 2ml of medium harvested and freeze at -80°C . The other samples were incubated for 1 hour at 37°C , then viral inoculum was removed, cells were washed with phosphate buffered saline (PBS: 137mM NaCl, 2,7mM KCl, 10mM Na_2HPO_4 , 1,8mM KH_2PO_4 , pH 7,4) and incubated for 3 minutes at RT with citrate buffer (1,35M NaCl, 0,1M KCl, 0,4M citric acid, pH 3). Then cells were washed twice with medium and finally left in 3ml of medium. The second time point (0h) was frozen and other plates were left at 37°C and freeze at the time points indicated. Finally every sample was titrated as previously described and the results were reported in a graph expressed in \log_{10} of the number of p.f.u./ml versus time.

The viruses replication activity was also tested by comparing the size of the plaques. Images of plaques were collected, with a microscope Nikon eclipse TE 2000-S, from plates of viral titration of samples collected 48 hours post infection and plaques diameters (n=30 for each virus) were measured using ImageJ software. Data collected were then reported in a graph, expressing the average diameter of plaques for each virus. Statistical significance was determined by student's t test.

2.2.12 Western Blot

Cells were harvested and resuspended in lysis buffer (10mM tris pH 7.6, 150mM NaCl, 5mM EDTA, 10% Glycerol, 1% Triton X100, 1mM Na_3VO_4 , 1mM NaF, 1mM PMSF, Protease inhibitor mix (Roche)) and boiled for 8 minutes. Samples were analyzed via 12% sodium dodecyl sulfate-polyacrylamide gel electrophoresis (SDS-PAGE). Proteins were then transferred to nitrocellulose membranes, that were blocked with PBS with 0,1% Tween 20 and 5% BSA, before being incubated for 1 hour with primary antibodies rabbit anti-Tau (phospho S202) 1:200 (ab108387, Abcam, Cambridge, UK); mouse anti-Phospho-PHF-tau AT100 1:500 (MN1060, Thermofisher scientific); mouse anti-class III β -tubulin, 1:1000 (TUJ1, Covance); mouse anti-GFP,1:5000 (JL-8, Clontech); rat anti-RFP, 1:2000 (5F8, Chromotek, Planegg, DE). After washing with PBS Tween 0,1%, with secondary antibodies goat anti-mouse IgG horseradish peroxidase-linked (GE Healthcare). Immunocomplexes were

detected by ECL detection kit (Thermofisher scientific). Membranes were stripped between antibodies by incubation in Restore Western blot stripping buffer (21059, Thermofisher scientific).

2.2.13 Immunofluorescence

Cells were fixed in 4% paraformaldehyde (PFA) in PBS for 20 minutes, permeabilized in 0,1% Triton X-100 in PBS, blocked for 1 hour in PBS containing 3% bovine serum albumin (BSA) and 2% normal goat serum (NGS) and labelled for 1 hour with primary antibodies rabbit Anti-Tau (phospho S202) 1:200 (ab108387, Abcam, Cambridge, UK); mouse Phospho-PHF-tau AT100 1:500 (MN1060, Thermofisher scientific); rabbit anti-HSV-1 (ab9533, Abcam); mouse anti-HSV-1 VP16 (kindly provided by prof. Efstathiou). After washing in PBS cells were incubated with the secondary antibodies Alexa Fluor 488-goat anti-rabbit IgG (green fluorescence) and Alexa Fluor 568-conjugated goat anti-mouse IgG (red fluorescence) pAb (Invitrogen, Carlsbad, CA, USA) diluted 1:1000 for 1 hour in the dark. Finally cell samples were mounted with ProLong® Gold Antifade Mountant (Invitrogen) containing DAPI (4',6-diamidino-2-phenylindole) to stain nuclei.

Fluorescent images were collected with a Leica SP5 confocal microscope and processed with ImageJ software.

2.3 Results

2.3.1 Construction of mutant viruses HSV-1 Δ UL13 and Δ US3 Δ UL13

HSV-1 mutant viruses lacking portions of the *UL13* or *US3* genes were constructed by homologous recombination between infectious wild-type HSV-1 F DNA and pBSSK Δ UL13-EGFP plasmid containing the Δ UL13 allele (166bp deletion in UL13 ORF) and GFP selection marker. The insertion of GFP expression cassettes into UL13 loci in the HSV-1 genome was verified by Southern blot. DNA samples were digested with KpnI restriction enzyme, transferred on a blot and stained with a 497bp probe corresponding to the short sequence between the two XhoI sites of pBSSK13 that spans from 2947 to 3444 bp (Fig. 2.1).

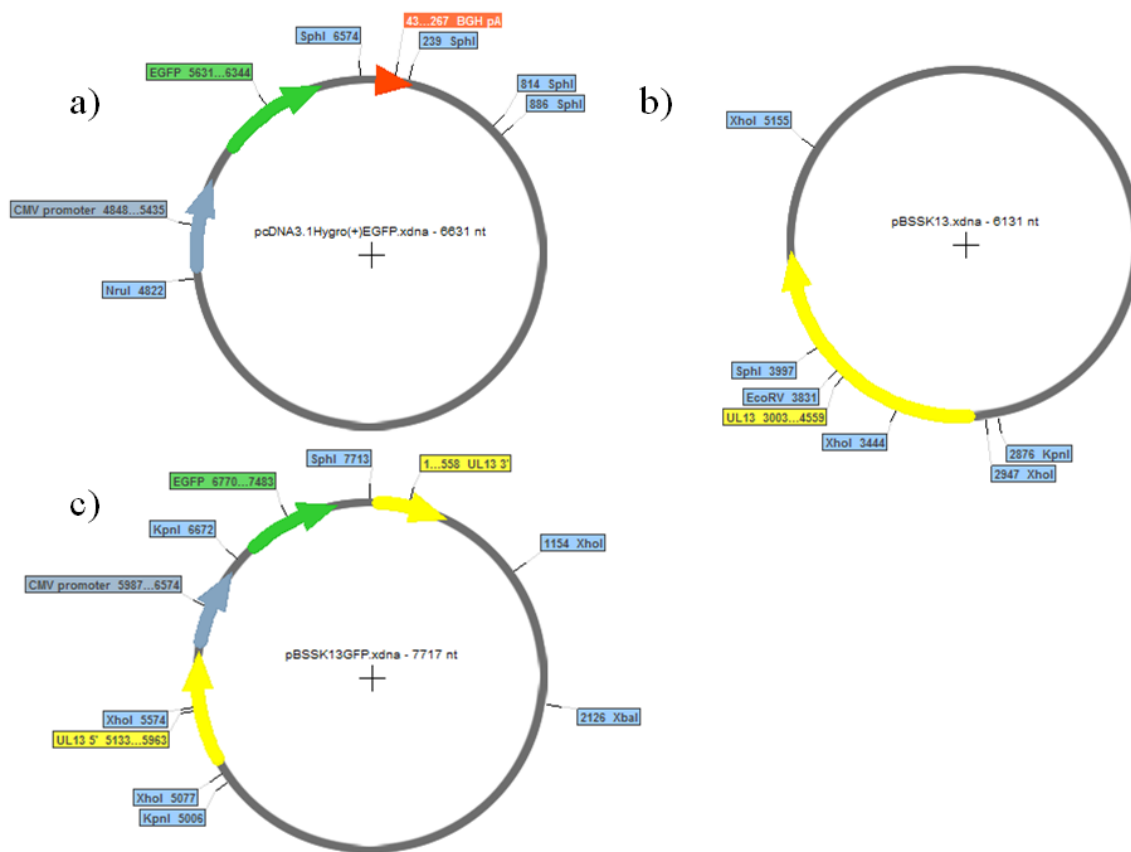


Fig. 2.1. Maps of the plasmids used to interrupt the ORF of UL13 in HSV-1 genome. They are evidenced the main features and the restriction sites of the enzymes used. a) Map of pcDNA3.1Hygro(+)-EGFP. b) Map of pBSSK13. c) Map of pBSSK13-EGFP.

This probe binds to a sequence upstream the site of deletion in UL13, thus it is possible to discriminate between recombined and not-recombined virus (Fig. 2.2). The HSV-1 $\Delta UL13/\Delta US3$ mutant virus was constructed by homologous recombination between infectious R7041 DNA (HSV-1 $\Delta Us3$) and pBSSK $\Delta UL13$ -EGFP DNA from HSV-1 F,wild-type virus, R7041 mutant and pBSSK13 plasmid were used as a negative control and pBSSK $\Delta UL13$ -EGFP as a positive control.

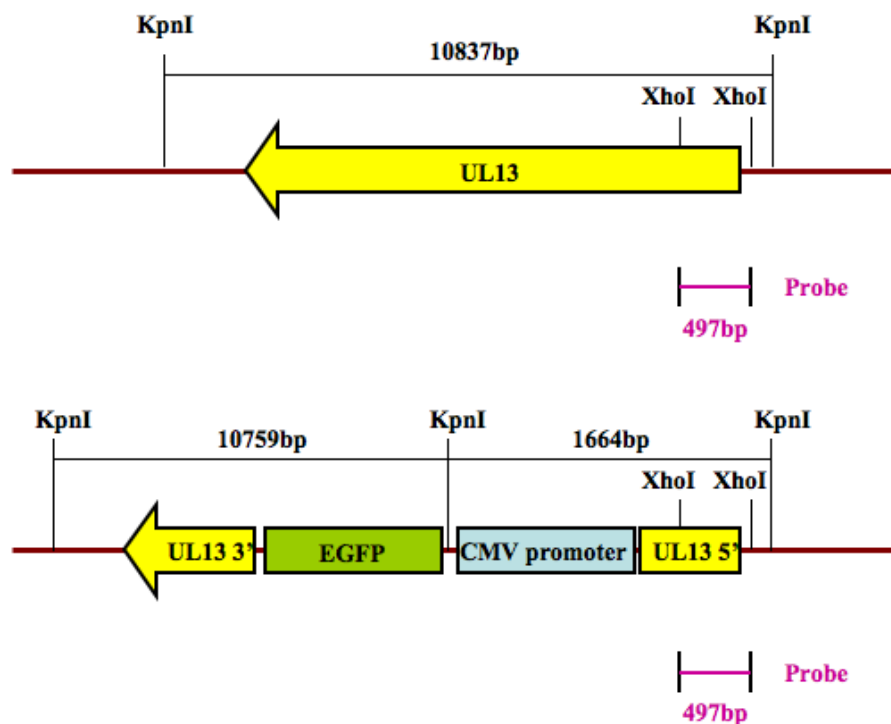


Fig. 2.2. Schematic representation of the sequences detected by southern blot. Pink bar represent the probe used, corresponding to the sequence between the two XhoI sites indicated. They are evidenced the restriction sites for KpnI, used to digest DNA samples. a) In samples negative for recombination, the probe detects a sequence of 10837bp corresponding to the two KpnI sites present in this area of HSV-1 genome. b) In samples positive for recombination, there is an extra KpnI sites, between CMV promoter and EGFP ORF, that make the probe recognises a sequence of 1664bp.

Southern blot analysis confirmed that each HSV-1 mutant virus carried an insertion of the expected size and restriction fragment. Fig. 2.3 and 2.4 show the results of the southern blots, respectively for $F\Delta UL13$ and $F\Delta US3\Delta UL13$ indicating that the intended mutations were effectively introduced into the HSV-1 genome. Once checked the correct insertion of the deletion, viral stocks were prepared and viral replication ability was tested by growth curve assay.

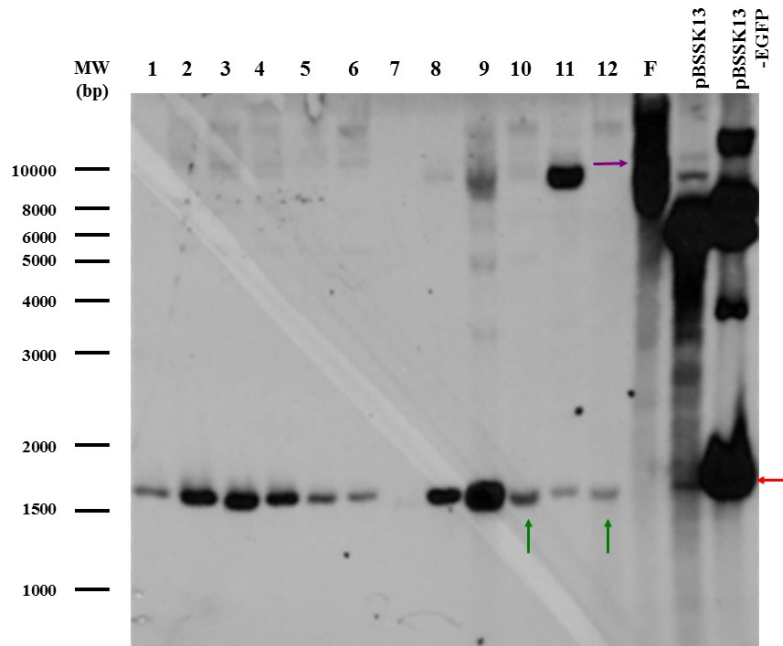


Fig. 2.3. Southern blot of F Δ UL13 recombinant virus DNAs. Lanes 1-12 are the samples to test; lane 13 is the backbone DNA HSV-1 F wild type and represent the negative control; lane 14 is pBSSK13, a further negative control, detected by the probe as the entire sequence of the plasmid (6131bp); lane 15 is pBSSK13-EGFP, the positive control. Red arrow indicates the 1664bp band detected by the probe in positive samples. Purple arrow indicates the 10837bp band detected in the backbone virus. Green arrows indicate the two samples chosen to prepare viral stocks.

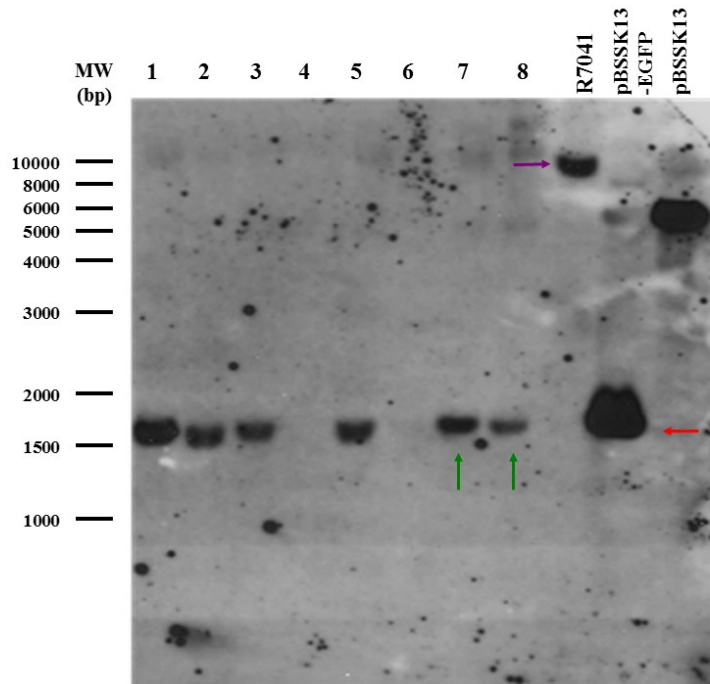


Fig. 2.4. Southern blot of F Δ US3 Δ UL13 recombinant virus DNAs. Lanes 1-8 are the samples to test; lane 9 is the backbone DNA HSV-1 R7041 and represent the negative control; lane 11 is pBSSK13-EGFP, the positive control; lane 10 is pBSSK13, a further negative control, detected by the probe as the entire sequence of the plasmid (6131bp). Red arrow indicates the 1664bp band detected by the probe in positive samples. Purple arrow indicates the 10837bp band detected in the backbone virus. Green arrows indicate the two samples chosen to prepare viral stocks.

2.3.2 Evaluation of replication activity of mutant viruses

Our initial experiment focused on testing if UL13 and US3 protein kinases play a role in the immediate-early and early phases of HSV-1 replication (prior to viral DNA synthesis). As described in material and methods, Vero cells were infected with 0,01 m.o.i. of every single virus separately, the two recombinant FΔUL13 and FΔUS3ΔUL13 and their respective backbone virus, i.e. F and R7041.

Infected cells were collected at several time points and viral load was determined by plaque assay.

As shown in Fig. 2.5 the deletion in UL13 alone doesn't affect viral yield, while the FΔUS3ΔUL13 mutant shows a reduction in viral yield of at least half logarithm than the other viruses.

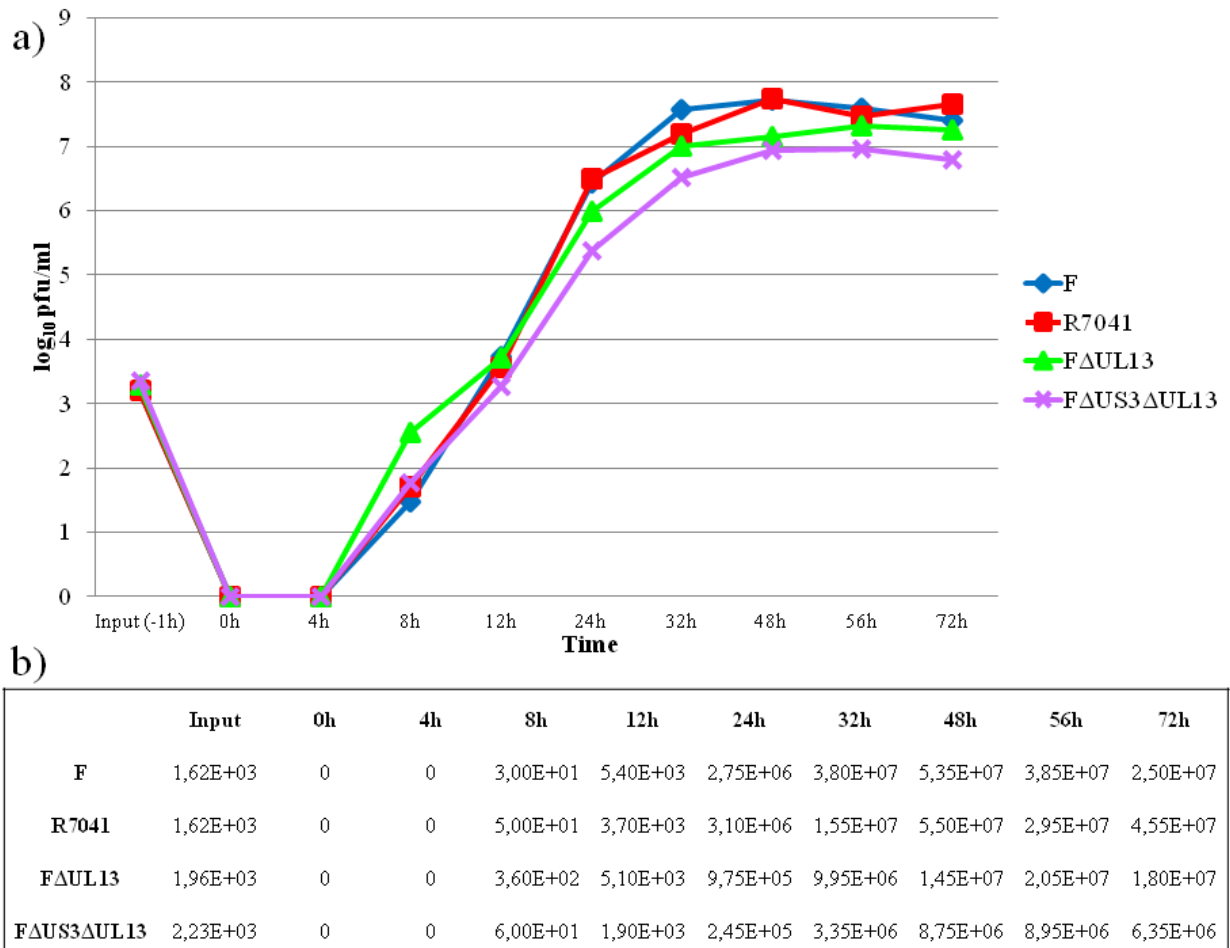


Fig. 2.5. Growth curves of recombinant viruses. a) Graph representing the viral load, expressed in \log_{10} of the p.f.u./ml, versus the time points analyzed, expressed in hours. b) Table reporting the number of p.f.u./ml scored at each time point.

To observe whether the lack of the viral protein kinases can lead to phenotype changes Vero cells were then infected with HSV-1 F or HSV-1 $\Delta UL13$ and/or $\Delta US3$ mutants as described above.

Consistent with the previous assay, plaques formed by the HSV-1 $\Delta UL13/\Delta US3$ mutant exhibit “small-plaque” phenotype as shown in figure 2.6

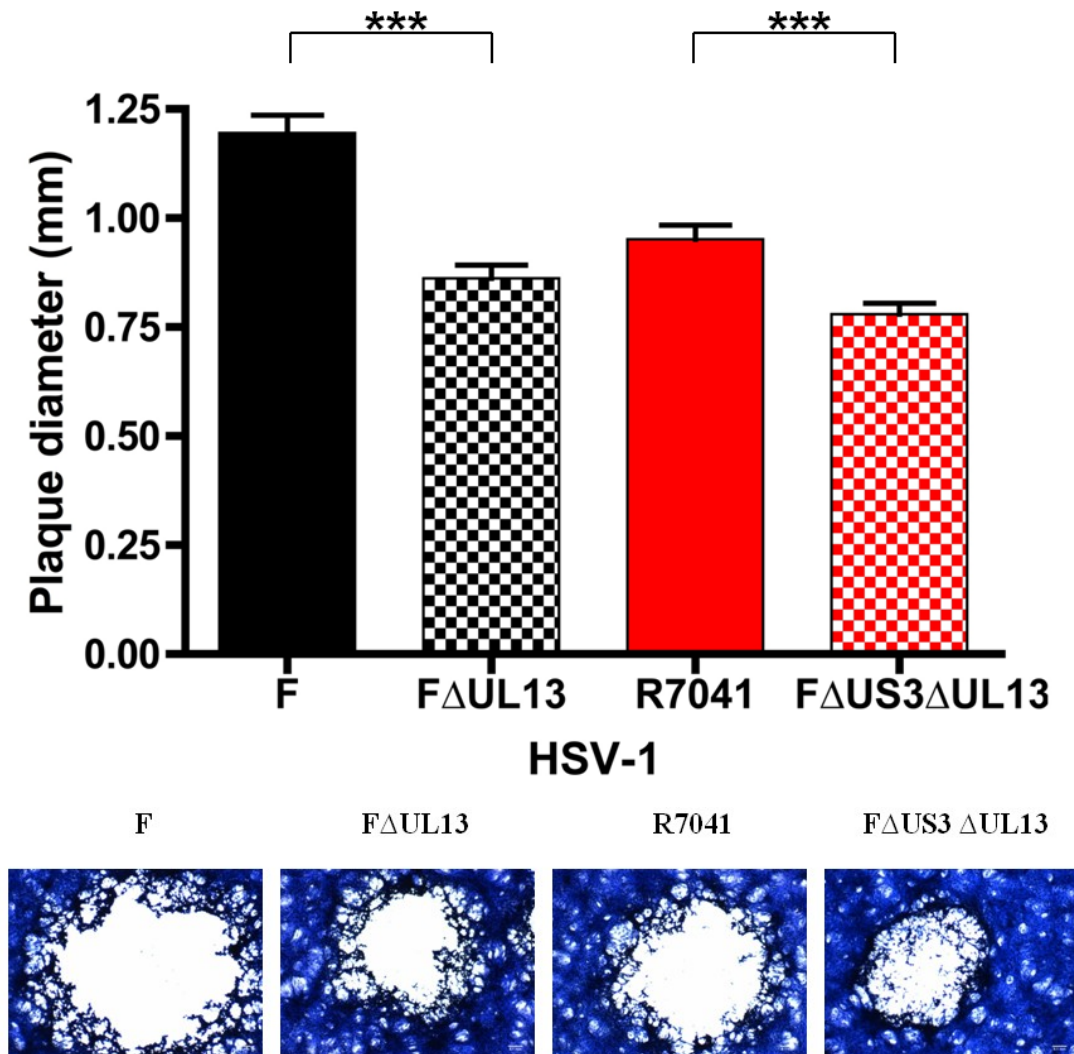


Fig. 2.6. Average diameters of viral plaques. The graph in the upper panel shows the mean of the diameter scores (expressed in mm) of viral plaques (n=30), measured for every virus. Student’s t test outcome a significant difference (p<0,0001) for both mutants deleted in UL13 compared with their relative backbone virus. In lower panel are reported representative pictures of plaques of each virus tested.

Together these results supported the hypothesis that these two protein kinases might act in a cooperative manner to support HSV-1 spread in Vero cells

2.3.3 Characterization of plasmid vectors expressing GFP-US3 and RFP-UL13

Meanwhile, when we constructed the viral mutants, two independent recombinant plasmids were generated expressing UL13 and US3 genes (Fig.2.7) in order to study the function of these protein kinases.

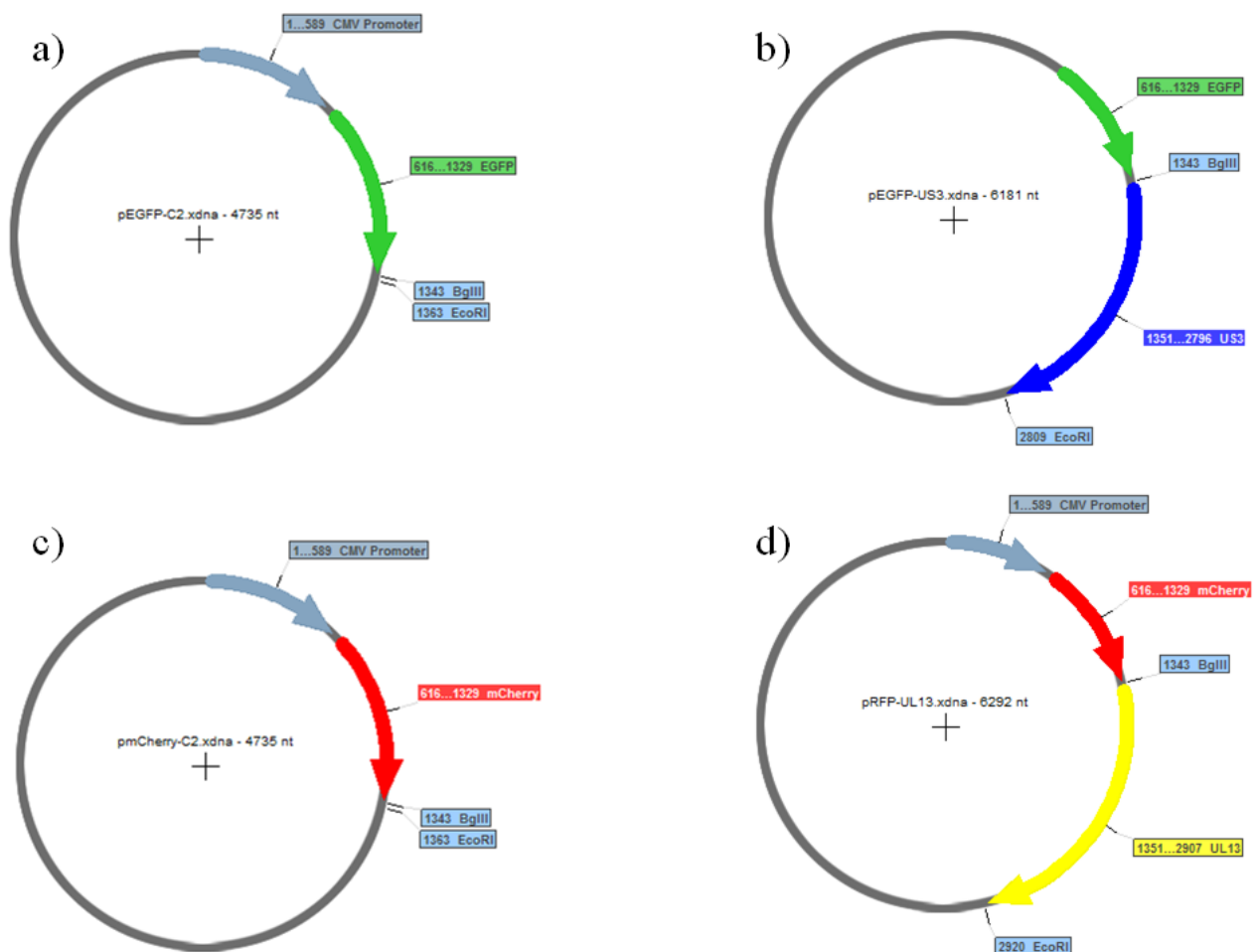


Fig. 2.7. Maps of the plasmid used to create fusion tag proteins GFP-US3 and RFP-UL13. They are evidenced the two restriction sites used for the cloning (BglIII and EcoRI), the sequences of the tags (EGFP in green and mCherry in Red) and those of the two viral kinases (US3 in blue and UL13 in yellow). a) Map of pEGFP-C2. b) Map of pEGFP-US3. c) Map of pmCherry-C2. d) Map of pRFP-UL13.

In order to check the correct expression of pEGFP-US3 and pRFP-UL13 plasmids that are expressing the viral kinases US3 and UL13 fused respectively to EGFP and mCherry, a red fluorescent protein, Vero (data not shown) and SH-SY5Y (Fig.2.8) cells were transfected with pEGFP-US3 or pRFP-UL13 and 24 hours post-transfection the samples were collected and processed for western blot. As negative control, cells were also transfected with backbone vectors pEGFP-C2 and pmCherry-C2.

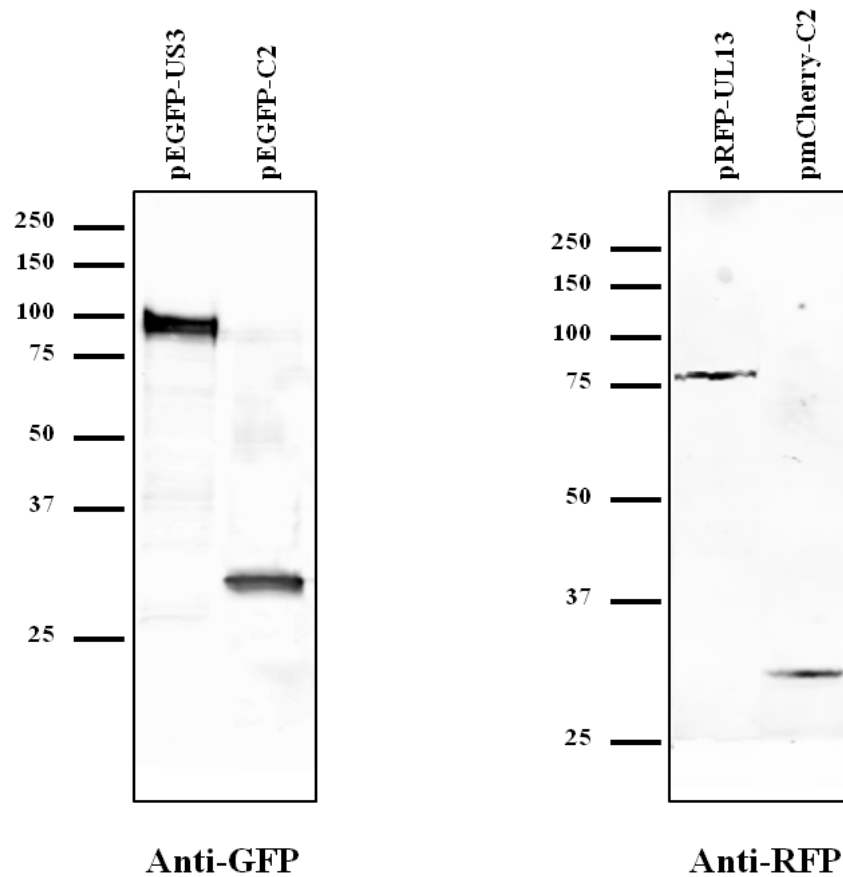


Fig. 2.8. Western blot for the characterization of the two plasmids pEGFP-US3 and pRFP-UL13. Right panel: staining with anti-GFP antibody of SH-SY5Y cells transfected with pEGFP-US3 (first lane) or pEGFP-C2 (second lane). Left panel: staining with anti-RFP antibody of SH-SY5Y cells transfected with pRFP-UL13 (first lane) or pmCherry-C2 (second lane).

The staining with an anti-GFP antibody, as shown in Fig. 2.8, revealed a band of approximately 95 kDa, while anti-RFP a band around 80 kDa respectively in samples transfected with pEGFP-US3 and pRFP-UL13. Given that the molecular weight of US3 is 68kDa [13], that of UL13 is 56kDa [14] and that of both GFP and RFP are approximately 27-30 kDa (as confirmed by the blot) the bands detected by the antibodies are related to the fusion proteins GFP-US3 and RFP-UL13.

2.3.4 Analysis of US3 and UL13 direct involvement in tau phosphorylation

To assess if the viral kinases US3 and UL13 may affect tau phosphorylation, western blot and immunofluorescence analysis were performed. SH-SY5Y cells were transfected with pEGFP-US3 and pRFP-UL13 or infected with 1 m.o.i. of F, R7041, FAUL13 and FAUS3ΔUL13 viruses. 24 hours post-infection/transfection the phosphorylation status of tau was tested using antibodies AT100 and anti-tau (pS202) directed against two phosphorylation dependent epitopes of the protein. In particular the first recognizes a specific region of PHF-associated tau in which is present phospho-serine 214, a potential phosphorylation site for US3, while the second detect tau when phosphorylated in serine 202, a possible target for UL13. As a control, blots were stained for β-tubulin. In figure 2.9, both transfected and infected samples show no significant differences compared to wild type infected sample. Moreover wild type virus doesn't seem to increase the signal of these two antibodies compared to mock infected cells (Fig 2.9).

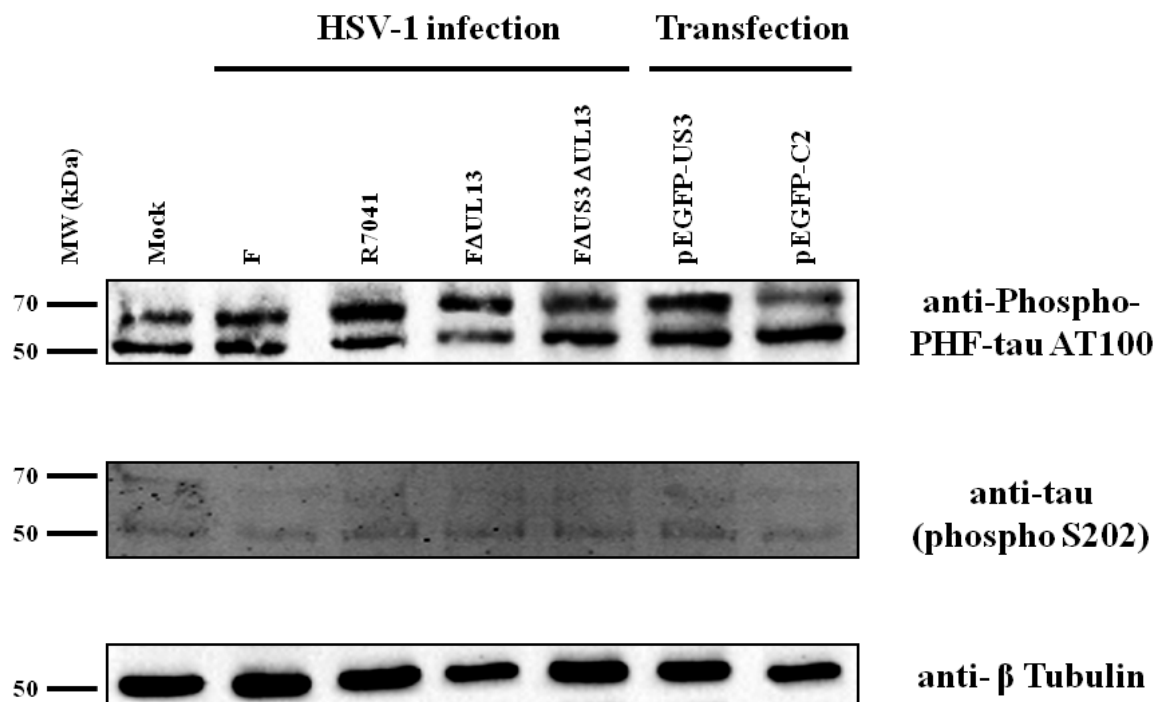


Fig. 2.9. Western blot of SH-SY5Y infected/transfected with the constructs to study the involvement of the viral kinases US3 and UL13 in tau phosphorylation. Lane 1 is the negative control; lanes 2-5 are samples infected with the virus indicated; lanes 6-7 are cells transfected with vectors for the expression of the two kinases. Upper panel represent the blot with anti-phospho tau AT100 antibody. Middle panel is the blot with anti-phospho tau Ser202. Lower panel is the staining of the same samples for β -tubulin as a control

This last observation was confirmed by immunofluorescence assay (Fig. 2.10). The staining for tau (pS202) was very hard to detect both in infected and uninfected cells, while with AT100 the signal was higher but almost equal independently of viral infection.

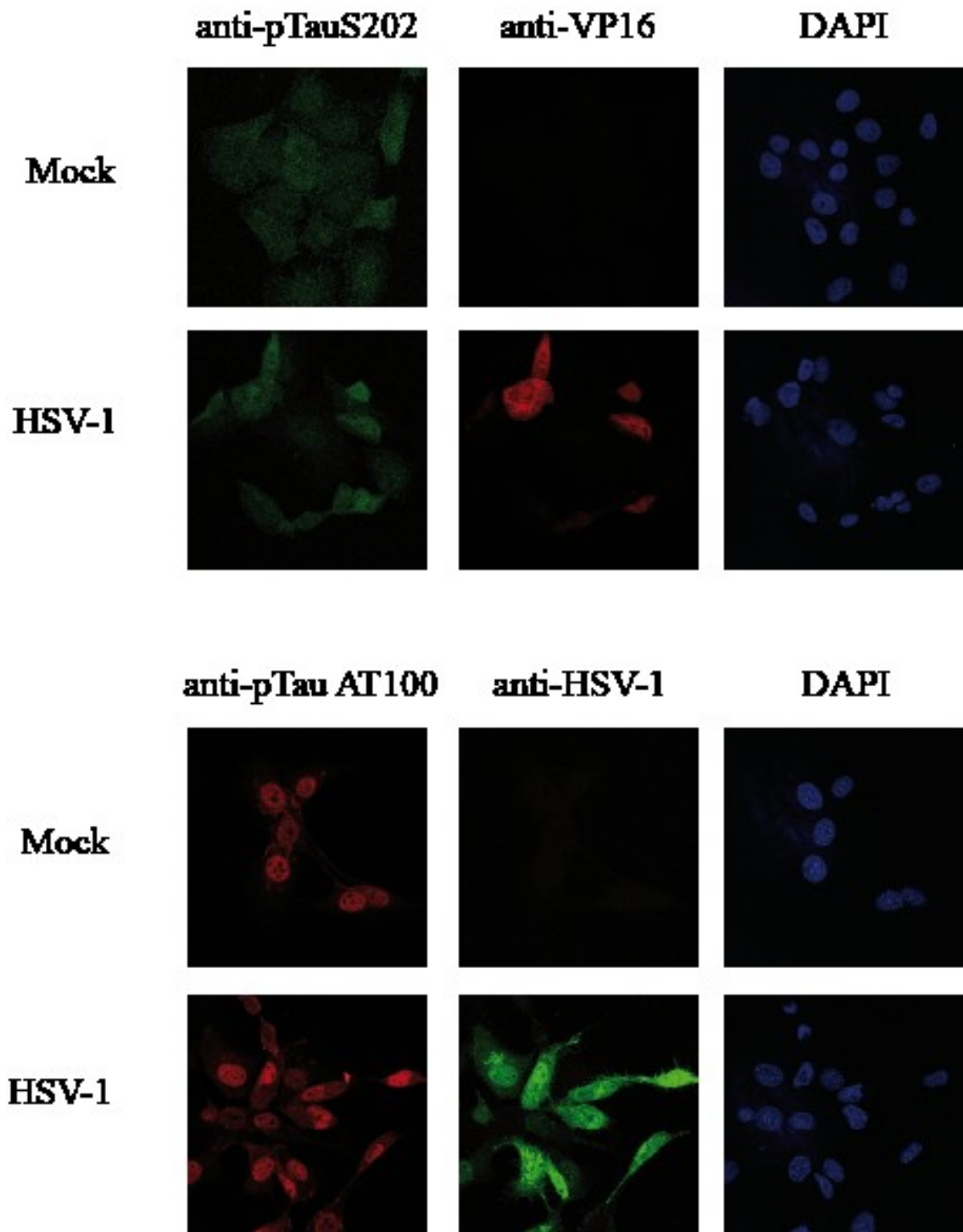


Fig. 2.10. Immunofluorescence for the detection of phospho-tau. Upper panel show the staining with the secondary antibodies Alexa Fluor 488-goat anti-rabbit IgG (green fluorescence) for phospho tau Ser202, lower panel, the staining with Alexa Fluor 568-conjugated goat anti-mouse IgG (red fluorescence) pAb against phospho tau AT100. Since there were no significant differences among all the samples tested, the figure shows only uninfected (first row of each panel) and HSV-1 wild type infected (second row of each panel) cells, as representative examples.

2.4 Discussion

To verify if viral kinases US3 and UL13 may have a role in tau phosphorylation, as suggested by the literature [4, 8], the constructs described in this chapter were generated. The mutant viruses lacking these genes were supposed to decrease the phosphorylation effect of HSV-1 on tau, while plasmid expressing the two kinases were supposed to increase this phenomenon, in case these are directly involved. As said above, it was chosen to analyse Ser202 and Ser214, because they are two of the sites possibly affected by these two kinases. However, in the system presented in this chapter, it was not possible to perform these evaluations because the antibodies used didn't reveal any changes in the phosphorylation status of tau after infection with viral mutants or wild type virus. This seems to be in contrast with the observation of Wozniak et al., who show a phosphorylation event in these two sites after viral infection [4]. Another contradictory results with their work, is that it was observed an immunofluorescent staining with AT100 also in uninfected cells, particularly in the nucleus, where it was demonstrated that this antibody recognise an epitope not related to tau [15].

We cannot however exclude the possibility that the virus can phosphorylate tau in different sites and that this effect may involve US3 and UL13. Indeed we just take a look at 2 out of 80 phosphorylation sites of tau protein, and the cellular kinases that potentially share a functional similarity with viral kinases affect many of them [9, 16]. Anyway the characterization of the constructs generated revealed their validity as a tool to study the role of the two viral kinases US3 and UL13, therefore it is planned to investigate if they can affect other phosphorylation sites of tau.

In further investigations it should be considered that the double mutant virus F Δ US3 Δ UL13 presents some defects in growth ability, thus an eventual decrease in tau phosphorylation may be due to a slower replication, rather than an the lacking of the two kinases. Therefore, further studies are needed to elucidate the mechanisms by which the HSV-1 UL13 and US3 protein kinases regulate viral replication and biologically relevant substrates. Interestingly HSV-1 has been found to phosphorylate tau at Ser396, Ser404 and Ser409 in neuroblastoma cells, and that this phosphorylated protein accumulate in the nucleus where it could play an important role for viral replication and/or transcription [3].

In order to elucidate this possible relation between HSV-1 and tau, the focus of the research was moved to the nuclear form of tau as detailed in the next chapter.

References

1. Hanger, D.P., et al., *Novel phosphorylation sites in tau from Alzheimer brain support a role for casein kinase 1 in disease pathogenesis*. J Biol Chem, 2007. **282**(32): p. 23645-54.
2. Tenreiro, S., K. Eckermann, and T.F. Outeiro, *Protein phosphorylation in neurodegeneration: friend or foe?* Front Mol Neurosci. **7**: p. 42.
3. Alvarez, G., et al., *Herpes simplex virus type 1 induces nuclear accumulation of hyperphosphorylated tau in neuronal cells*. J Neurosci Res. **90**(5): p. 1020-9.
4. Wozniak, M.A., A.L. Frost, and R.F. Itzhaki, *Alzheimer's disease-specific tau phosphorylation is induced by herpes simplex virus type 1*. J Alzheimers Dis, 2009. **16**(2): p. 341-50.
5. Roizman, B., Knipe D. M., *Herpes simplex viruses and their replication*. Fields virology, 4th ed. Lippincott-Williams &Wilkins, Philadelphia, Pa., 2001: p. 2399-2459.
6. Benetti, L. and B. Roizman, *Herpes simplex virus protein kinase US3 activates and functionally overlaps protein kinase A to block apoptosis*. Proc Natl Acad Sci U S A, 2004. **101**(25): p. 9411-6.
7. Tanaka, M., et al., *The role of protein kinase activity expressed by the UL13 gene of herpes simplex virus 1: the activity is not essential for optimal expression of UL41 and ICP0*. Virology, 2005. **341**(2): p. 301-12.
8. Ball, M.J., et al., *Intracerebral propagation of Alzheimer's disease: strengthening evidence of a herpes simplex virus etiology*. Alzheimers Dement. **9**(2): p. 169-75.
9. Pei, J.J., et al., *Up-regulation of cell division cycle (cdc) 2 kinase in neurons with early stage Alzheimer's disease neurofibrillary degeneration*. Acta Neuropathol, 2002. **104**(4): p. 369-76.
10. Jicha, G.A., et al., *cAMP-dependent protein kinase phosphorylations on tau in Alzheimer's disease*. J Neurosci, 1999. **19**(17): p. 7486-94.
11. Cunningham, C. and A.J. Davison, *A cosmid-based system for constructing mutants of herpes simplex virus type 1*. Virology, 1993. **197**(1): p. 116-24.
12. Longnecker, R. and B. Roizman, *Clustering of genes dispensable for growth in culture in the S component of the HSV-1 genome*. Science, 1987. **236**(4801): p. 573-6.
13. Frame, M.C., et al., *Identification of the herpes simplex virus protein kinase as the product of viral gene US3*. J Gen Virol, 1987. **68 (Pt 10)**: p. 2699-704.
14. Roizman, B. and G. Campadelli-Fiume, *Alphaherpes viral genes and their functions*. 2007.
15. Whiteman, I.T., et al., *Rapid changes in phospho-MAP/tau epitopes during neuronal stress: cofilin-actin rods primarily recruit microtubule binding domain epitopes*. PLoS One. **6**(6): p. e20878.
16. Duka, V., et al., *Identification of the sites of tau hyperphosphorylation and activation of tau kinases in synucleinopathies and Alzheimer's diseases*. PLoS One. **8**(9): p. e75025.

3. HSV-1 and Nuclear Tau

3.1 Introduction

Tau is a low molecular weight protein expressed in higher eukaryotes in both neuronal and non-neuronal cells, but prevalently in neurons [1-4].

Although tau was originally found associated to microtubules, this protein, as well as other eukaryotic proteins, displays a wide functional diversity and different cellular compartments have been described to host this protein, such as dendrites, ribosomes, plasma membrane and nucleus. In this last compartment an unphosphorylated tau, at residues 189-207 [4-9], has been found to be present mainly in neuronal cells but also in non-neuronal cells [6]. The function of this protein inside the nucleus is not yet fully understood, anyway it has been observed that in normal condition is associated with the nucleolar organizer regions and it has been suggested that Tau plays a role in the nucleolar organization and/or heterochromatinization of rRNA genes [8]. In addition tau has been observed to bind DNA [6] [10], and to protect neuronal genome from heat and acute oxidative stress damage [7].

The nucleolus is the largest nuclear compartment of eukaryotic cell, formed around specific loci of acrocentric chromosomes, named nucleolar organizing regions (NORs). The main task of nucleolus is ribosome synthesis and assembly, and it plays an important role in cell-cycle control, stress sensing and senescence, as well as in viral infection [11].

The presence of tau in the nucleolus and its partial colocalization with nucleolin, one of the most abundant nucleolar proteins, has been confirmed by different studies. Nuclear and nucleolar tau are detected mainly by Tau-1 antibody that recognises tau when dephosphorylated at serine 195, 198, 199 and 202 [4-9]. The phosphorylates sites on Tau could play a dual role by enhancing nuclear translocation exclusively in their dephosphorylated state and in promoting cytoplasmic localization when phosphorylated. A possible role of this nuclear form of the protein in neurodegeneration is still under debate and the major hypothesis is that pathological alterations of Tau, e.g. hyperphosphorylation, might impair its ability to shuttle between the cytoplasm and the nucleus and/or affect its affinity for DNA. Altered forms of tau can act also as a trigger for tau aggregation and consequent neurodegeneration [4], representing an essential mechanism of AD etiopathogenesis. In recent years nuclear tau has gained a great interest in AD research and since several viral

functions such as transcription, DNA replication, assembly of new capsids and packaging of DNA occur in the host cell nucleus, it is worth to investigate if HSV-1 may alter this particular form of tau. After the initial observation of HSV-1 DNA in AD brains [12, 13], several authors investigated if the virus may perturb protein tau physiology, paying particular attention to its phosphorylation state [14-16]. As it has been described previously, hyperphosphorylated tau is the main component of the AD hallmarks NFTs, a high insoluble protein deposit. A possible interference of HSV-1 with nuclear tau stems from different observations. First, the virus induces oxidative stress [17], a type of injury to which neurons respond by recruiting tau in the nucleus [7]. Second HSV-1 induces chromatin relaxation, by promoting histone acetylation, and tau was found to bind DNA in a similar manner to histones [10]. The acetylation of histones, the nuclear proteins around which DNA is packaged in structures named nucleosomes, promotes the removal of DNA that became more accessible for transcription. This is valid not only for cellular DNA but also for the viral genome that is tightly packaged in nucleosomes during latency, while during lytic infection releases itself thanks also to histone acetylation [18]. Third HSV-1 is known to induce nucleolar alteration, manipulating the cell cycle, and among the viral proteins reported to localize inside the nucleolus, the tegument protein US11 has been found to physically interact with nucleolin and this interaction is fundamental for the egress of HSV-1 nucleocapsid [19]. Since tau was observed to colocalize with nucleolin [6] it is likely that US11 may compete with tau for the binding to this protein.

Therefore, to investigate a possible correlation between HSV-1 and nuclear tau, Western blot and Immunofluorescence analysis were done using Tau-1 antibody that stains for the isoform of tau, when is dephosphorylated at serine 195, 198, 199 and 202.

The first experiments were performed in different cell lines, with epithelial or neuronal phenotype, in order to study how viral infection can affect nuclear tau cellular distribution and to identify HSV-1 genes involved in this mechanism. At this regard we tried to assess if the viral protein US11 can interact with tau.

A second set of experiments, were done in primary neurons of newborn 3xTG mice, which is the model that most closely mimics human AD hallmarks. Tau levels were evaluated with Tau-1 antibody in cellular explant at day 5 and 12, respectively, after 24 hours of infection, in order to observe if HSV-1 may anticipate the outcome of the pathological phenotype and/or its worsening.

3.2 Material and methods

3.2.1 Cells

Vero cells, epithelial cells from kidney of adult African green monkey (ATCC), were grown in Dulbecco's minimal essential medium (DMEM) containing 100 U/ml penicillin, 100 µg/ml streptomycin, 2mM L-glutamine and 10% heat-inactivated fetal calf serum (FCS), and were used to the preparation of viral stocks as described below.

SH-SY5Y cells, human neuroblastoma (ATCC), were grown in a mixture 1:1 of Eagle's minimal essential medium and nutrient F12 Ham (EMEM-F12) supplemented with 100 U/ml penicillin, 100 µg/ml streptomycin, 2mM L-glutamine and 15% FCS. Cultures were maintained at 37°C in 5% CO₂ atmosphere. 24 hours prior to infection or transfection cells were seeded at a concentration of $2 \cdot 10^4$ cells per well in a 24-well plate for immunofluorescence assay and $5 \cdot 10^5$ per well in a 6-well plate for western blot.

3.2.2 Animals and neuronal cultures

Primary cortical neurons were prepared from newborn 3xTG mice as previously described [20]. Briefly, cerebral cortices were removed and dissociated by mild trypsinization at 37°C, followed by trituration in a DNase solution (0.005% w/v) containing a soybean trypsin inhibitor (0.05% w/v). The cells were resuspended in DMEM supplemented with p-amino benzoate, insulin, penicillin and 10% foetal calf serum. The cell suspension was seeded in 12mm or 24mm glass coverslips precoated with poly-D-lysine and incubated in respectively 24 or 6 multiwell plates for 5–12 days in vitro (DIV) in a humidified 5% CO₂/95% air atmosphere at 37°C. Cytosine arabinoside, 2 M was added before 48 h in culture to prevent glial proliferation.

Cortical neurons were then infected, as described below, at DIV 4 and 11.

3.2.3 Infection

The viruses used were a HSV-1 wild type strain F, FΔUS11 and T0Z.

FΔUS11 is a US11-negative mutant kindly provided by I. Mohr and previously described [21] T0Z is a non-replicating virus with a deletion in ICP4, ICP27, ICP22 and in UL41, previously described [22].

Cells were infected with a HSV-1 f wild type strain with a multiplicity of infection (m.o.i.) of 1 plaque forming unit (p.f.u.) per cell. Viral particles were diluted in culture medium and

added to cell monolayer, after 1 hour at 37°C, the viral inoculum was removed and replaced with fresh medium.

At the time points indicated in the results, i. e. 8 or 24 hours post-infection (hpi), samples were collected for immunofluorescence and western blot analysis.

3.2.4 Transfections

pUS11, a plasmid expressing the 149 aa of full length US11 under the control of the CMV promoter, was a kind gift of prof. A. Greco, for details in its sequence see [19].

0µl of Lipofectamine reagent (Invitrogen, Carlsbad, CA, USA) were added in 50µl of Optimem medium (Gibco) and 2µg of pUS11, were added in 50µl of Optimem medium (Gibco). The two solutions were left separated for 5 minutes and then mixed. After 20 minutes, 100µl of the mix were added to cells. 24 hours post-transfection cells were subjected to immunofluorescence assay.

3.2.5 Drugs

Drugs added to culture medium to induce chromatin relaxation and their relative concentration were: 100µM 2-Hydroxy-4-[[[(4-methylphenyl)sulfonyl]oxy]acetyl]amino]-benzoic acid, a STAT 3 inhibitor; 500µM N-(4-Chloro-3-trifluoromethyl-phenyl)-2-ethoxybenzamide (CTB), an activator of Histone acetyltransferase p300/CBP; 1µM Thricostatin A, a broad-spectrum inhibitor of histone deacetylase (SML0330, C6499, T1952, Sigma-Aldrich, St. Louis, MO, USA). 24 hours post treatment cells were analysed by immunofluorescence.

To inhibit viral DNA synthesis, together with virus 100µM ganciclovir (GCV) (G2536, Sigma-Aldrich) was added to culture medium.

3.2.6 Immunofluorescence

Cells were fixed in 4% paraformaldehyde (PFA) in phosphate-buffered saline (PBS) for 20 minutes, permeabilized in 0,1% Triton X-100 in PBS, blocked for 1 hour in PBS containing 3% bovine serum albumin (BSA) and 2% normal goat serum (NGS) and labelled for 1 hour with primary antibodies mouse anti-Tau1 clone PC1C6 (MAB3420, Merck Millipore); mouse anti ICP0 (5H7) (ab6513, Abcam); rabbit anti-HSV-1 (ab9533, Abcam); polyclonal rabbit anti US11 previously produced in prof. Marconi's laboratory. After washing in PBS cells were incubated with the secondary antibodies Alexa Fluor 488-goat anti-rabbit IgG and Alexa Fluor 568-conjugated goat anti-mouse IgG pAb (Invitrogen, Carlsbad, CA, USA) diluted

1:1000 for 1 hour in the dark. Finally cells samples were mounted with ProLong® Gold Antifade Mountant (Invitrogen) containing DAPI (4',6-diamidino-2-phenylindole) to stain nuclei.

Fluorescence was visualized using mainly a Nikon eclipse TE 2000-S fluorescent microscope and for some samples, images were collected with a Leica SP5 confocal microscope and analyzed with ImageJ software.

3.2.7 Western Blot

Cells were harvested and resuspended in lysis buffer (10mM tris pH 7.6, 150mM NaCl, 5mM EDTA, 10% Glycerol, 1% Triton X100, 1mM Na₃VO₄, 1mM NaF, 1mM PMSF, Protease inhibitor mix (Roche)) and boiled for 8 minutes. Samples were analyzed via 12% sodium dodecyl sulfate-polyacrylamide gel electrophoresis (SDS-PAGE). Proteins were then transferred to nitrocellulose membranes, that were blocked with PBS with 0,1% Tween 20 and 5% BSA, before being incubated for 1 hour with primary antibodies mouse anti-Tau1 clone PC1C6, 1:500 (MAB3420, Merck Millipore) and mouse anti-class III β -tubulin, 1:1000 (TUJ1, Covance). After washing with PBS Tween 0,1%, with secondary antibodies goat anti-mouse IgG horseradish peroxidase-linked (GE Healthcare, Little Chalfont, UK). Immunocomplexes were detected by ECL detection kit (Thermo scientific, Waltham, USA). Membranes were stripped between antibodies by incubation in Restore Western blot stripping buffer (21059, Thermo scientific)

3.3 Results

3.3.1 HSV-1 increases and relocalizes nuclear Tau in epithelial and neuroblastoma infected cells

Tau's localisation within the nucleus is particularly interesting, considering the importance of the nucleus in cellular processes. It may be important therefore to make a distinction between the nuclear tau ubiquitously distributed within the nucleus and tau predominantly localised to the nucleolus. The difference in its nuclear distribution could assign different roles for the protein in neuronal physiology and pathology. Localization of tau in the nucleolus could play a role in rRNA gene silencing and as a potential regulator of rDNA stability. Vero, HRPE and SH-SY5Y cell lines, were infected with a multiplicity of infection (m. o. i.) of 1 plaque forming unit (pfu) per cell. After 24 hours, infected and uninfected, samples were collected and processed for Western blot and Immunofluorescence assay as described in material and methods. Immunoblots showed a marked increase of Tau-1 staining, in infected compared to uninfected samples (Fig. 3.1).

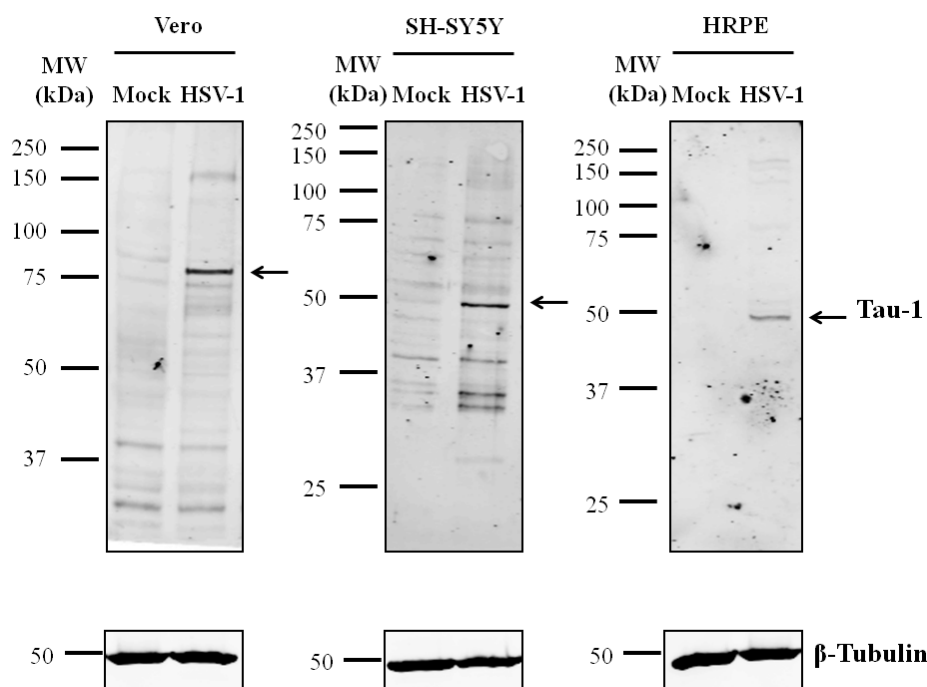


Fig. 3.1. Western blot showing the marked increase of nuclear tau in infected cells 24 hpi. Tau-1 staining (upper panels) in HSV-1 infected cells marked a strong increase for a band at ≈ 80 kDa in Vero cells (left panel) and at 50 kDa in SH-SY5Y and HRPE (respectively middle and right panel). Staining for β -tubulin (bottom panels) revealed the same amount of total proteins for both mock and HSV-1 infected samples.

The different molecular weight, 80KDa for Vero and 50 KDa for HRPE and SH-SY5Y, might be simply related to a specific expression of the protein in the different cell lines (Fig. 3.1). Immunofluorescence assay, with a double staining for the monoclonal antibody anti-Tau-1 (red) and a polyclonal antibody anti-HSV-1 (green) confirmed that the increase of tau occur only in infected cells. In figure 3.2 we can observe that tau was clustered as small dots confined to the nucleoli in non-infected cells, whereas in infected cells it appeared as larger strongly fluorescing spots dispersed in the whole nucleus after 24 hours post infection (Fig. 3.2 and 3.3).

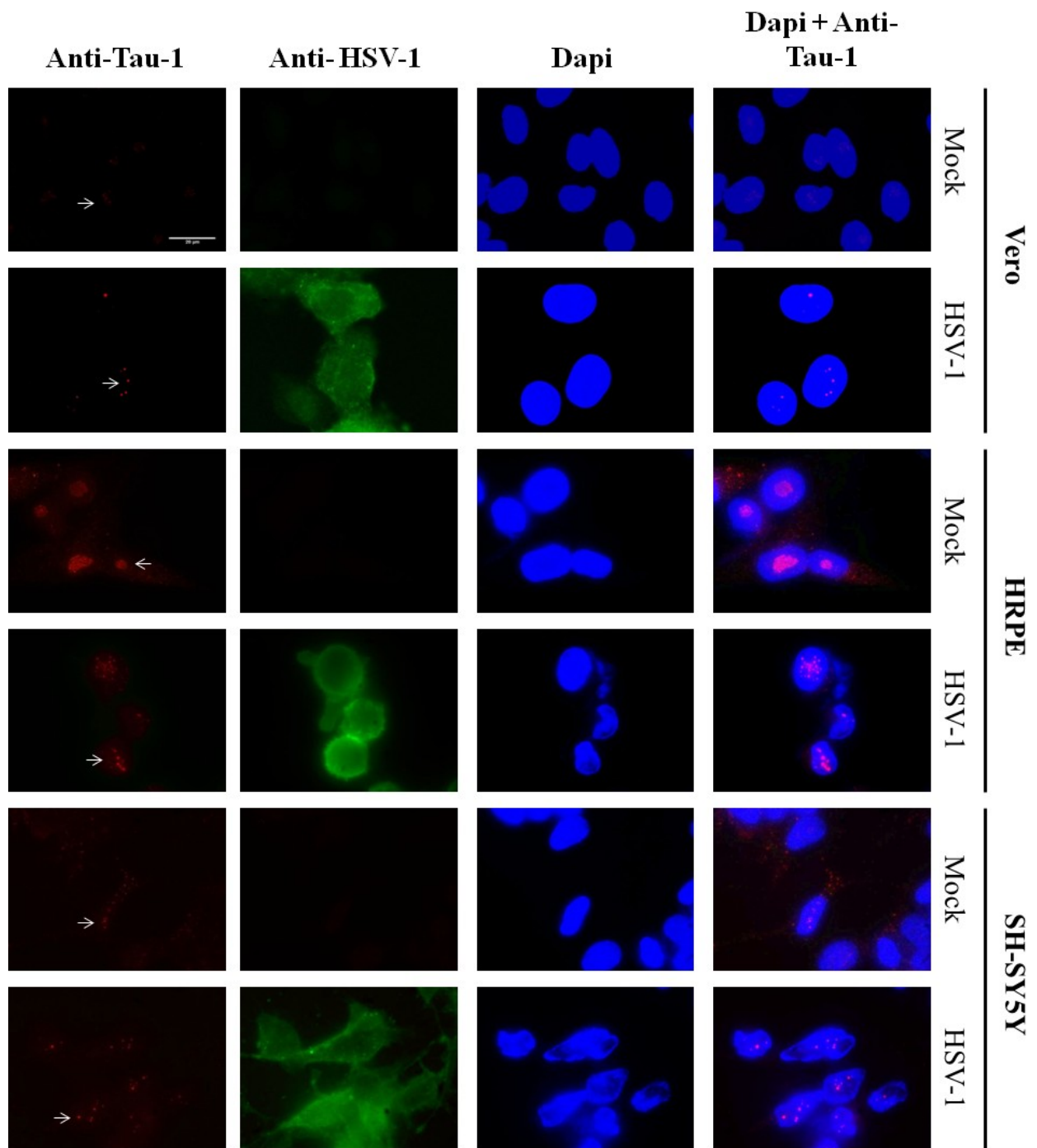


Fig. 3.2. Fluorescence microscope images of immunofluorescence assay performed with Tau-1 (red fluorescence) and HSV-1 antibody (green fluorescence) showing the redistribution of nuclear tau 24 hpi. In all cell line, i. e. Vero, SH-SY5Y and HRPE, immunofluorescent staining with Tau-1 antibody (first column) and Dapi (third column) detect tau in the nucleus as shown by merging these two channel (fourth column). In mock infected cells tau (red) is present in small dots clustered in nucleolar areas, while in HSV-1 infected cells tau forms big aggregates dispersed all over the nucleus, as indicated by the white arrows. The presence of the virus in infected samples is checked with a polyclonal antibody anti-HSV-1 (green) (second column). The nuclei are revealed with Dapi.

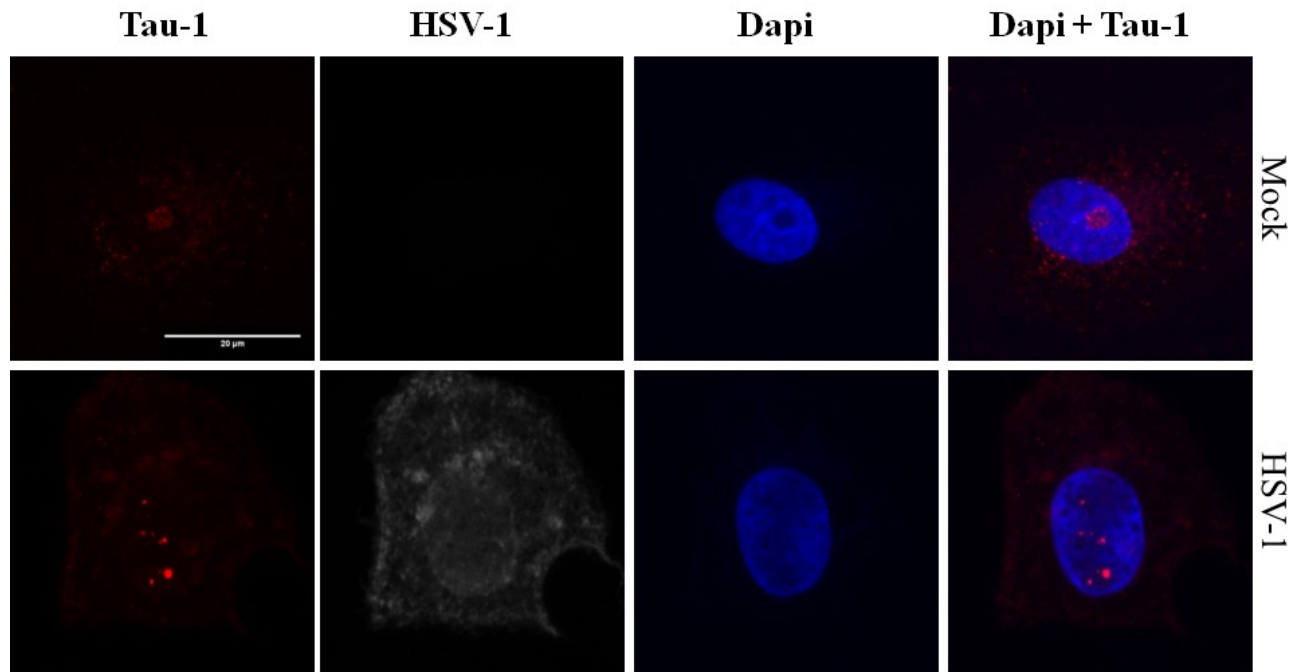


Fig. 3.3 Confocal microscope images of immunofluorescence assay performed with Tau-1 and HSV-1 antibody showing the redistribution of nuclear tau 24 hpi. Detail of two single Vero cells, mock and infected, marked for Tau-1 (first column) and HSV-1 (second column). Confocal microscope allows a more detailed observation of the Dapi stained nucleus (third column). The combination of Dapi and Tau-1 channel (fourth column) confirm that nuclear tau is mainly located to the nucleolus in uninfected cells and it spread throughout the nucleus 24hpi.

3.3.2 The nucleolar viral protein US11 does not cause the redistribution of nuclear tau outside the nucleolus

The observation that tau exit the nucleolus during viral infection, lead to suggest that this may happen for a competition with some viral product for the use of this nucleolar compartment. Therefore, the viral protein US11, which has been found to localize inside the nucleolus and to physically interact with nucleolin after 8 hours post infection [19], can be the viral component that competes with tau for the binding to this protein. To test this hypothesis, cells were infected with wild-type HSV-1 and with the HSV-1 Δ US11 mutant deleted on US11 and double stained for Tau-1 and an antibody anti-US11. In Vero cells 8 hours post infection US11 (green) is visible inside nucleoli and in the cytoplasm, while Tau appears aggregated in other areas of the nucleus but not in the nucleolus (Fig. 3.4).

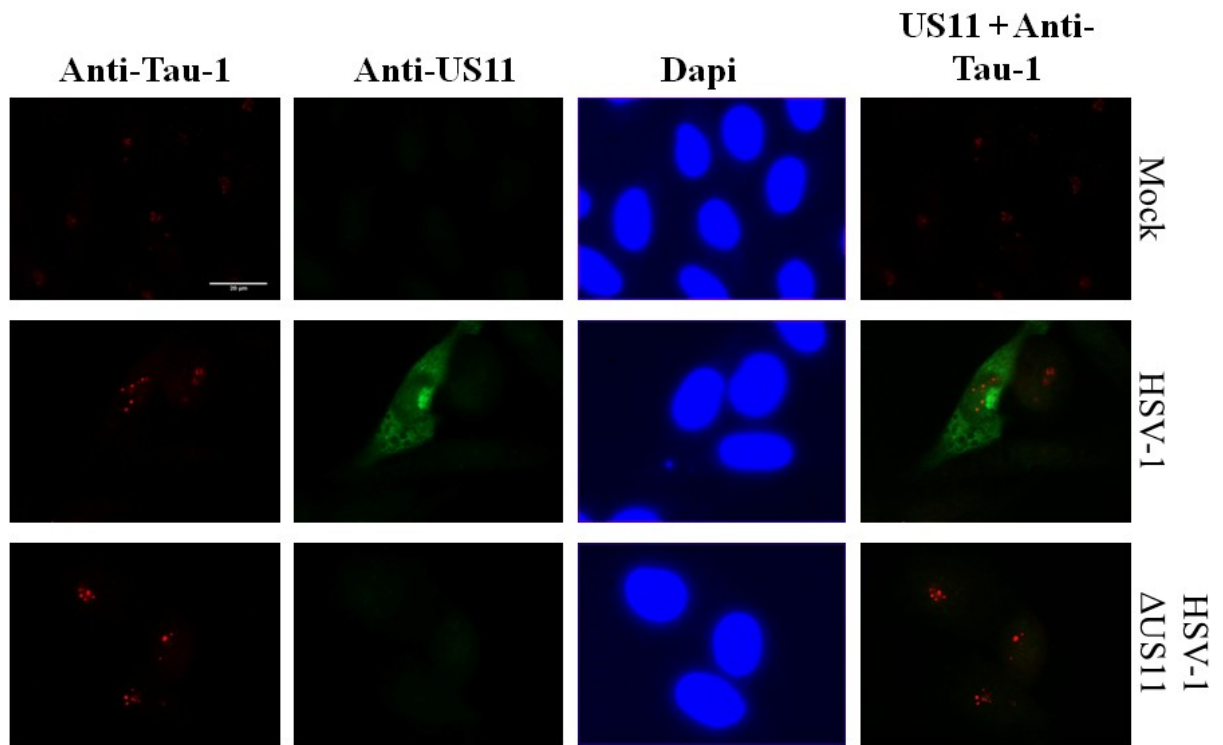


Fig. 3.4. The deletion of US11 doesn't affect the redistribution of tau during infection. Vero cells were infected with a HSV-1 wild type or Δ US11 and 8 h.p.i the distribution of tau was evaluated. The staining of with Tau-1 antibody (red, first column) revealed that in cells infected with the wild type (second row) or with the mutant virus (third row) tau is dispersed in the nucleus and is not confined to the nucleolus like in uninfected cells (first row). The expression of US11 was checked by staining with a polyclonal antibody (second column) and revealed a distribution of the protein both in the cytoplasm and in the nucleolus only for the wild type virus, as expected. Combining the signal of the two antibodies (fourth column) it was observed the relative localization of the two proteins.

To test if US11 alone was sufficient to provoke the egress of tau from the nucleolus, Vero cells were transfected with a US11 expressing plasmid and infected with wild-type HSV-1 and with the HSV-1 Δ US11 mutant. After 24 hours post transfection or infection, US11 was well expressed in transfected cells and it was distributed both in the cytoplasm and in the nucleolus, instead tau was entirely localized in the nucleolus like in non-transfected cells (Fig. 3.5). Moreover, after 24 hours post-infection with a mutant HSV-1 depleted for US11 or HSV-1 wild-type, the virus retains the ability to modify nuclear tau amount and distribution (Fig.3.5).

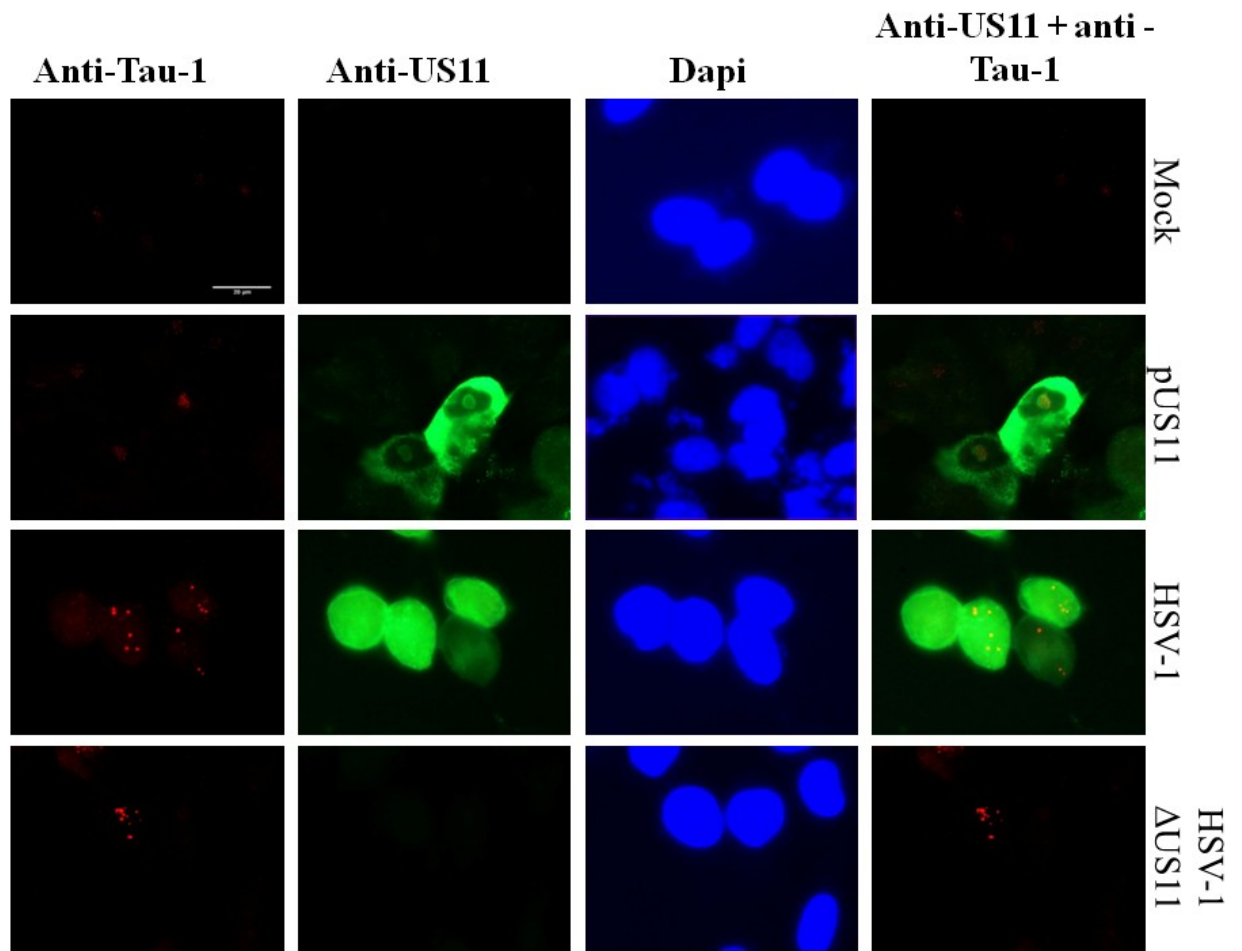


Fig. 3.5. The expression of the single protein US11 doesn't induce nuclear redistribution of tau. Cells were transfected with pUS11 (second row) and 24 hours post transfection the localization of tau detected by tau-1 (first column) was compared with uninfected cells (first row) and cells infected at the same time with HSV-1 wild type or Δ US11 (respectively third and fourth row). Tau doesn't exit the nucleolus in pUS11-transfected cells, like in untreated cells, contrarily to infected cells with both viruses. Expression of US11 was checked with a polyclonal antibody (second column) that revealed a nucleolar and cytoplasmic distribution of the protein in transfected cells, and a cytoplasmic and nuclear localization after 24 hours post infection. Combining the signal of the two antibodies (fourth column) it was observed the relative localization of the two proteins.

Therefore we can conclude that changes in nucleolar tau are not depending on Us11 but several other viral proteins, perhaps among those able to usurp the nucleolus, might be directly involved in this phenomenon. In prior studies, several HSV-1 proteins (ICP0, ICP4, ICP27, ICP34.5, UL12, UL24 and US11) were reported to associate with the nucleolus, in some cases causing nucleolar reorganization or redistribution of nucleolar components. Therefore, before to identify these viral players we focused our attention to demonstrate if these tau changes are linked to the viral lytic cycle and to the ability of tau to bind DNA.

3.3.3 Alterations in nuclear tau doesn't seem to be related to viral replication

Due to tau's ability to bind DNA in a histone-like manner, to correlate the delocalization of nucleolar tau with chromatin relaxation, uninfected Vero cells were treated with a combination of drugs: Thricostatin A, CTB and NSC74859 that are, respectively, a potent pan histone deacetylase inhibitor, an activator of the histone acetyltransferase p300/CBP and an inhibitor of STAT3 transcriptional factor [23]. After 24 hours, treated cells show tau aggregated in dots bigger than untreated cells, and they were dispersed all over the nucleus instead of being restricted only to the nucleolus proving a similar behaviour to cells infected with wild-type virus (Fig. 3.6). These data strongly suggest that an increase of nuclear tau and its relocalization is related to a more relaxed conformation of chromatin, condition that promotes the lytic cycle of the virus, and thus its replication.

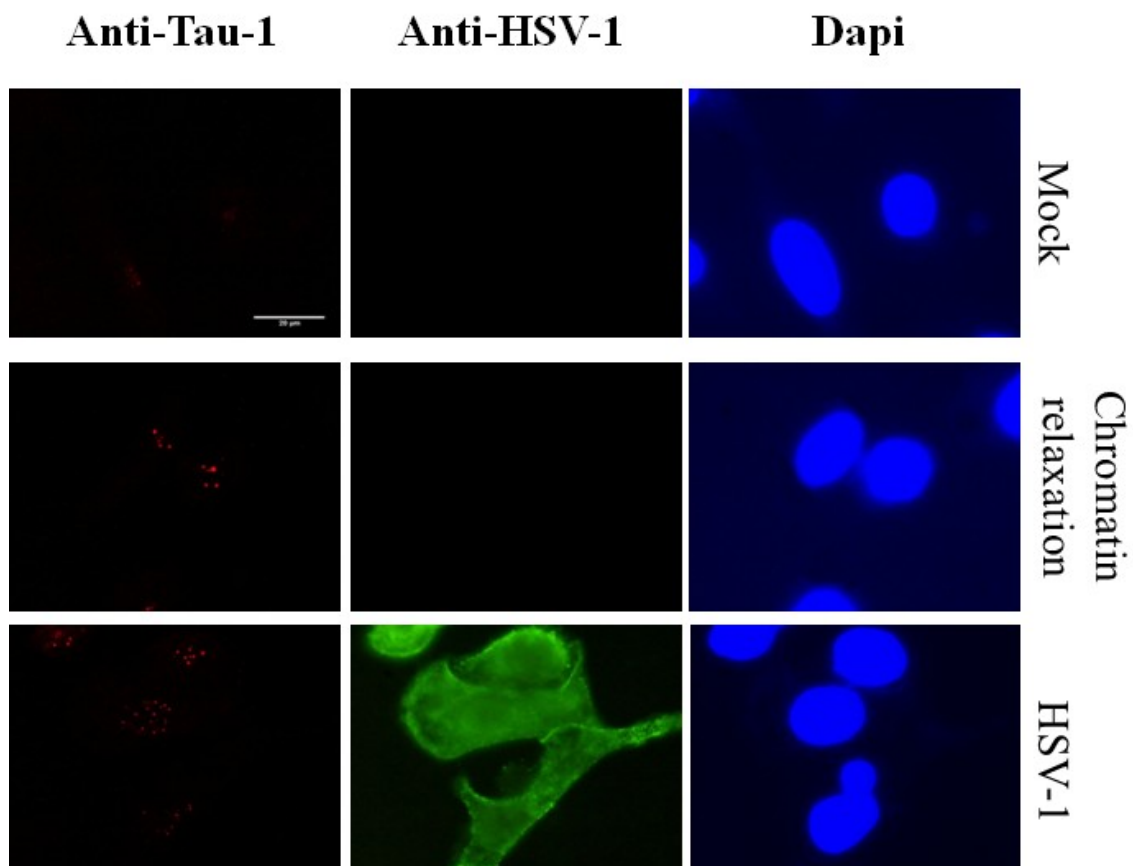


Fig. 3.6. Immunofluorescent evidence of the redistribution of nuclear tau in Vero cells 24 hours after a treatment to induce chromatin relaxation. Tau-1 staining (first column) in Vero treated with drugs, i.e. TSA, CTB and STAT3 inhibitor, that promote histone acetylation (second row) shows a pattern of distribution of nuclear tau similar to infected cells (third row). HSV-1 staining (second column) confirms that these cells are not infected.

Therefore to test if nuclear tau increases and aggregates in other nuclear regions than nucleolus occurs only during lytic infection, when chromatin is more dynamic, we did two types of infection without viral replication. The first employ T0Z, a mutant HSV-1 lacking three genes: infected cell polypeptides (ICP) 4, 27 and 22. These genes, together with ICP0 and ICP47, belong to the family of IE genes, those that are primarily expressed during viral infection, and that regulate its progression. The absence of these genes allows the virus to infect cells, but it cannot start viral transcription and replication unless it is in a complementing cell line [22]. The second model, cells were infected with a wild type virus in a medium containing ganciclovir (GCV), the antiviral drug whose mechanism of action is to block viral DNA replication but not the initial viral genes expression [24]. In these experiments we analysed the expression of an immediate early gene (ICP0) and of a true late gene (US11) whose expression are respectively independent and dependent by viral DNA synthesis [25].

Vero cells were infected with T0Z the HSV-1 mutant described above. After 24 hours of infection, immunofluorescence analysis with Tau-1 staining antibody, revealed no differences between infected and uninfected cells, highlighting that in T0Z mutant the absence not only of viral replication but also viral transcription, due to the deletion of IE genes, can have a crucial role in expression and relocation of nuclear tau during infection (Fig. 3.7).

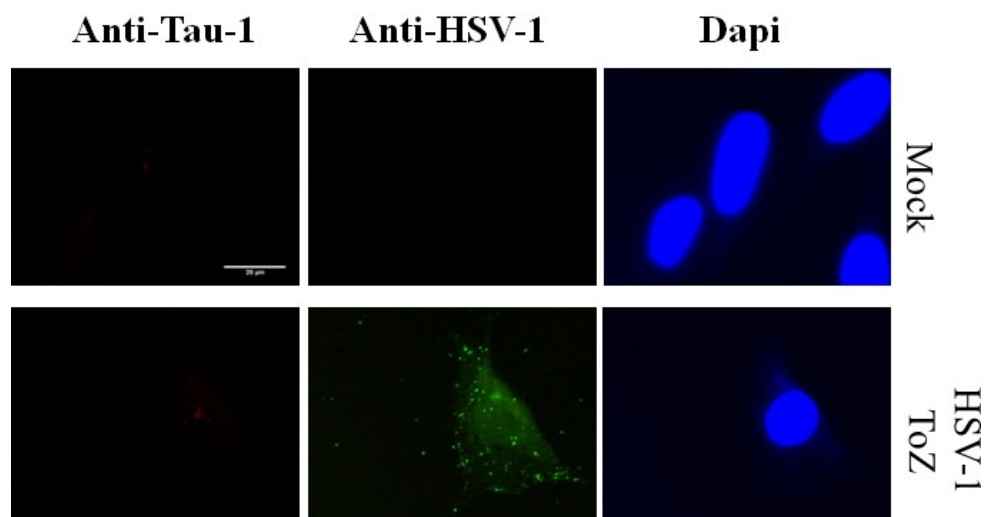


Fig.3.7. Immunofluorescence analysis of nuclear tau distribution 24hpi with ToZ, a triple mutant replication defective virus. Tau-1 staining (first column) revealed a similar distribution for mock (first row) and ToZ (second row) infected cells. HSV-1 staining (second column) confirms the presence of HSV-1 only in infected cells.

In the second experimental system infection without viral replication, Vero were infected with a HSV-1 wild type virus in the presence or absence of the antiviral drug ganciclovir (GCV), in order to block viral DNA synthesis. Opposed to the first experiment, 24 hours post infection, nuclear tau appeared in small dots dispersed in various area of the nucleus independently on the presence of GCV (Fig.3.8).

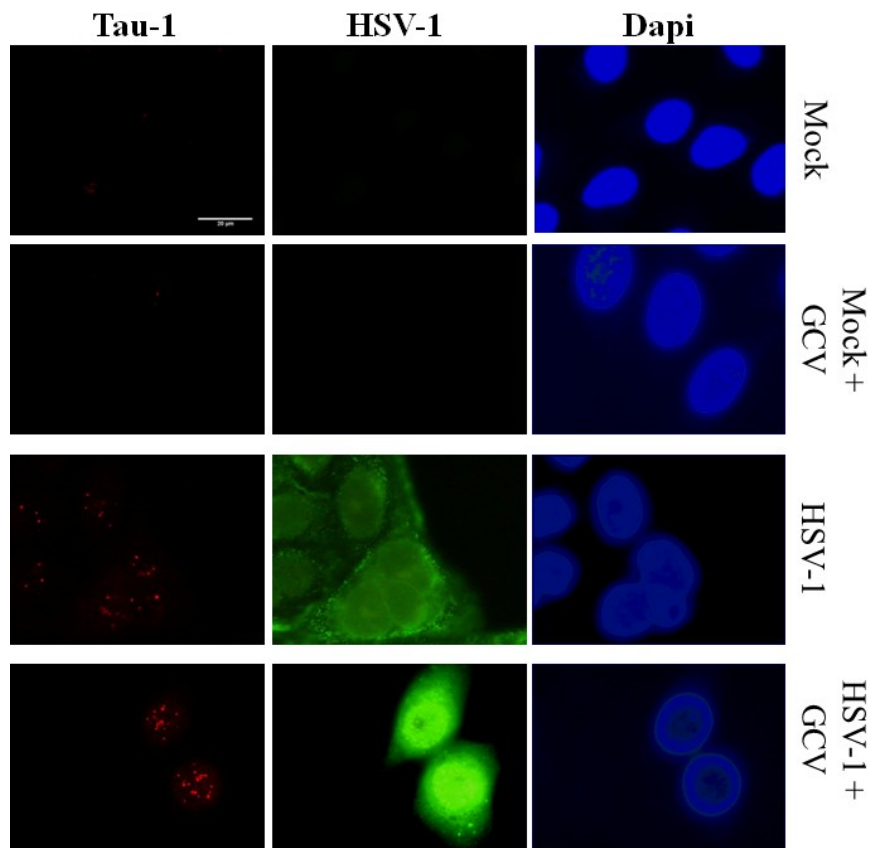


Fig. 3.8. Immunofluorescence analysis of nuclear tau (red) localization in HSV-1 (green) wild type infected or uninfected cells, in the presence or absence of the inhibitor of viral DNA synthesis GCV. Tau-1 antibody (first column) detect tau in the nucleolus of uninfected cells (first and second raw) and dispersed through the whole nucleus in infected cells (third and fourth raw) both in presence (second and fourth raw) or absence (first and third raw) of the antiviral drug GCV, that blocks viral DNA replication.

To verify that GCV was efficient in inhibiting viral replication, the infected cells treated and untreated with GCV, were marked with two antibodies directed for two different viral proteins: the immediate early ICP0 and the late protein US11, whose expression are

respectively independent and dependent by viral DNA synthesis. As expected 24 hours post infection Immunofluorescence staining was positive for ICP0 but not for US11 (Fig. 3.9).

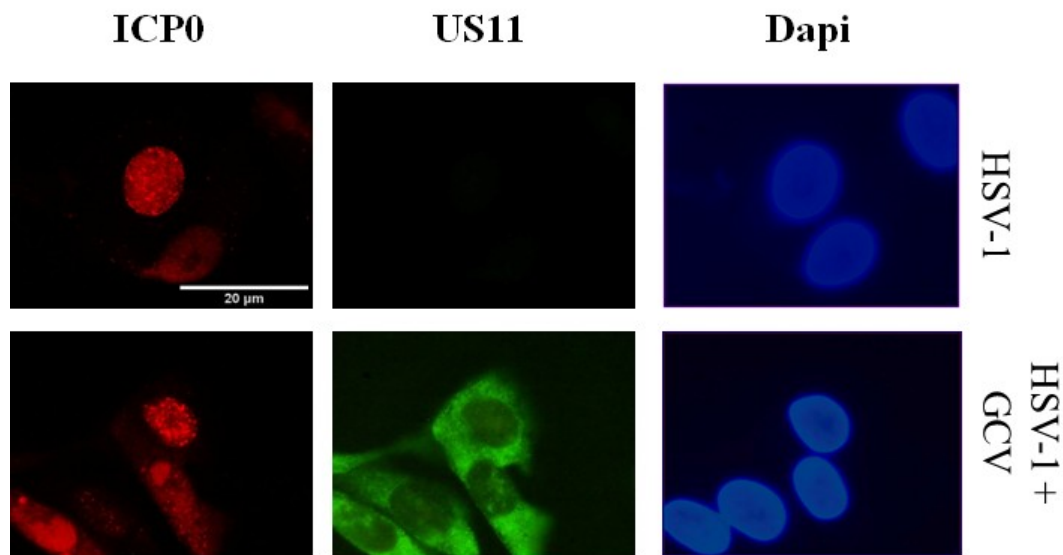


Fig. 3.9. Confirm of the efficacy of GCV to block viral replication. HSV-1 infected cells treated (second row) or untreated (first row) with GCV were stained 24hpi for the IE gene ICP0 (red) (first column) and the L gene US11 (green) (second column), whose expression is respectively not affected and affected by GCV. As expected, US11 is expressed only in untreated cells (second column, first row).

These data suggest that the mobilization of tau during infection is not affected, using GCV, by inhibition of viral DNA synthesis and thus of the expression of true late genes, but requires transcriptional activity that doesn't occur in the absence of ICP4, ICP22 and ICP27.

3.3.4 HSV-1 increases Tau-1 staining in Alzheimer's Disease mouse model neurons

Once we have observed that HSV-1 induces expression and aggregation of nuclear tau in neuronal and non-neuronal cell lines, although the reasons why this happen remain to be confirmed, we want to establish if the same effect can be visible in a more AD-related ex vivo cell system.

Neurons were extracted, according to the protocol described in material and methods, from newborn 3xTG mice, an animal model that most closely mimics human AD hallmarks. These mice carry 3 human transgenes harbouring mutations associated with AD: PS1_{M146V}, APP_{Swe} and Tau_{P301L}. The first is an alteration in Presenilin1, an enzyme involved in the cleavage of amyloid precursor protein (APP), the second is a mutation in APP itself found in a particular form of hereditary Alzheimer's disease, and the third lead protein tau to be more prone to

aggregate [23]. In the brain of these mice it's possible to observe the formation of SP starting from the age of 6 months, while NFT are not visible until 12 months. In explanted neurons from newborn animals, the human transgenes expressions, *in vitro*, are well detectable between day in vitro (DIV) 6 and 12 [26].

Since cells, from these transgenic mice, spontaneously show an optimal expression of tau and amyloid beta between postnatal day 6 and 12, we decided to infect the cells before that days to first evaluate if the virus may anticipate or worsen the expression of aberrant isoform of tau. Neurons were infected, *in vitro*, with 1 m.o.i. at Day In Vitro (DIV) 4, and then fixed at 24 hours post infection (DIV 5) (Fig. 3.10).

DIV 5

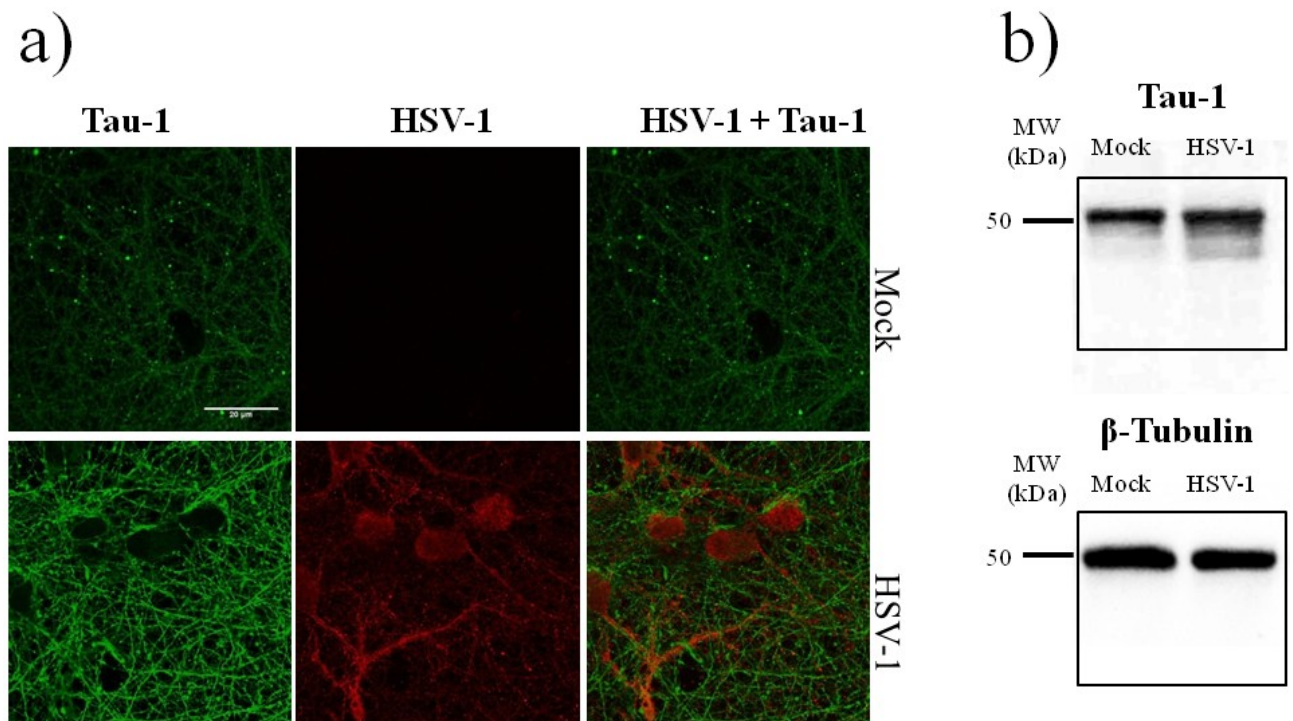


Fig. 3.10. Detection of tau with Tau-1 antibody in 3xTG explanted neurons at DIV5. DIV4 neurons were infected and 24 h.p.i. at DIV5, were analysed by immunofluorescence and western blot; control cells were DIV5 uninfected neurons. a) Immunofluorescent staining of Tau-1 (green) (left column) is slightly increased in infected (bottom row) versus uninfected (upper row) cells. HSV-1 staining (middle column) helps to discriminate between infected and uninfected samples. Right column show the combination of the two staining. b) Western blot confirm immunofluorescence observation: 2 bands below 50 kDa are slightly more marked in infected than uninfected neurons. β -Tubulin (lower panel) is shown as a control.

Immunoblot of figure 3.10 demonstrates in infected cells only a low increase of 50 KDa band of dephosphorylated tau recognized by the tau-1 antibody and the appearance of new isoforms

while Tau-1 immunofluorescence stain for dephosphorylated tau at high levels in the middle and distal axon in infected 3xTG neurons in comparison with uninfected cells (Fig. 3.10). The results are very different from the ones obtained in neuronal e fibroblast cells line where dephosphorylated tau was found in the nucleus.

This results lead to conclude that the virus induces increase levels of this protein that can contribute the outbreak of the pathological phenotype in these cells.

In order to observe if the virus can also aggravate an already pathological situation, accelerating the progression of the disease, the experiments were then repeated when the level of expression of the human transgenes in this 3xTG model were higher. Neurons were infected, *in vitro*, with a 1 m.o.i. at day DIV11 and fixed 24 hours post-infection (DIV12). Figure 3.11 show that Tau-1 staining was higher in cells infected than in control samples.

DIV 12

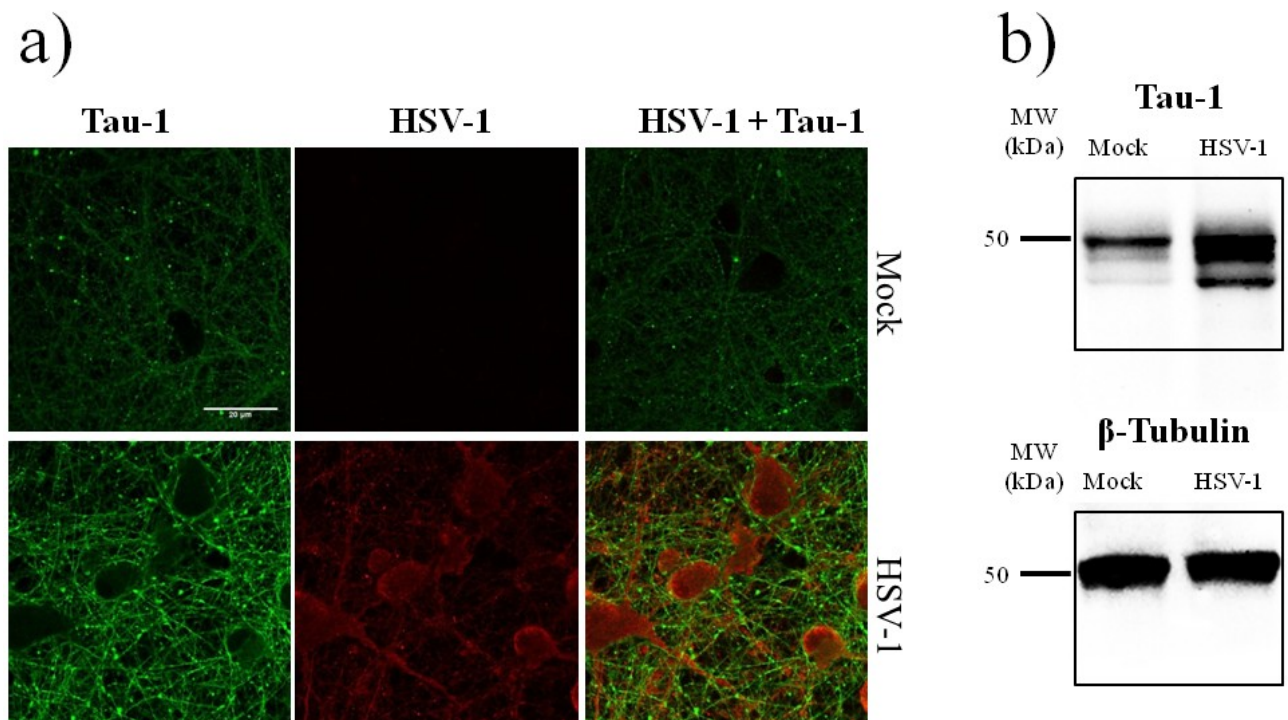


Fig. 3.11 Detection of tau with Tau-1 antibody in 3xTG explanted neurons at DIV12. DIV11 neurons were infected and 24 h.p.i, at DIV12, were analysed by immunofluorescence and western blot; control cells were DIV12 uninfected neurons. a) Immunofluorescence revealed a staining for Tau-1 markedly more increased in infected samples compared to uninfected (respectively first and second column). b) Western blot analysis outcome a strong detection for the 2 bands below 50 kDa (upper panel). β-Tubulin (lower panel) is shown as a control.

Western Blot showed a marked increase of different isoforms of tau dephosphorylated at the site recognized by the tau-1 antibody displayed by the band at 50 KDa and two lower bands below 50 KDa, in infected neurons. Immunofluorescence, in infected 3xTG neurons, reveals again a stronger staining for dephosphorylated tau that appears clustered in dots and dispersed along the axons and poorly in the nucleus, while in uninfected cells, anti-tau-1 stains tau clustered as small dots only in some areas of the axons (Fig. 3.11).

Therefore, independently on its localization, the amount of tau increases after HSV-1 infection, suggesting that HSV-1 can play a role in anticipate or aggravate an already pathological situation, leading to the progression of the disease.

3.4 Discussion

The data presented in this chapter focus on the influence of HSV-1 on dephosphorylated isoform of protein tau found mainly in the nucleus.

A function for tau protein in this cellular compartment has not been fully elucidated but several studies [4-9] suggest that, if altered, it might contribute to the onset of AD. The antibody that best recognized the nuclear isoform of tau dephosphorylated at serine 195, 198, 199 and 202, in neuronal and non-neuronal cells, is Tau-1[4-9].

The effect of HSV-1 on this protein was first evaluated in two different cell types: epithelial and neuroblastoma. In the cell lines tested, Western blot analysis have shown a drastic increase of the nuclear tau isoform. Immunofluorescence revealed that tau protein in uninfected cells is mainly localised in small dots inside the nucleolus, as previously observed in other cell lines [4-9], whereas in infected cells, 24 hours post-infection, tau distributes in bigger aggregates throughout the whole nucleus.

Thus, despite the viral proteins implicated in the alterations of nuclear tau during viral infection are still to be identified, the focus of our research moved to the causes that lead to this outcome.

First of all we studied if this effect might dependent by the interaction of tau with the viral protein US11 due to the localization of this tegument protein in the nucleolus. Our experimental data indicate that there are no evidence of a link between US11 and nucleolar Tau, because: (i) in cells infected with wild type HSV-1 US11 is located in the cytoplasm and in the nucleolus while tau is not, (ii) the infection with a mutant virus deleted for US11

behaves as wild-type virus regarding expression and localization of tau, and (iii) the transfection with a US11 expressing plasmid is not sufficient to influence tau nucleolar behaviour that is similar to untreated cells.

Nuclear tau has been proved to bind DNA in a manner similar to histones [10] and a role in nucleolar and chromatin organization has been suggested [6]. These facts might be linked to the ability of HSV-1 to induce chromatin remodelling [18]. This hypothesis seems to be strengthened by the observation of a profile for Tau-1 immunofluorescent staining in cells pharmacologically treated to induce chromatin relaxation that behave similar to infected cells. A more relaxed chromatin means more accessibility to viral gene transcription, thus the progression of productive cycle of viral infection.

To test if nuclear tau changes occur only in lytic infection we infect the cells with a replication defective HSV mutant, T0Z, or with a wild-type virus where the cells were treated with GCV. In both these experimental models the virus infects the cells but do not produce viral progeny. However, the data obtained from these experiments were different inasmuch as the alterations in nuclear tau were absent only in the cells infected with a replication defective virus lacking three IE genes but not in cells infected with wild-type and treated with GCV. Therefore the block of lytic cycle is not necessarily a limit to develop nuclear tau alterations, what is more important probably is the step on which the cycle is arrested. The three proteins ICP4, ICP22 and ICP27, are required for the transcription of viral genes, and its depletion arrest viral gene expression at the immediate early stages. While new viral DNA synthesis occurs later during infection and its inhibition affects the expression of only a small number of viral genes, named true late [25]. Therefore nuclear tau seems to have a role in viral gene transcription, but not in the synthesis of new DNA. This strengthens a functional similarity between tau and histones. The chromatin dynamics during HSV-1 infection, including the mobilization of histones, are a new area of epigenetic regulation of viral gene expression. Indeed, immediately after nuclear entry, viral genomes are complexed in silencing chromatin by the cell and, in productive infection, HSV-1 proteins mobilize away histones from viral DNA, while, in latent or quiescent infections, initial silencing is not disrupted and progress to almost fully block viral chromatin. Interestingly for the mobilization of the core histones is not required the ability of viral DNA to replicate (and consequently express true late genes), but it is necessary transcriptional activity [18].

After giving a partial explanation to viral induced nuclear tau changes, the profile for Tau-1 staining was investigated in a more AD related system: ex vivo cultured neurons from new born 3xTG mice, a widely used experimental model of AD [27].

Also in these cells the signal for Tau-1 was higher in infected than uninfected samples, but the results differed to those obtained in other cell lines for two aspects. First in Immunofluorescence the antibody stains mainly the axons and very weakly the nucleus. Second Western blot marked three bands, of which the two lower, placed below 50 KDa, are those more intense after viral infection.

The information achieved from these data are essentially two: in neurons dephosphorylated form of tau is mainly located along the axons, and it is present in at least three isoform the shortest of which are those increasing in response to viral infection and may be correlated to pathological isoforms since they are appearing, even if in a less amount, in uninfected 3xTG neurons at DIV12 when human transgenes carrying Alzheimer-like mutations are well expressed [26]. This might imply that HSV-1 can anticipate the outbreak of the pathological hallmarks and/or can aggravate an already pathological situation, accelerating the progression of the disease.

The different distribution of Tau-1 signal between 3xTG neurons and the other cell lines used in this work might depend on the diverse morphology of these cells. In fact, epithelial and neuroblastoma cells are mitotically active and Tau-1 stains a nuclear protein, while in neurons, which are differentiated cells, stains a dephosphorylated form of tau long axons. We cannot exclude that tau might increase also in neuronal nuclei, where it can play the same role that it plays in epithelial and neuroblastoma cells. Therefore the role of dephosphorylated form of tau remains to be elucidated.

In conclusion what is more remarkable from these data, however, is that levels of tau, despite its cellular-dependent localization, seems to increase and accumulate in altered isoforms after HSV-1 infection. Moreover we can suggest that alterations of tau itself, the substrate of tau kinases and phosphatases, can also play a role in its hyperphosphorylation and aggregation contributing to the formation of PHF, and thus to NFT that are not able to migrate inside the nucleus in response to HSV-1 induced stress, leading to a possible DNA damage and consequently neurodegeneration.

3.5 References

1. Martin, L., X. Latypova, and F. Terro, *Post-translational modifications of tau protein: implications for Alzheimer's disease*. *Neurochem Int.* **58**(4): p. 458-71.
2. Rossi, G., et al., *A new function of microtubule-associated protein tau: involvement in chromosome stability*. *Cell Cycle*, 2008. **7**(12): p. 1788-94.
3. Stoothoff, W.H. and G.V. Johnson, *Tau phosphorylation: physiological and pathological consequences*. *Biochim Biophys Acta*, 2005. **1739**(2-3): p. 280-97.
4. Loomis, P.A., et al., *Identification of nuclear tau isoforms in human neuroblastoma cells*. *Proc Natl Acad Sci U S A*, 1990. **87**(21): p. 8422-6.
5. Lu, J., et al., *Visualizing the microtubule-associated protein tau in the nucleus*. *Sci China Life Sci.* **57**(4): p. 422-31.
6. Sjoberg, M.K., et al., *Tau protein binds to pericentromeric DNA: a putative role for nuclear tau in nucleolar organization*. *J Cell Sci*, 2006. **119**(Pt 10): p. 2025-34.
7. Sultan, A., et al., *Nuclear tau, a key player in neuronal DNA protection*. *J Biol Chem.* **286**(6): p. 4566-75.
8. Thurston, V.C., et al., *Nucleolar localization of the microtubule-associated protein tau in neuroblastomas using sense and anti-sense transfection strategies*. *Cell Motil Cytoskeleton*, 1997. **38**(1): p. 100-10.
9. Wang, Y., et al., *A novel tau transcript in cultured human neuroblastoma cells expressing nuclear tau*. *J Cell Biol*, 1993. **121**(2): p. 257-67.
10. Camero, S., et al., *Tau protein provides DNA with thermodynamic and structural features which are similar to those found in histone-DNA complex*. *J Alzheimers Dis.* **39**(3): p. 649-60.
11. Ni, L., S. Wang, and C. Zheng, *The nucleolus and herpesviral usurpation*. *J Med Microbiol.* **61**(Pt 12): p. 1637-43.
12. Jamieson, G.A., et al., *Latent herpes simplex virus type 1 in normal and Alzheimer's disease brains*. *J Med Virol*, 1991. **33**(4): p. 224-7.
13. Jamieson, G.A., et al., *Herpes simplex virus type 1 DNA is present in specific regions of brain from aged people with and without senile dementia of the Alzheimer type*. *J Pathol*, 1992. **167**(4): p. 365-8.
14. Wozniak, M.A., A.L. Frost, and R.F. Itzhaki, *Alzheimer's disease-specific tau phosphorylation is induced by herpes simplex virus type 1*. *J Alzheimers Dis*, 2009. **16**(2): p. 341-50.
15. Wozniak, M.A., et al., *Antivirals reduce the formation of key Alzheimer's disease molecules in cell cultures acutely infected with herpes simplex virus type 1*. *PLoS One.* **6**(10): p. e25152.
16. Alvarez, G., et al., *Herpes simplex virus type 1 induces nuclear accumulation of hyperphosphorylated tau in neuronal cells*. *J Neurosci Res.* **90**(5): p. 1020-9.
17. Kavouras, J.H., et al., *Herpes simplex virus type 1 infection induces oxidative stress and the release of bioactive lipid peroxidation by-products in mouse P19N neural cell cultures*. *J Neurovirol*, 2007. **13**(5): p. 416-25.
18. Conn, K.L. and L.M. Schang, *Chromatin dynamics during lytic infection with herpes simplex virus 1*. *Viruses.* **5**(7): p. 1758-86.
19. Greco, A., et al., *Nucleolin interacts with US11 protein of herpes simplex virus 1 and is involved in its trafficking*. *J Virol.* **86**(3): p. 1449-57.
20. Vale, C., et al., *Cytotoxic action of lindane in neocortical GABAergic neurons is primarily mediated by interaction with flunitrazepam-sensitive GABA(A) receptors*. *J Neurosci Res*, 1998. **52**(3): p. 276-85.
21. Mulvey, M., et al., *Regulation of eIF2alpha phosphorylation by different functions that act during discrete phases in the herpes simplex virus type 1 life cycle*. *J Virol*, 2003. **77**(20): p. 10917-28.
22. Goins, W.F., et al., *Generation of replication-competent and -defective HSV vectors*. *Cold Spring Harb Protoc.* **2011**(5): p. pdb prot5615.

23. Du, T., G. Zhou, and B. Roizman, *Modulation of reactivation of latent herpes simplex virus 1 in ganglionic organ cultures by p300/CBP and STAT3*. Proc Natl Acad Sci U S A. **110**(28): p. E2621-8.
24. Kimberlin, D.W. and R.J. Whitley, *Antiviral therapy of HSV-1 and -2*. 2007.
25. Kibler, P.K., et al., *Regulation of herpes simplex virus true late gene expression: sequences downstream from the US11 TATA box inhibit expression from an unreplicated template*. J Virol, 1991. **65**(12): p. 6749-60.
26. Vale, C., et al., *Profile for amyloid-beta and tau expression in primary cortical cultures from 3xTg-AD mice*. Cell Mol Neurobiol. **30**(4): p. 577-90.
27. Oddo, S., et al., *Triple-transgenic model of Alzheimer's disease with plaques and tangles: intracellular A β and synaptic dysfunction*. Neuron, 2003. **39**(3): p. 409-21.

4. HSV-1 and Ca²⁺ signalling

4.1 Introduction

Calcium ions (Ca²⁺) play a pivotal role in the cell since participate as protagonist in signal transduction pathways where they act as a second messenger, in neurotransmitter release from neurons, in contraction of all muscle cell types, and in fertilization. In most eukaryotic cells, calcium levels are tightly regulated. Extracellular calcium is important for maintaining the potential difference across excitable cell membranes while the concentration of Ca²⁺ ions is kept very low at nanomolar levels in the cytosol, 10,000 times lower than in the extracellular space, by means of Ca²⁺ pumps that pump these ions out of the cell or into the endoplasmic reticulum (ER). Therefore intracellular organelles, include mitochondria and the endoplasmic reticulum, constantly accumulate Ca²⁺ ions and release them during certain cellular events. Calcium ions are important for cellular signalling as once they enter the cytosol of the cytoplasm they exert allosteric regulatory effects on many enzymes and proteins.

Cells maintain a rigid control over the intracellular level of Ca²⁺, thus ensuring that the level is kept low during periods of inactivity. In order to use Ca²⁺ as a messenger, cells overcome this tight homeostatic control by using sophisticated mechanisms. An increase in the intracellular level of Ca²⁺ depends upon entry channels in the plasma membrane and release channels in the membranes of the internal stores, the ER or the Golgi apparatus. In first case, there are many different plasma membrane channels that control Ca²⁺ entry from the external medium in response to stimuli that include membrane depolarization, stretch, noxious stimuli, extracellular agonists.

The release of Ca²⁺ from internal store is controlled by Ca²⁺ itself, or by an expanding group of messengers, the most ubiquitous of which is inositol-1,4,5-triphosphate (IP₃), which acts by binding to a specific receptor on the endoplasmic reticulum.

During the course of a typical Ca²⁺ transient, the generation of Ca²⁺ signalling is counteracted by the systems of switching off of Ca²⁺ signalling, during which time various pumps and exchangers remove Ca²⁺ from the cytoplasm.

Mitochondria also have an active function during the recovery process in that they sequester Ca²⁺ rapidly through a uniporter, and release more slowly back into the cytosol to be dealt with by pumps.

To distinguish between these different responses, their subtle regulation in time, space and amplitude, the characterization of the Ca^{2+} signalling requires measurement with tools of precise localization, high dynamic range and as little disturbance of cell physiology as possible, such as recombinant aequorin and Fura-2-acetoxymethyl ester (Fura-2AM).

Aequorin is a Ca^{2+} sensitive photoprotein of a coelenterate, isolated from the jellyfish *Aequorea Victoria*. The protein is composed of a 21 kDa apoprotein and a hydrophobic prosthetic group, coelenterazine (MW~400 Da). Upon high affinity binding of 3 Ca^{2+} ions, the coelenterazine is oxidized to coelenteramide, with a concomitant release of carbon dioxide and emission of light, this is an irreversible reaction where one photon is emitted.

Although this reaction is irreversible, in vitro an active aequorin can be obtained by incubating the apoprotein with coelenterazine in the presence of oxygen and 2-mercaptoethanol [1].

In particular, recombinant aequorin can be expressed not only in the cytoplasm, but also in specific cellular locations by including specific targeting sequences in the engineered cDNAs. The recombinant aequorin variants used in this work are a cytoplasmic and a mitochondrial isoform, respectively named cytAeq and mtAeq.

Fura-2AM is a membrane permeable derivative of Fura-2, an aminopolycarboxylic acid. Fura-2 is excited at 380 nm when free and at 340 nm when bound to Ca^{2+} , and the absorbance at those wavelengths is directly related to the amount of intracellular calcium. Regardless of the presence of calcium, Fura-2 emits at 510 nm of light. The use of the ratio between the light absorbed at 340 nm and at 380 nm (340/380) automatically cancels out confounding variables, such as variable dye concentration and cell thickness, making Fura-2 one of the most appreciated tools to quantify calcium levels. The high photon yield of Fura-2 allows the real time (video rate) measurements of calcium inside living cells [2].

These 2 systems allows to perform 2 different evaluations: Aequorin can be targeted to measure the $[\text{Ca}^{2+}]$ in different cellular compartments, and can be useful to detect changes in intracellular distribution of Ca^{2+} occurred after an incubation time of the cells with a possible Ca^{2+} agonist, while Fura-2 measure free cytoplasmic $[\text{Ca}^{2+}]$, but in real time.

The increased cellular calcium concentration could certainly play a part in the cytopathic effects induced by virus infection or in virus particle morphogenesis. It is known that HSV-1 triggers the activation of Ca^{2+} signalling [3] and that this is necessary for viral entry. The entry of HSV-1 inside the cell is a very complex process orchestrated by the envelope glycoproteins gB, gC, gD, gH/gL, that play a role in different cellular pathways involved during infection which remain to be elucidated. Cheshenko et al. demonstrated that the binding of the virus to

the ubiquitous surface co-receptors heparan-sulfate proteoglycans (HSPG) and the engagement of the gD coreceptor nectin-1 induce the release of a small amount of Ca^{2+} near the plasma membrane, that may start the entry process [4]. However to complete this process and to allow the intracellular transport of the viral capsid, into the nucleus, it is required the release of global intracellular Ca^{2+} stores, activation of IP_3Rs , and the presence of the essential viral envelope glycoproteins (gB, gD, gH/gL).

The binding of the virus to HSPG is dispensable for viral entry, and it is mediated by two glycoproteins: gC and gB. The absence of the first affects the ability of the virus to bind to cell surface, but not its entry. The second, in addition to HSPG binds to membrane also with other receptors, the main known of which are paired immunoglobulin-like type 2 receptor (PILR) α [5], myelin associated glycoproteins [6] and non-muscle myosin heavy chain (NMHC) IIA [7]. gB performs also a fundamental role in the fusion of viral envelope with cell membrane, and viruses deleted in gB are not able to infect cells, while a deletion in only a polylysine (pK) sequence located in the N terminus of gB, that is responsible for interaction of gB with HSPG, doesn't prevent viral infection, albeit it reduces viral attachment [8].

gB has been proposed to have a possible influence in the development of AD because of the observation of the homology between an its internal sequence and the carboxyl-terminal region of $\text{A}\beta$ and it has been demonstrated to promote $\text{A}\beta$ aggregation in vitro [9].

$\text{A}\beta$ and Ca^{2+} interact reciprocally during the development of AD, alterations in Ca^{2+} signalling accelerates the deposition of $\text{A}\beta$, while $\text{A}\beta$ peptides especially in soluble oligomeric forms alter intracellular Ca^{2+} , as reviewed in [10]. HSV-1 has been reported to play a role in this dualism between Ca^{2+} and $\text{A}\beta$, since the Ca^{2+} signalling attendant to viral attachment and entry induce modifications in APP that lead to its cleavage and the consequent formation of $\text{A}\beta$ [11].

Interestingly $\text{A}\beta$, like gB, has the ability to interact with HSPG, and this binding contribute to AD pathogenesis [12].

In attempt to elucidate a possible link between gB and $\text{A}\beta$ in intracellular Ca^{2+} dysregulation, it was planned to, first of all, investigate Ca^{2+} responses to gB and the implication of the binding to HSPG.

Therefore, two different systems have been used to study the changes in calcium concentration in HSV infected cells by means of two sensitive calcium binding probes: Aequorin and FURA-2.

Ca²⁺ homeostasis is altered in AD, for several reasons discussed in the general introduction of this thesis, and it is characterized by an overload of this ion inside the cytoplasm, resulting in loss of neuronal physiology and functionality therefore contributing to the pathogenesis of the disease.

Therefore preliminary data presented in this chapter show, in epithelial and neuronal cells, a release of Ca²⁺ from intracellular stores induced by a purified recombinant gB, analyzed by the aequorin system while an intracellular Ca²⁺ increase, detected by the FURA-2 probe, was provoked by infecting the cells with a wild type HSV-1 and a mutant virus deleted in the pK domain of gB.

The preliminary results obtained from the present work are the basis to study the alteration of Ca²⁺ signalling as a possible link between AD and HSV-1.

4.2 Material and Methods

4.2.1 Cells and viruses

Vero, HRPE and neurons from 3xTG AD mice were cultured as described in previous chapters.

293 and 293-gB1s were grown in Dulbecco's minimal essential medium (DMEM) containing 100 U/ml penicillin, 100 µg/ml streptomycin, 2mM L-glutamine and 10% heat-inactivated foetal calf serum (FCS).

For Aequorin experiments, 24 hours prior to transfection 10⁵ HRPE cells were seeded on 13mm coverslips in 24 well plates.

For Fura-2 experiments, 5·10⁵ HRPE or Vero were seeded 24 hours prior to the experiment on 24mm coverslips in 6-well plates, while 10⁶ 3xTG neurons were seeded on the same support immediately after the extraction and the experiment was performed at DIV 7.

The viruses used for Fura-2 experiments were an HSV-1 strain Kos wild type and a mutant deleted in pK domain of gB, named KgBpK⁻ and described in [8]. 5·10⁵ viral plaques were diluted in 100µl of PBS and added during the experiment to cells (see below) in order to infect them with 1 m.o.i.

4.2.2 gB purification

Glycoprotein B1s (gB1s), used in aequorin measurements, is a 662 amino acids derivative of the mature protein lacking the transmembrane anchor sequences, reconstructed with the

extracellular and intracytoplasmic domains, the gB1s gene was cloned into pRP-RSV, an eukaryotic expression vector [13]. The pRP-RSV gB1s expression vector was transfected in 293 cells, to create a cell line, 293-gB1s, that constitutively express and secrete in the culture medium gB1s.

The 293-gB1s cells were grown at confluence. Growth medium deprived of FCS was added for 24 hours and then the medium was collected.

After addition of protease inhibitors, the medium was frozen and lyophilized, to allow the concentration of the gB1s protein. gB1s was purified as reported in [14]. Briefly the lyophilized medium was dialyzed, and gB1s was purified by affinity chromatography on a column in which an anti gB1 monoclonal antibody had been conjugated. The positive fractions for gB1s were pooled, dialyzed, aliquoted and stored at -80°C . The concentration of gB1s ($25\text{ ng}/\mu\text{l}$) and BSA contamination ($7,5\text{ ng}/\mu\text{l}$) were determined by quantitative analysis with the Chemi Doc MP system and Image Lab Software (Biorad) of the sample on a Coomassie Brilliant Blue stained SDS-PAGE gel.

4.2.3 Transfection and Aequorin measurements

The probes employed (cytAEQ and mtAEQ) are chimeric aequorins targeted to the cytosol and mitochondria, respectively. For a map of the constructs and detailed informations on their characteristics see [15].

36 hours prior to the experiments, $1\mu\text{g}$ of each plasmids for the expression of the probes were transfected separately in HRPE cells seeded on 13mm coverslips with jetPEI® (polyplus transfection) according to manufacturer's instructions.

For the reconstitution of the probe HRPE cells were incubated with $5\mu\text{M}$ coelenterazine for 1,5 h in DMEM supplemented with 1% FCS. 1 hour prior to the measurement 500 ng of purified recombinant gB1s were added to cells. As a negative control cells were incubated with 150ng of BSA, the same amount of this contaminant found in the volume of the protein solution that contains 500 ng of gB1s.

Then the coverslip with transfected cells was placed in a perfused, thermostated chamber located in the close proximity of a low noise photomultiplier, with a built-in amplifier-discriminator [16].

All aequorin measurements were carried out in Krebs's ringer bicarbonate buffer (KRB: 10mM D-Glucose, $0,49\text{mM}$ MgCl_2 , $119,78\text{mM}$ NaCl , $4,56\text{mM}$ KCl , $0,7\text{mM}$ Na_2HPO_4 , $1,3\text{mM}$ NaH_2PO_4 , $14,99\text{mM}$ NaHCO_3) supplemented with 1 mM CaCl_2 . The agonist histamine was added to the same medium with a concentration of $1\mu\text{M}$. The experiments were

terminated by lysing the cells with 100 μ M digitonin in a hypotonic Ca²⁺-containing solution (10 mM CaCl₂ in H₂O), thus discharging the remaining aequorin pool. The output of the discriminator was captured by a Thorn-EMI photon counting board and stored in an IBM-compatible computer for further analyses. The aequorin luminescence data were calibrated off-line into [Ca²⁺] values, using a computer algorithm based on the Ca²⁺ response curve of wild type and mutant aequorins, as described in [17]. Chemicals and reagents were from Sigma or from Merck except for coelenterazine, that was from Molecular Probes. Statistical data are presented as mean \pm S.E.

4.2.4 Fura-2/AM measurements

The cytosolic free Ca²⁺ concentration [Ca²⁺]_c was evaluated using the fluorescent Ca²⁺ indicator Fura-2 acetoxymethyl ester (Fura-2/AM; Molecular Probes). Briefly, Vero, HRPE and 3xTG neurons were incubated in medium supplemented with 2.5 μ M Fura-2/AM for 30 min, washed with KRB buffer to remove the extracellular probe, supplied with preheated KRB buffer (supplemented with 1 mM CaCl₂), and placed in a thermostated (37 °C) incubation chamber on the stage of an inverted fluorescence microscope (Zeiss Axiovert 200). Dynamic video imaging was performed using the Metafluor software (Universal Imaging Corporation, USA). HSV-1 Kos wild type or KgBpK⁻ were added to cells with a m.o.i. of 1 and fluorescence was measured every 100 ms with the excitation wavelength alternating between 340 and 380 nm and the emission fluorescence being recorded at 510 nm. At the end of the experiment, a region free of cells was selected, and one averaged background frame was collected at each excitation wavelength for background correction. The [Ca²⁺]_c was calculated by the ratio method using the equation: $[Ca^{2+}]_c = Kd (R - R_{min}) / (R - R_{max}) \times Sf2 / Sf1$ where Kd is dissociation constant of Fura-2/AM for (Ca²⁺) taken as 240 nM at 37 °C, R is ratio of fluorescence for Fura-2/AM at the two excitation wavelengths, F340/F380, R_{max} is ratio of fluorescence in the presence of excess of calcium obtained by lysing the cells with 10 μ M ionomycin (Sigma Aldrich), R_{min} is ratio of fluorescence in the presence of minimal calcium obtained by lysing the cells and then chelating all the Ca²⁺ with 0.5 M EGTA, Sf2 is fluorescence of Ca²⁺ free form of Fura-2/AM at 380nm excitation wavelength and Sf1 is fluorescence of Ca²⁺ bound form of Fura-2/AM at 380 nm excitation wavelength.

4.3 Results

4.3.1 A soluble recombinant gB is able to induce Ca^{2+} release from intracellular stores of HRPE cells

As described in material and methods, after 1 hour of incubation with 500ng of gB or with 150ng of BSA, as a negative control, HRPE cells were stimulated to release Ca^{2+} from ER with the Ca^{2+} agonist histamine. The egress of Ca^{2+} from these intracellular stores reflects in an increase of $[\text{Ca}^{2+}]$ in cytoplasm and mitochondria that can be detected by the luminescence signal emitted by the recombinant aequorins.

The level of Ca^{2+} detected in cytoplasm is significantly lower in gB treated cells than in control samples: the peak reached by the signal after histamine stimulation is approximately 1,4 μM in the former versus 1,8 μM in the latter (Fig. 4.1). Also mitochondrial Ca^{2+} seems slightly lower after gB treatment compared to control samples (approximately 4,3 vs 4,1 μM), but this difference is not significative (Fig. 4.2).

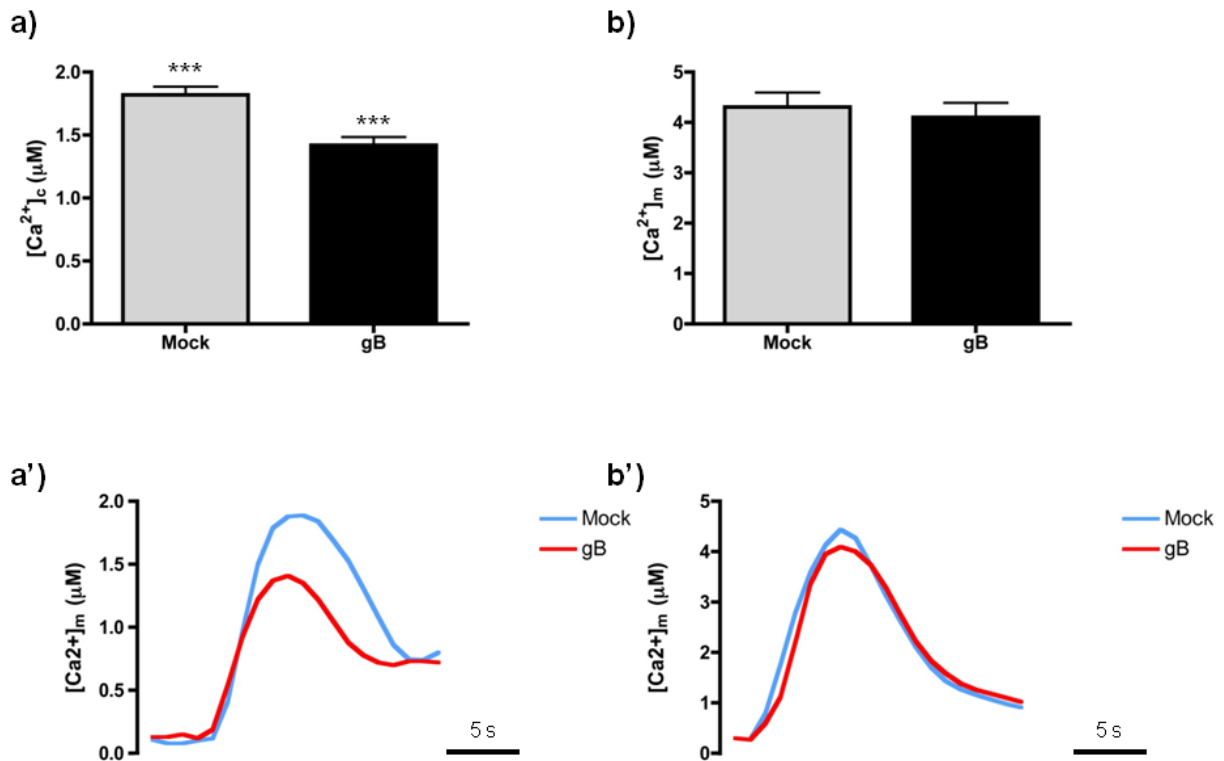


Fig. 4.1. gB1s induce the release of Ca^{2+} from intracellular stores. a) Mean of the $[\text{Ca}^{2+}]_c$ peaks registered during agonist stimulation. The average value of $[\text{Ca}^{2+}]_c$ detected is significantly lower after 1 hour of incubation with gB1s ($1,82 \pm 0,06 \mu\text{M}$ n=13 for control samples; $1,42 \pm 0,06 \mu\text{M}$ n=18; $p < 0,001$). a') Representative measure of the Ca^{2+} released in the cytoplasm during stimulation with the agonist histamine. b) Mean of the $[\text{Ca}^{2+}]_m$ peaks registered during agonist stimulation. The average value of $[\text{Ca}^{2+}]_m$ detected is slightly, but not significantly, lower after 1 hour of incubation with gB1s ($4,3 \pm 0,29 \mu\text{M/s}$ n=27 for control samples; $4,1 \pm 0,29 \mu\text{M/s}$ n=23; $p > 0,05$). b') Representative measure of the Ca^{2+} released in the mitochondria during stimulation with the agonist histamine.

These data shows that gB is able to induce a release of Ca^{2+} from ER: after 1 hour of treatment with the protein, $[\text{Ca}^{2+}]$ in ER is lower than in control samples and this results in a lower increase in cytoplasmic $[\text{Ca}^{2+}]$ after stimulation with an agonist. The observation of this difference only in the cytoplasm and not in mitochondria may indicate that the amount of Ca^{2+} moved by gB in this experimental system is quite exiguous and can be detected only in the cytoplasm where the level of Ca^{2+} under resting conditions is very low compared to other cellular compartments.

4.2.2 Interaction of gB with HSPG down-regulate Ca^{2+} signalling triggered by HSV-1

To test if the particular binding of gB to HSPG was involved in the Ca^{2+} signalling characteristic of HSV-1 entry, Vero, HRPE and 3xTG neurons were incubated with the fluorescent dye Fura-2AM, then intracellular $[\text{Ca}^{2+}]$ changes occurring after the addition of the virus were followed in real time, as described in material and methods.

Surprisingly the mutant virus KgbpK⁻ in all the three cell lines used promotes a major increase in intracellular $[\text{Ca}^{2+}]$ compared to the wild type virus.

The average peak of $[\text{Ca}^{2+}]$ reached in Vero cells with KgbpK⁻ is approximately $1\mu\text{M}$, while with the wild type virus is $0,6\mu\text{M}$ (Fig. 4.3).

A major difference between the two samples was observed in 3xTG neurons: the mean value of the $[\text{Ca}^{2+}]$ peaks detected were $1,5\mu\text{M}$ for the mutant virus and $0,6\mu\text{M}$ for the wild type (Fig. 4.4).

In HRPE cells the increase of $[\text{Ca}^{2+}]$ provoked by the two viruses is not drastic and transient like in other cells, but it follows a more gradual progression, indicating a slower response, therefore it was arbitrary chosen to analyze $[\text{Ca}^{2+}]$ at 1 minute after the adding of the virus to cells. Mutant virus at that time point induce an increase of $[\text{Ca}^{2+}]$ up to $150\mu\text{M}$ versus $80\mu\text{M}$ registered with the wild type virus (Fig. 4.5).

These data show that the lacking of the interaction between gB and HSPG leads to an enhanced Ca^{2+} signalling triggered by HSV-1, suggesting a regulatory function of this binding on the influx of Ca^{2+} that follows HSV-1 attachment to cell membrane.

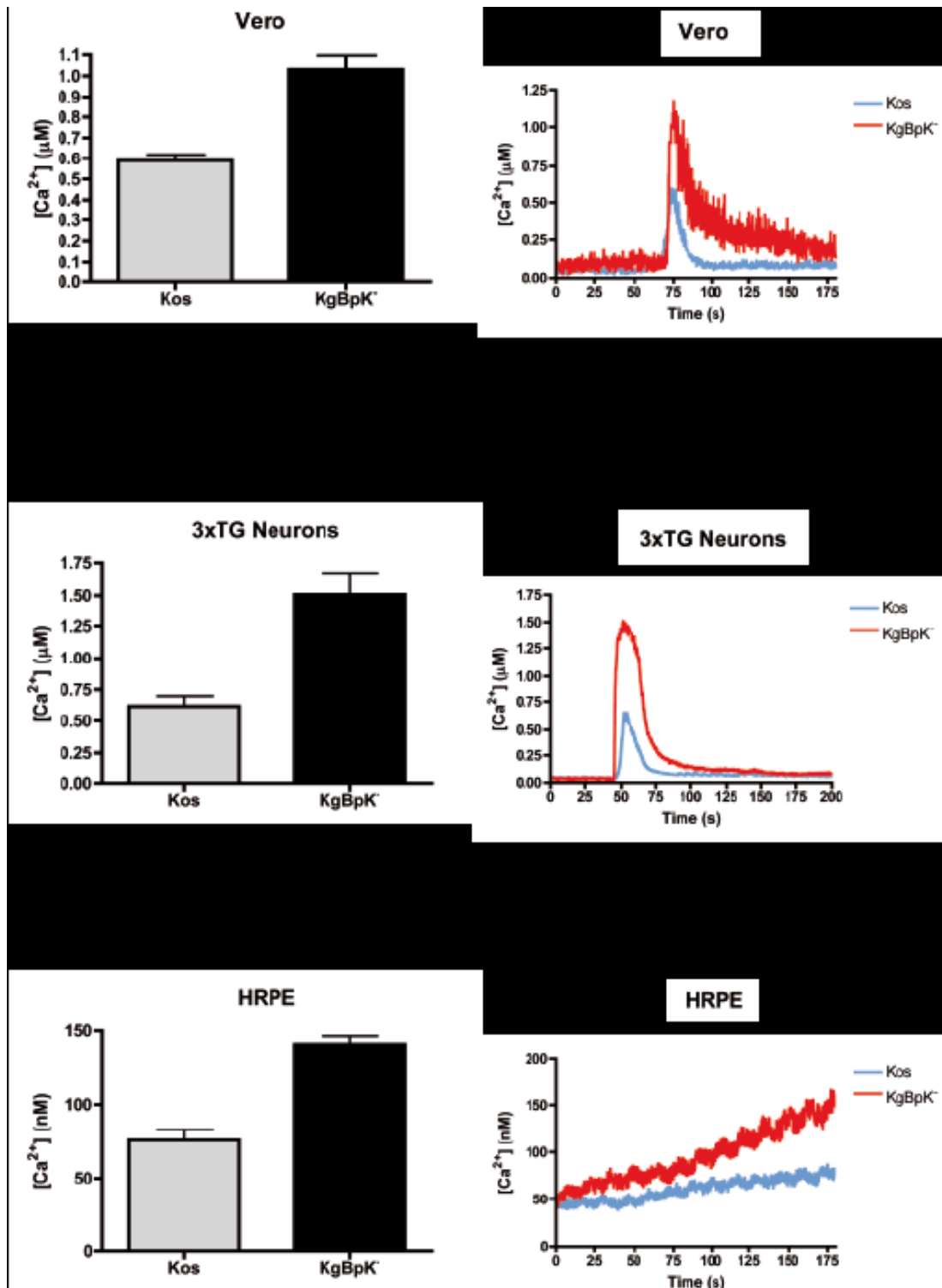


Fig. 4.2. pK domain of gB has a down-regulatory effect on Ca²⁺ signalling induced by HSV-1. The figure shows the results of the measures of [Ca²⁺]_c detected with the Fura-2 dye immediately after the addition of wild type HSV-1 Kos strain or the mutant KgBpK⁻ to cells. In left panels it is reported the graph of the mean value of the [Ca²⁺]_c recorded in the transient peak for Vero (0,59 ± 0,03 μM, n=72 for Kos; 1,03 ± 0,07 μM, n=32 for KgBpK⁻; p<0,0001) and 3xTG neurons (0,62 ± 0,08 μM, n=13 for Kos; 1,50 ± 0,16 μM, n=13 for KgBpK⁻; p<0,0001), while at 160'' after the beginning of the experiment for HRPE cells (75,82 ± 6,85nM , n=18 for Kos; 140,80 ± 5,65 nM, n=70, p<0,0001 for KgBpK⁻). Right panels show a representative trend of [Ca²⁺]_c in the cell line indicated. In Vero and 3xTG neurons both the virus induced an instantaneous transient peak, while in HRPE [Ca²⁺]_c increase in a more progressive and slow way.

4.4 Discussion

HSV-1 infection is known to be accompanied by transient intracellular Ca^{2+} influx, therefore it can be reasonably supposed to contribute to the dysregulation of this ion that lead to neurodegeneration in AD. Indeed the Ca^{2+} signalling triggered by HSV-1 infection is reported to promote APP processing and $\text{A}\beta$ accumulation [11].

HSV-1 gB and $\text{A}\beta$ have been proposed to have a correlation in the development of AD after the initial observation that a gB-derived peptide in vitro can induce the formation of $\text{A}\beta$ plaques, and that the two proteins present sequence homology [9]. In addition these proteins are implied in intracellular Ca^{2+} perturbation, because $\text{A}\beta$ formation can both affect or be affected by Ca^{2+} dyshomeostasis [10], and gB is an essential protein for the entry of the virus into the cell, a process mediated by Ca^{2+} signalling. The binding of gB to cell membrane is first mediated by HSPG and interestingly also $\text{A}\beta$ can interact with this surface molecule.

Given these observations it was planned to investigate if there might be some relationship between $\text{A}\beta$ and gB linked to alterations in intracellular $[\text{Ca}^{2+}]$.

The preliminary data presented in this chapter provide some insights in cellular response to gB.

After the first observation that a purified secreted form of gB showed the ability to induce Ca^{2+} release from intracellular stores in HRPE cells, it was evaluated how the interaction between the envelope protein and HSPG influence the movement of Ca^{2+} attendant viral entry. In all the cell lines tested the mutant HSV-1 deleted in the pK domain responsible for this binding provoke a higher increase of $[\text{Ca}^{2+}]$ compared to that registered with the wild type virus, suggesting that this interaction may down regulate the signal. Future experiments will be directed to elucidate if this is a specific effect given by gB or if also the lacking of gC, the other viral envelope glycoprotein reported to bind to HSPG, may produce the same effect. It can be speculated that in aged brains where viral reactivations occur more frequently because of systemic impairment, an excessive amount of $\text{A}\beta$ is produced and accumulate in the inter-synaptic space. Given the sequence homology with gB, the two proteins may compete for the binding to HSPG, thus an excessive amount of $\text{A}\beta$ prevent the interaction of gB with HSPG and the possible regulatory role that this may have in intracellular Ca^{2+} influx triggered by the virus.

The lacking of this interaction lead to an excessive Ca^{2+} signalling during HSV-1 attachment and entry, therefore amplifying the production of $\text{A}\beta$ and contributing to neurodegeneration.

4.5 References

1. Shimomura, O., F.H. Johnson, and Y. Saiga, *Extraction, purification and properties of aequorin, a bioluminescent protein from the luminous hydromedusa, Aequorea*. J Cell Comp Physiol, 1962. **59**: p. 223-39.
2. Grynkiewicz, G., M. Poenie, and R.Y. Tsien, *A new generation of Ca²⁺ indicators with greatly improved fluorescence properties*. J Biol Chem, 1985. **260**(6): p. 3440-50.
3. Cheshenko, N., et al., *Herpes simplex virus triggers activation of calcium-signaling pathways*. J Cell Biol, 2003. **163**(2): p. 283-93.
4. Cheshenko, N., et al., *Multiple receptor interactions trigger release of membrane and intracellular calcium stores critical for herpes simplex virus entry*. Mol Biol Cell, 2007. **18**(8): p. 3119-30.
5. Satoh, T., et al., *PILRalpha is a herpes simplex virus-1 entry coreceptor that associates with glycoprotein B*. Cell, 2008. **132**(6): p. 935-44.
6. Suenaga, T., et al., *Myelin-associated glycoprotein mediates membrane fusion and entry of neurotropic herpesviruses*. Proc Natl Acad Sci U S A. **107**(2): p. 866-71.
7. Arii, J., et al., *Non-muscle myosin IIA is a functional entry receptor for herpes simplex virus-1*. Nature. **467**(7317): p. 859-62.
8. Laquerre, S., et al., *Heparan sulfate proteoglycan binding by herpes simplex virus type 1 glycoproteins B and C, which differ in their contributions to virus attachment, penetration, and cell-to-cell spread*. J Virol, 1998. **72**(7): p. 6119-30.
9. Cribbs, D.H., et al., *Fibril formation and neurotoxicity by a herpes simplex virus glycoprotein B fragment with homology to the Alzheimer's A beta peptide*. Biochemistry, 2000. **39**(20): p. 5988-94.
10. Demuro, A., I. Parker, and G.E. Stutzmann, *Calcium signaling and amyloid toxicity in Alzheimer disease*. J Biol Chem. **285**(17): p. 12463-8.
11. Piacentini, R., et al., *HSV-1 promotes Ca²⁺ -mediated APP phosphorylation and Abeta accumulation in rat cortical neurons*. Neurobiol Aging. **32**(12): p. 2323 e13-26.
12. Zhang, G.L., et al., *Towards understanding the roles of heparan sulfate proteoglycans in Alzheimer's disease*. Biomed Res Int. **2014**: p. 516028.
13. Manservigi, R., et al., *Protection from herpes simplex virus type 1 lethal and latent infections by secreted recombinant glycoprotein B constitutively expressed in human cells with a BK virus episomal vector*. J Virol, 1990. **64**(1): p. 431-6.
14. Manservigi, R., et al., *Experimental keratitis in rabbits by human HSV-1 variants: prevention and treatment*. J Med Virol, 1990. **32**(3): p. 148-54.
15. Chiesa, A., et al., *Recombinant aequorin and green fluorescent protein as valuable tools in the study of cell signalling*. Biochem J, 2001. **355**(Pt 1): p. 1-12.
16. Brini, M., et al., *Targeting of aequorin for calcium monitoring in intracellular compartments*. J Biolumin Chemilumin, 1994. **9**(3): p. 177-84.
17. Brini, M., et al., *Transfected aequorin in the measurement of cytosolic Ca²⁺ concentration ([Ca²⁺]_c). A critical evaluation*. J Biol Chem, 1995. **270**(17): p. 9896-903.

5. An *in vivo* model to study the correlation between HSV-1 and neurodegeneration

5.1 Introduction

The classical pathological hallmarks of Alzheimer's disease are the presence of abnormal protein aggregates represented by intraneuronal neurofibrillary tangles and extraneuronal senile plaques. Despite great stride in AD research, the causes that lead to the formation of these pathological markers and thus to the development and progression of the disease are not fully understood.

In the last 10 years another important factor that has been included among the characteristic of AD is the inflammation. At present it is not clear if inflammation is a cause or a consequence of AD progression, but it has been implicated in neuronal damage, increased A β and hyperphosphorylated tau generation and cognitive impairment.

Ageing, the main risk factor for AD, is often accompanied by enhanced chronic inflammation [1], in addition A β is able to initiate an inflammatory response that lead to neuronal and synaptic damage [2]. Many other factors, genetic and environmental, seem to be involved in inflammatory processes in nervous system that start with activation of microglia and macrophages, which represent the innate immunity response in this compartment. These cells generate inflammatory mediators, like chemokines, cytokines, prostaglandins, free radicals, cyclooxygenase-2 (COX-2) and inducible nitric oxide synthase (iNOS) and activate components of the adaptive immune system, such as T lymphocytes, as well their presence is necessary for the clearing of toxic products and damaged tissue [3]. Infectious agents are gaining a growing relevance [4] in the inflammatory process in central nervous system (CNS) and Herpes simplex virus type 1 (HSV-1) is one of these.

The rationale for implicating HSV-1 in AD stems mainly from its neurotropism that enable it to establish latency in peripheral nervous system, in particular in trigeminal ganglia (TG), while, with age, it can also reach the CNS [5, 6]. In addition herpes simplex encephalitis (HSE), a rare but severe disorder, affects areas leading the main pathological changes in AD [7], such as frontal and temporal cortices, and where HSV-1 DNA has been detected by polymerase chain reaction (PCR) also in normal brains [5, 8].

Therefore, it is reasonable to suppose that, besides a direct involvement of HSV-1 infection in tau phosphorylation and APP cleavage [9-12], another important contribution of the virus to the progression of the disease may result by inflammatory processes due to reactivation and latency episodes.

In order to address this issue we have used an *in vivo* system consisting of Ai6 RosaZsGreen reporter mice that contain a ZsGreen reporter gene in the Rosa26 locus and a recombinant HSV-1 expressing Cre recombinase under the control of Cytomegalovirus immediate early promoter (HSV CMVCre). Ai6 is a transgenic strain that conditionally expresses ZsGreen fluorescent protein upon Cre recombinase excision of a stop cassette, following infection with HSV CMVCre. The strong fluorescence afforded by this reporter mouse strain allows the direct visualization of live infected cells in the nervous system. Our results have shown that the virus is able to activate macrophages and microglia and to recruit some T lymphocytes in the area of infection, whereas it was not possible to detect amyloid plaques or neurofibrillary tangles

5.2 Material and methods

5.2.1 Virus

The virus used for mice infection was an SC16 strain-based recombinant HSV-1 carrying the CRE recombinase under the control of the human cytomegalovirus (HCMV) major immediate early promoter (MIEP) [13].

5.2.2 Mice

All the *in vivo* experiments were conducted in the transgenic reporter mouse Ai6 carrying, in the ROSA26 locus, a CRE recombinase-controlled ZsGreen, one of the brightest green fluorescent protein [14].

8 weeks old mice were infected by scarification of whisker pads with $2 \cdot 10^6$ p.f.u. of virus. At different times after infection, i.e. 4, 11, 40, 126 days post-infection, groups of three mice were killed by CO₂ asphyxiation. As a control a group of three mice was left uninfected and sacrificed with the first group of infected mice. Mice brains and TG were dissected, washed in PBS and fixed in 1% formaldehyde-10 mM sodium periodate-75 mM l-lysine. After 24 h at 4°C of fixation samples were equilibrated in 30% sucrose at 4°C for 18 h, and then frozen in OCT and sectioned, in slices of 9 µm thick, on a cryostat.

5.2.3 Immunofluorescence

Sections of TG and brains were air dried for 2 h at room temperature (RT), post-fixed with 4% paraformaldehyde (PFA) in PBS and blocked with 2% goat serum-2% BSA-PBS for 1 h at RT. Samples were then incubated with the primary antibody for 1 hour, washed with Tween 0,1% in PBS and incubated with the secondary antibody for 1 hour in the dark. All primary and secondary antibodies were diluted in 2% BSA-PBS and are listed below. Finally samples were washed with Tween 0,1% in PBS and mounted with ProLong® Gold Antifade Mountant (Invitrogen) containing DAPI (4',6-diamidino-2-phenylindole) to stain nuclei. Fluorescence was visualized using a Leica SP5 confocal microscope and analyzed with ImageJ.

5.2.4 Antibodies

Primary antibodies were as follows: rabbit anti-beta Amyloid, 1:200 (ab2539, Abcam, Cambridge, UK); anti-Tau (phospho S202), 1.200 (ab108387, Abcam); anti-HSV-1, 1:10000 (ab9533, Abcam, Cambridge); rat anti-F4/80 (A3-1), 1:200 (ab6640, Abcam); goat anti-Iba 1, 1:200 (ab107159, Abcam).

Secondary antibodies, all purchased from Invitrogen, Carlsbad, CA, USA and diluted 1:1000, were as follows: Alexa Fluor 488- or 568- or 633-conjugated goat anti-rabbit IgG pAb; Alexa Fluor 488- or 568- or 633-conjugated goat anti-mouse IgG pAb; Alexa Fluor 568- conjugated goat anti-rat IgG pAb and Alexa Fluor 568-conjugated donkey anti-goat IgG pAb.

5.2.5 DNA extraction and PCR

Brains from 2 uninfected mice were homogenized separately and genomic DNA was extracted using Wizard® Genomic DNA purification kit (Promega) according to manufacturer's protocol.

Genomic DNA was amplified with polymerase chain reaction (PCR) performed with Phusion High-Fidelity DNA Polymerase (Finnzymes). To detect possible event of recombination of the two loxP sites, the sequence of the primers used were based upon the map of Ai6 plasmid, used for the generation of Ai6 recombinant mice, available here: <https://www.addgene.org/22798/> and represented in fig. 1. Primer forward is the sequence reported in the map as pCAG_F_primer (5'-GCAACGTGCTGGTTATTGTG-3') and primer reverse corresponds to pBluescriptKS_primer: (5'-TCGAGGTCGACGGTATC-3'). As shown in fig. 1 these two primers are external to the loxP sites, thus PCR may outcome 2

amplificates with different length: 1576 bp in case of recombination and 2448 bp in case of no recombination.

The PCR was performed with an initial denaturation step (98 °C for 30 s) followed by amplification steps carried out over 40 cycles (denaturation, 98 °C for 10 s; annealing, 60 °C for 30 s; extension, 72 °C for 60 s) and a final extension at 72 °C for 5 min.

Products of PCR were analysed by electrophoresis on 2% agarose gel in TAE with 0,2µM ethidium bromide.

5.3 Results

5.3.1 Route of HSV-1 in the nervous system of Ai6 mice

Ai6 reporter mice were infected, by scarification in both whisker pads, with 2×10^6 pfu of a recombinant HSV-1 expressing CRE recombinase under the control of human cytomegalovirus major immediate early promoter that is transiently active prior to the establishment of latency [15]. The expression of ZsGreen allows following the track of the virus in infected neurons. Brains and trigeminal ganglia (TG) from infected and uninfected Ai6 were sectioned and analysed by immunofluorescence assay, as described in material and methods, at different time points, i. e. 4, 11, 40, 126 days post infection (Fig. 5.1).

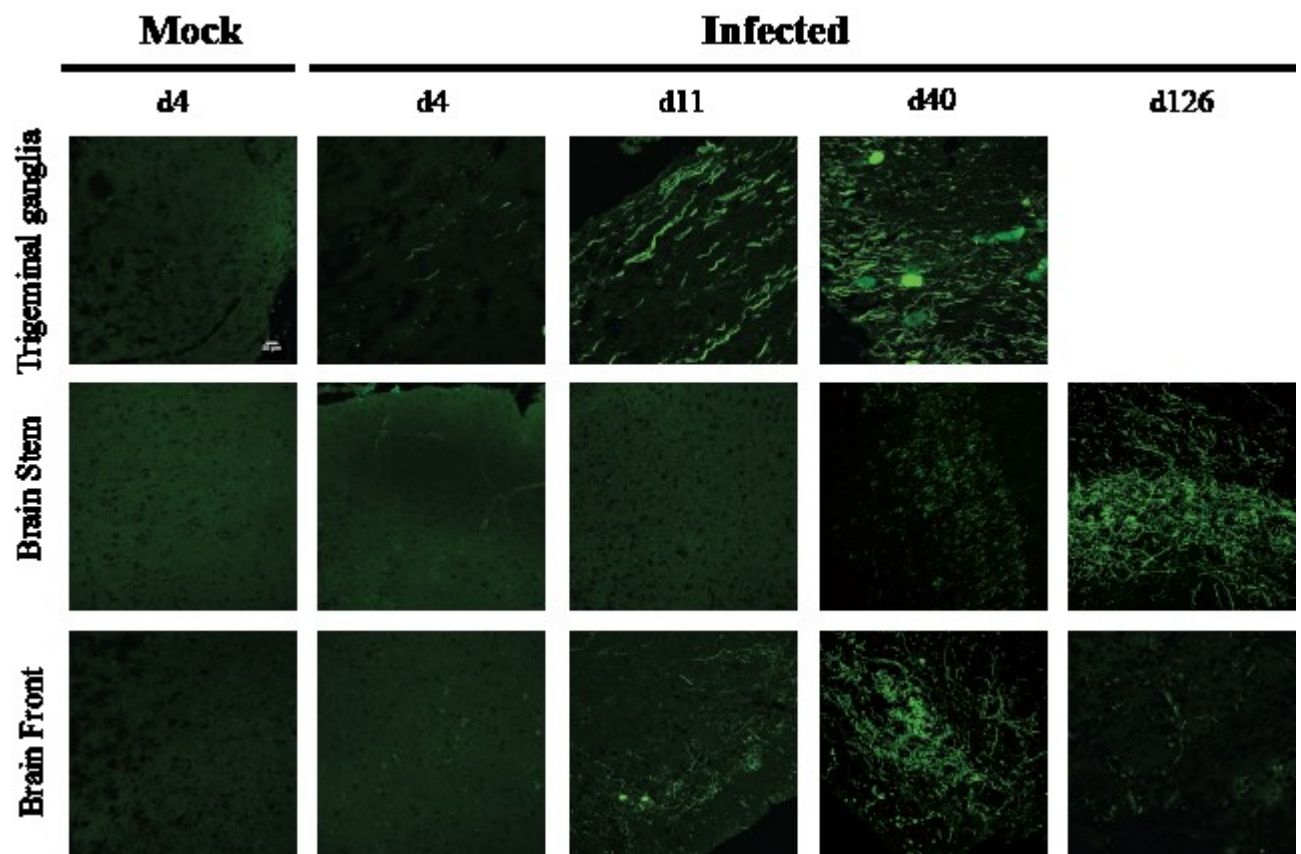


Fig. 5.1. Time point analysis of the ZsGreen signal. The figure shows examples, for each time point analysed, of the expression of ZsGreen in the nervous system of infected Ai6 mice. The fluorescent signal of sample slices was detected with a confocal fluorescent microscope. In the first row are reported TG slices, in the second brain stem and in the third frontal cortex. Time points are disposed in columns and ordered from left to right. First column shows uninfected samples.

The virus was observed through expression of ZsGreen in TG and in the two external edges of the brain: frontal cortex and stem (Fig. 5.1).

The presence of HSV-1, expressing Cre recombinase, was evident in TG sections at day 4 post-inoculation and at day 11 when it started to appear also in the frontal cortex but not in brain stem while at day 40 the virus, besides being very abundant in the frontal regions, begins to be present in the dorsal part of the brain, showing its ability to reach that area (fig. 5.1).

These images suggest that following primary infection in the whisker pads the virus reaches the TG, as expected, and then invades the brain from the front and moves back to the stem. Surprisingly after 126 days from infection, ZsGreen signal disappears from the frontal cortex and becomes very high in the stem. This may be due to viral reactivation/replication through a mechanism of clearance of the infected cells that it is still to be elucidated.

5.3.2 Validation of the system

During the analysis a green signal was also observed in brains of uninfected mice (fig. 5.2a), consequently, it was necessary to check if a non-specific recombination in the Rosa 26 locus had occurred.

PCR analysis were performed with primers designed to cover the region between the two loxP sites, containing a STOP codon sequence that blocks transcription of ZsGreen gene, in case of recombination the amplified should have been 1576 bp long, otherwise 2448 bp (Fig. 5.2b-b'). As shown in figure 5.2c, PCR gave only one product of approximately 2500 bp, indicating that no recombination occurred on the genome of uninfected mice.

Whatever causes the presence of this aspecific signal is to be elucidated, but it's clear that it is not the excision of the stop cassette upstream of the ZsGreen gene. In addition, confirming the reliability of this model, this "fake" marker can be distinguished from the real one because of some differences: the first is present as a group of tiny dots very close to each other in the central area of brain slice, while the second highlight the morphology of infected neurons, whose localization is mainly in external cortex (Fig. 5.2a).

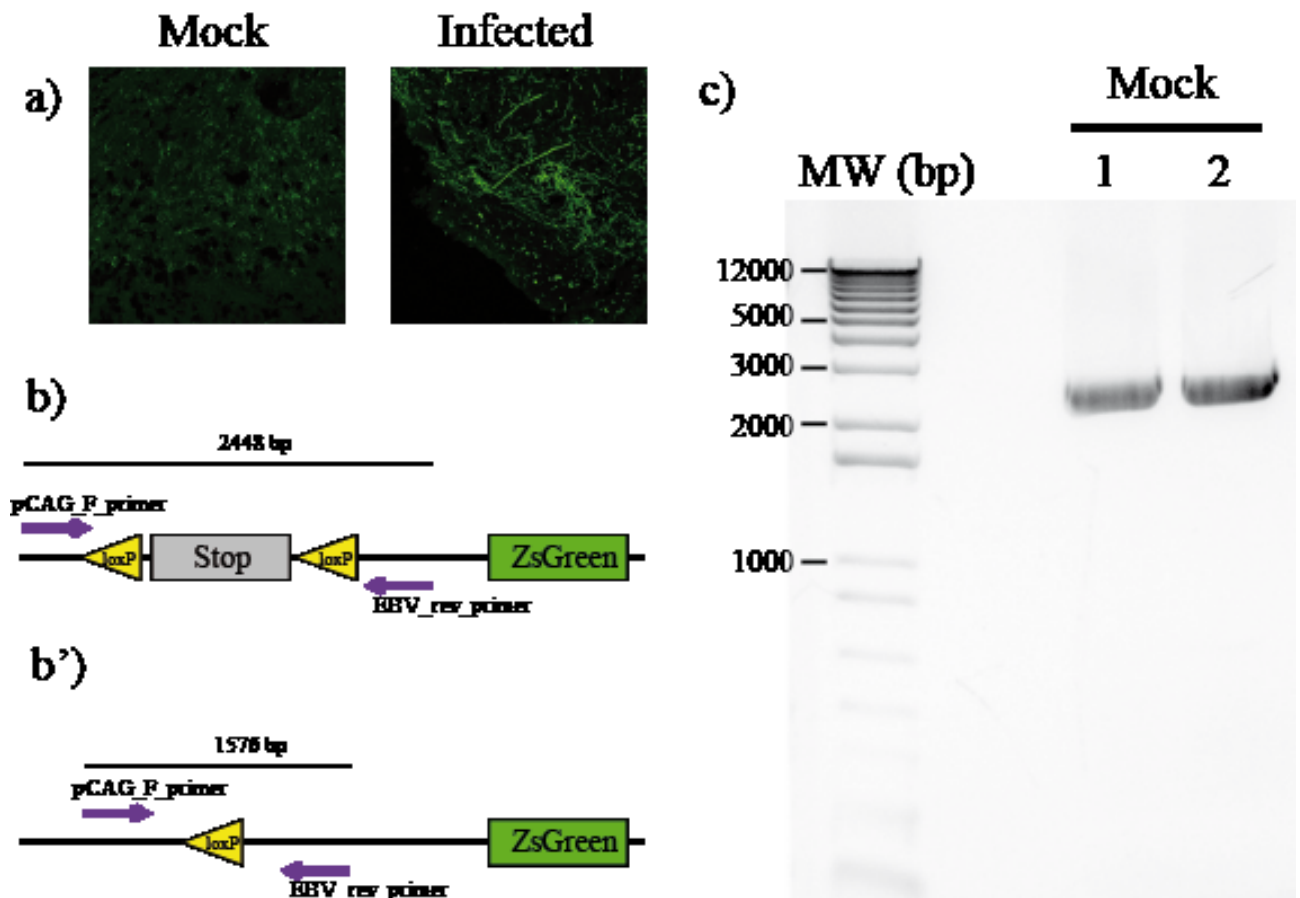


Fig. 5.2. Validation of the system. a) Comparison between the confocal images of “fake” ZsGreen signal found in brain tissue of mock infected (left picture) Ai6 mice and real signal found in infected Ai6 mice (right picture). In infected mice the green signal highlights the morphology of neurons, while in uninfected mice it is more spotted and not well defined. b-b’) Schematic representation of the ROSA26 locus with the two primers (pCAG_F_primer and EBV_rev_primer, indicated by purple arrows) used to analyze the sequence. b) In case of no recombination the PCR product is 2448bp. b’) In case of recombination the PCR product is 1576 bp. Yellow triangles indicate the loxP sites, gray rectangle the stop cassette and green rectangle the ZsGreen ORF. c) PCR analysis of DNA extracted from brains of two different uninfected Ai6 mice (1, 2). In both samples the PCR product was only one of approximately 2500 bp, indicating no recombination event in the ROSA26 locus.

5.3.3 Characterization of HSV-1 infection in Ai6 mice nervous system

HSV-1 persists in a latent state in neurons, and in response to a variety of diverse stimuli it can reactivate. The observation, reported above, that the infected cells of different area in the brain increase in time indicates that the virus replicates and produces new viral progeny. To

verify this hypothesis, brain sections were stained with a polyclonal antibody (Fig. 5.3) to HSV-1 and monoclonal antibodies to CP0 and ICP4, the two immediate early proteins expressed during viral reactivation from latency. As shown in Fig. 5.4, the expression of ICP0 and ICP4 was detected in TG only at day 4, in the acute phase of infection, due to the viral replication that occurs shortly before the virus enter in latency. Later on, it is reasonable to suppose that the virus is prevalent latent in the nervous system with short micro-reactivations that are not detected by immunoblot analyses, whereas are evidenced by the expression of Cre recombinase. The data from these experiments show the natural route of HSV-1 in the nervous system and support the idea that using a transgenic mouse model carrying a reporter gene under the control of the CRE recombinase expressed by the virus, is the best system to track the presence of HSV-1 in the CNS.

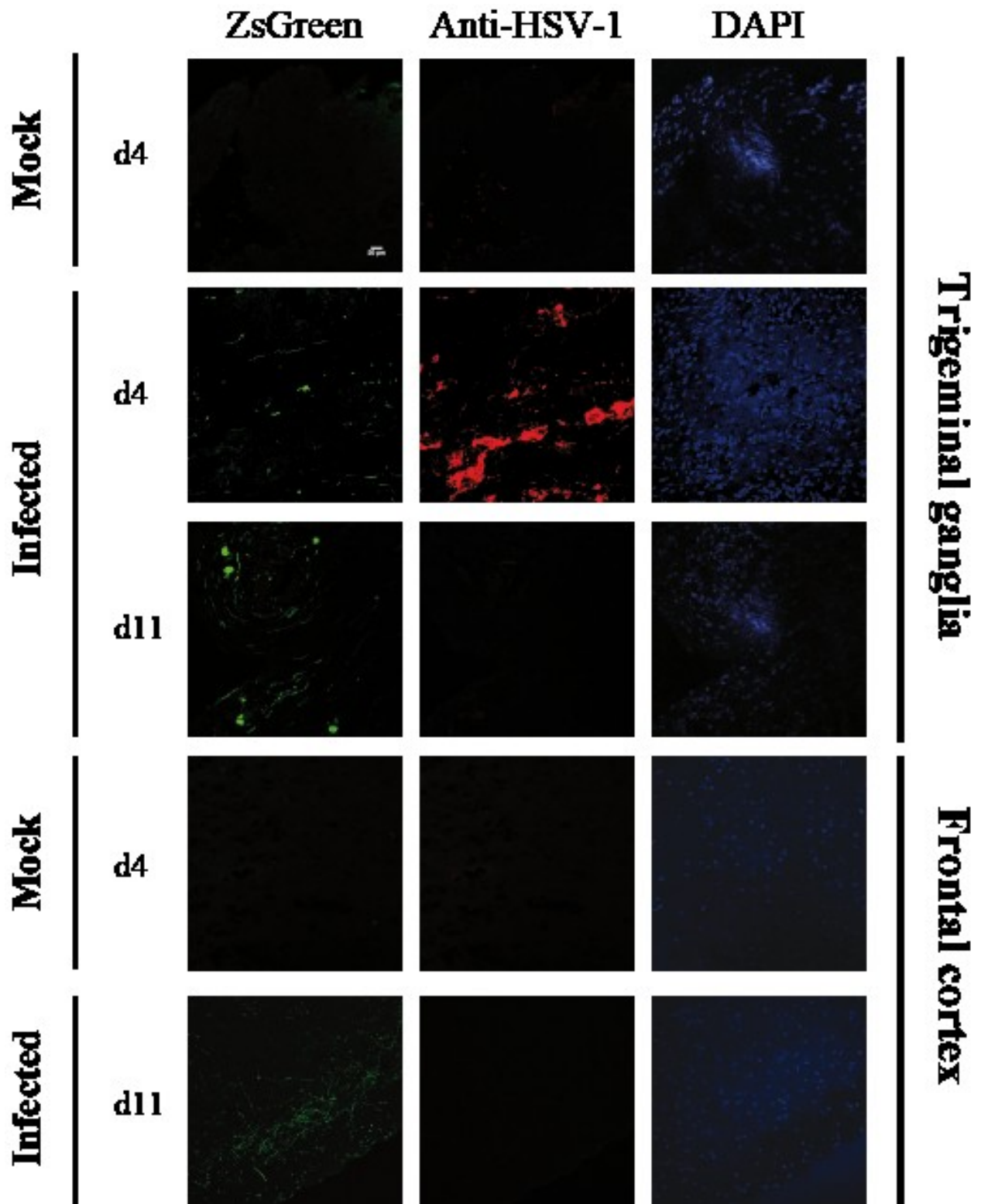


Fig. 5.3. Detection of HSV-1 with a polyclonal antibody only in acute infection. The first 3 row shows the staining of TG slices with a polyclonal antibody anti-HSV-1. The antibody can detect the virus only at d4 (second row). As example of the absence of signal in later times it is shown d11 (third row), to indicate that after acute infection the virus can be detectable only with ZsGreen. The fourth and fifth row shows a representative example of the staining for HSV-1 in brain tissue, respectively in uninfected and infected mice, in both these samples HSV-1 is not detectable by immunofluorescence staining, but it is by ZsGreen.

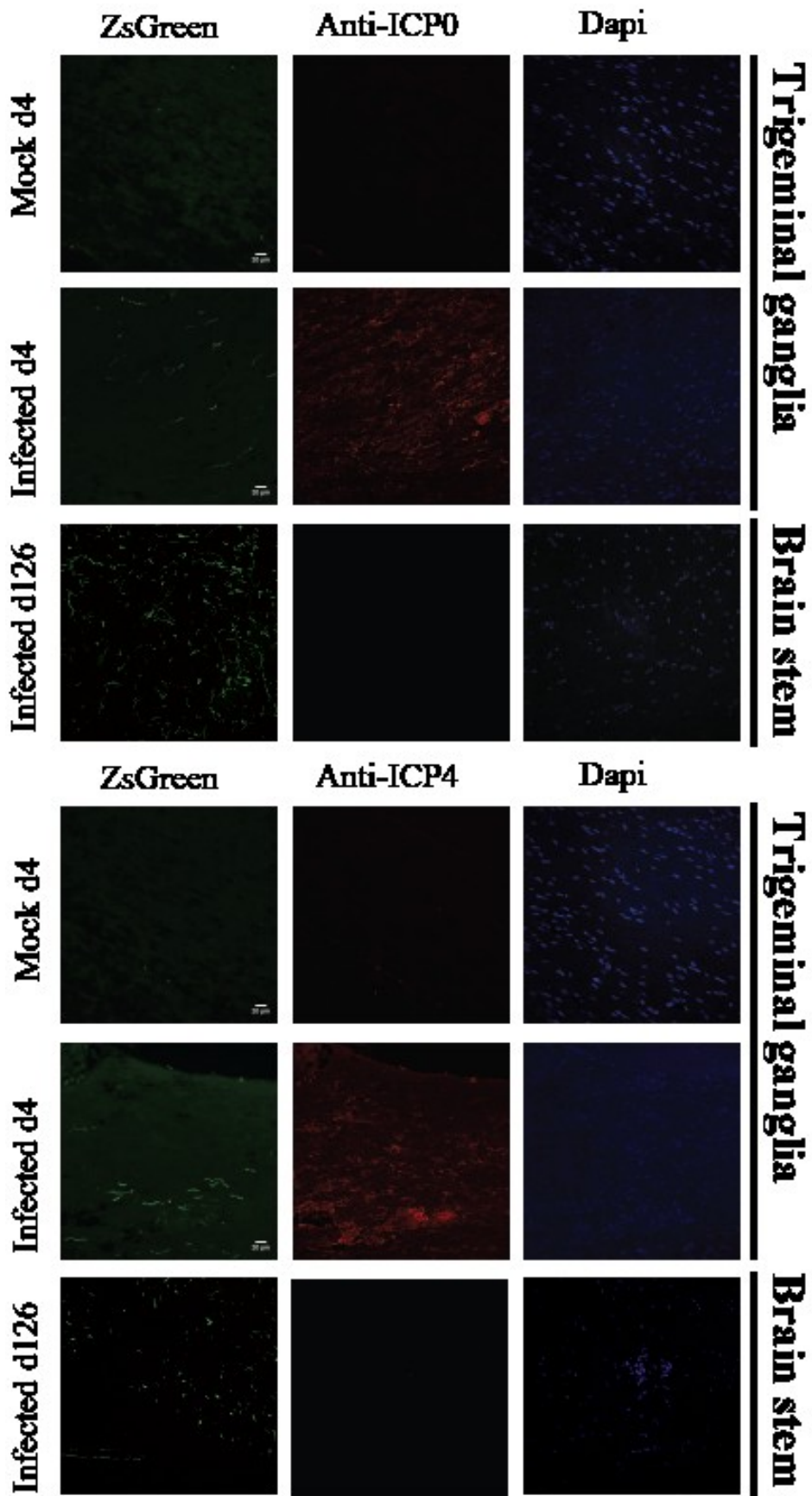


Fig. 5.4. Detection of ICP0 (upper panel) and ICP4 (lower panel) only in acute infection. Also these two early gene products were detected only in acute infection, i.e. in TG at d4 (second row of each

panel). As example of no detection in later time points in both TG and brains, it is reported a brain stem slice of d126 post infection (third row of each panel).

5.3.4 HSV-1 activates inflammatory cells

In order to investigate a possible link between HSV-1 and the neuroinflammation, which is one of the characteristics of AD, it was first considered the involvement of innate immunity in the inflammatory processes in the CNS. The infiltration of activated macrophages and microglia was assessed by immunofluorescence microscopy for F4/80 and Iba markers. As evidenced in Fig. 5.5 and 5.6 in trigeminal ganglia, 4 days post infection the two markers were not detected, whereas these antigens were strongly detectable at d11 with a slight decrease at d40. These data highlight that a high infiltration of these cells are concentrate in the areas infected by the virus. In the brain slice we observed similar results with a positive staining at d11 only in ZsGreen positive areas, i. e. the frontal cortex but not brain stem (Fig. 5.7-5.10). However, even if the virus proceeds on spreading, the presence of these cells at d40 is drastically reduced (Fig. 5.7-5.10 fourth row) to be completely absent at d126 (Fig. 5.7-5.10 fifth row).

These data demonstrate that the innate immune response, represented by macrophages and microglia, is triggered in the nervous system during early stages of HSV-1 infection and even it is particular intense in trigeminal ganglia it is also present in brain. Later on, although the virus is still detectable, the involvement of macrophages and microglia become weaker, presumably giving space to other compartments of the immune system in fighting the infection.

In conclusion these data show that HSV-1 is able to activate the same immune compartment mainly involved in the neuroinflammatory process characteristic of AD, suggesting a potential strong link between viral infection and the disease.

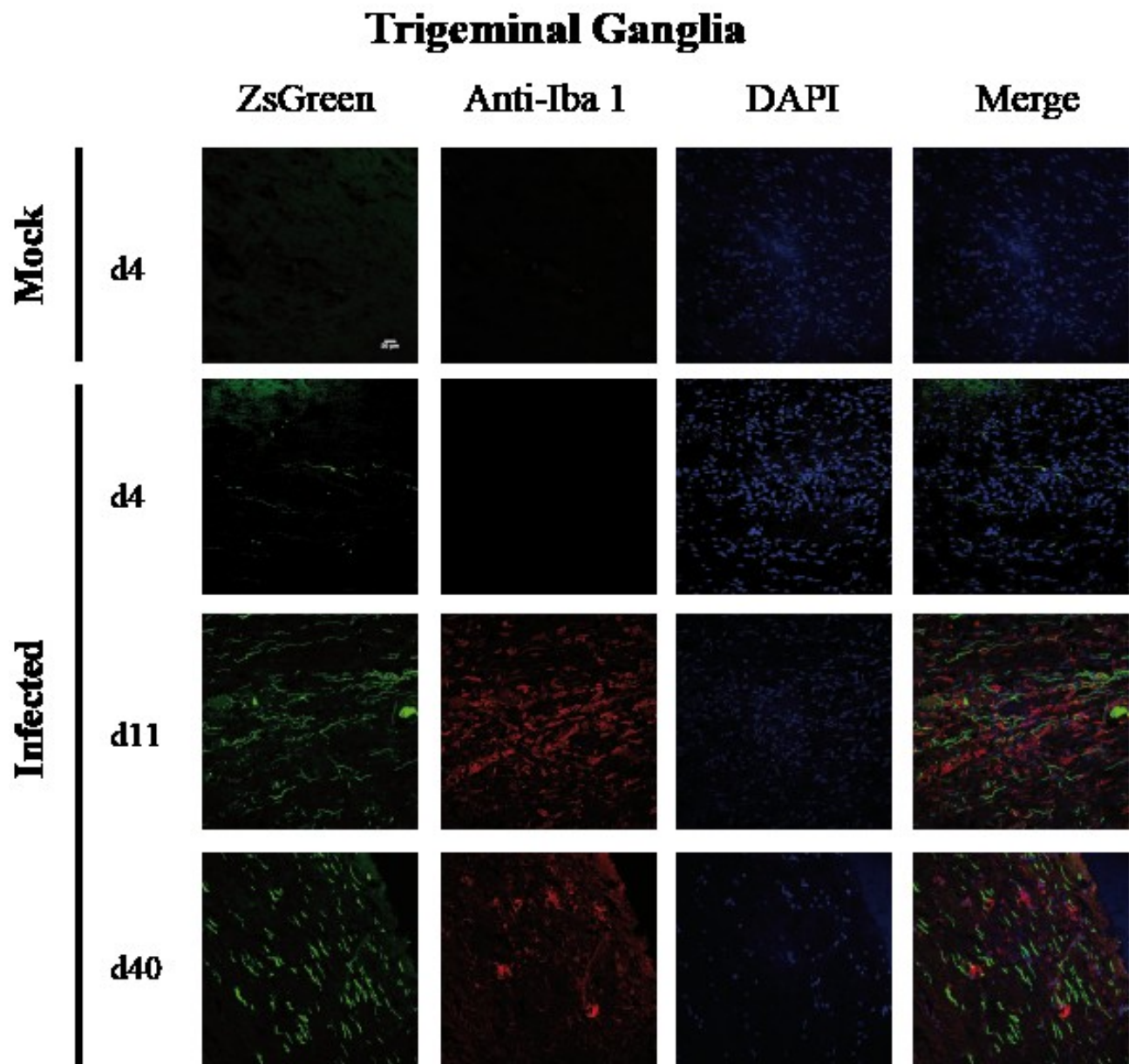


Fig. 5.5. Detection of activated microglial cells in TG. Activated microglia was detected by an antibody directed against Iba 1 (red), a surface antigen expressed by these cells when activated. First column shows the ZsGreen signal, second Iba 1, third Dapi staining of the nucleus and fourth the combination of these channels. The first row shows mock infected sample, while from the second to the last row there are shown infected samples ordered from the earliest to the latest time point as indicated in the figure.

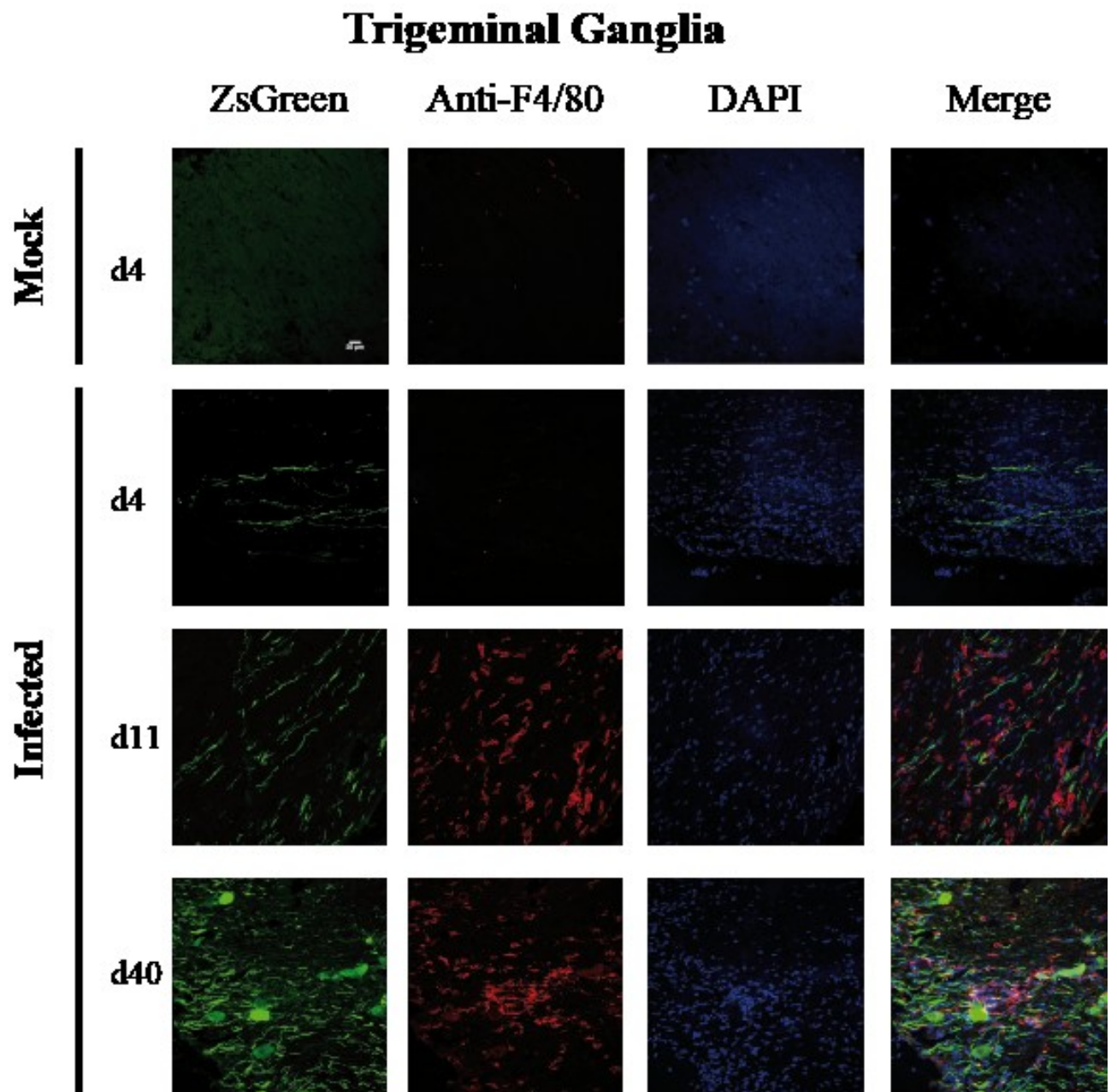


Fig. 5.6. Detection of activated macrophages in TG. Activated macrophages were detected by an antibody directed against F4/80, a surface antigen expressed by these cells when activated. First column shows the ZsGreen signal, second F4/80 (red), third Dapi staining of the nucleus and fourth the combination of these channels. The first row shows mock infected sample, while from the second to the last row there are shown infected samples ordered from the earliest to the latest time point as indicated in the figure.

Frontal cortex

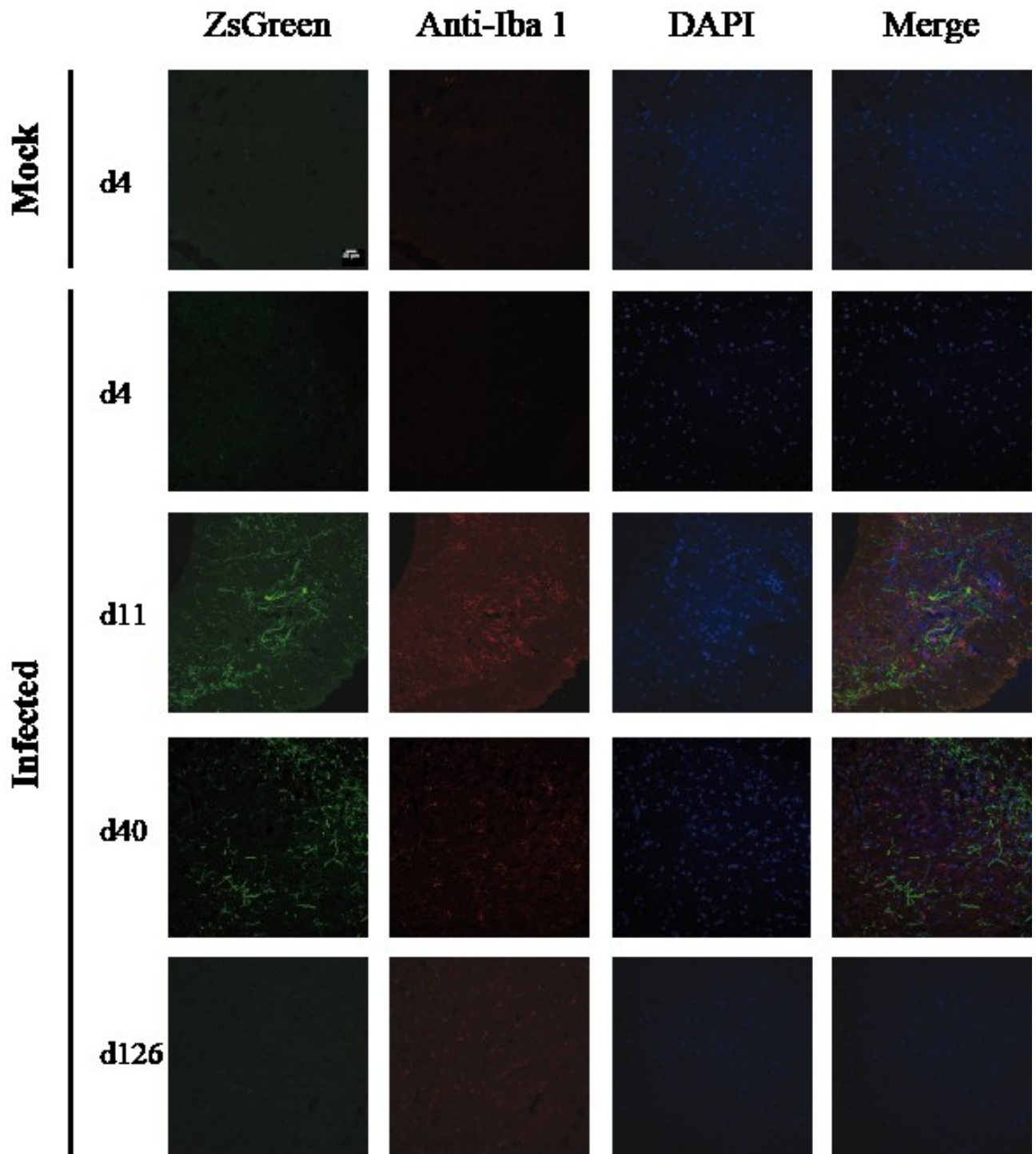


Fig. 5.7. Detection of activated microglial cells in brain frontal cortex. Activated microglia was detected by an antibody directed against Iba 1, a surface antigen expressed by these cells when activated. First column shows the ZsGreen signal, second Iba 1, third Dapi staining of the nucleus and fourth the combination of these channels. The first row shows mock infected sample, while from the second to the last row there are shown infected samples ordered from the earliest to the latest time point as indicated in the figure.

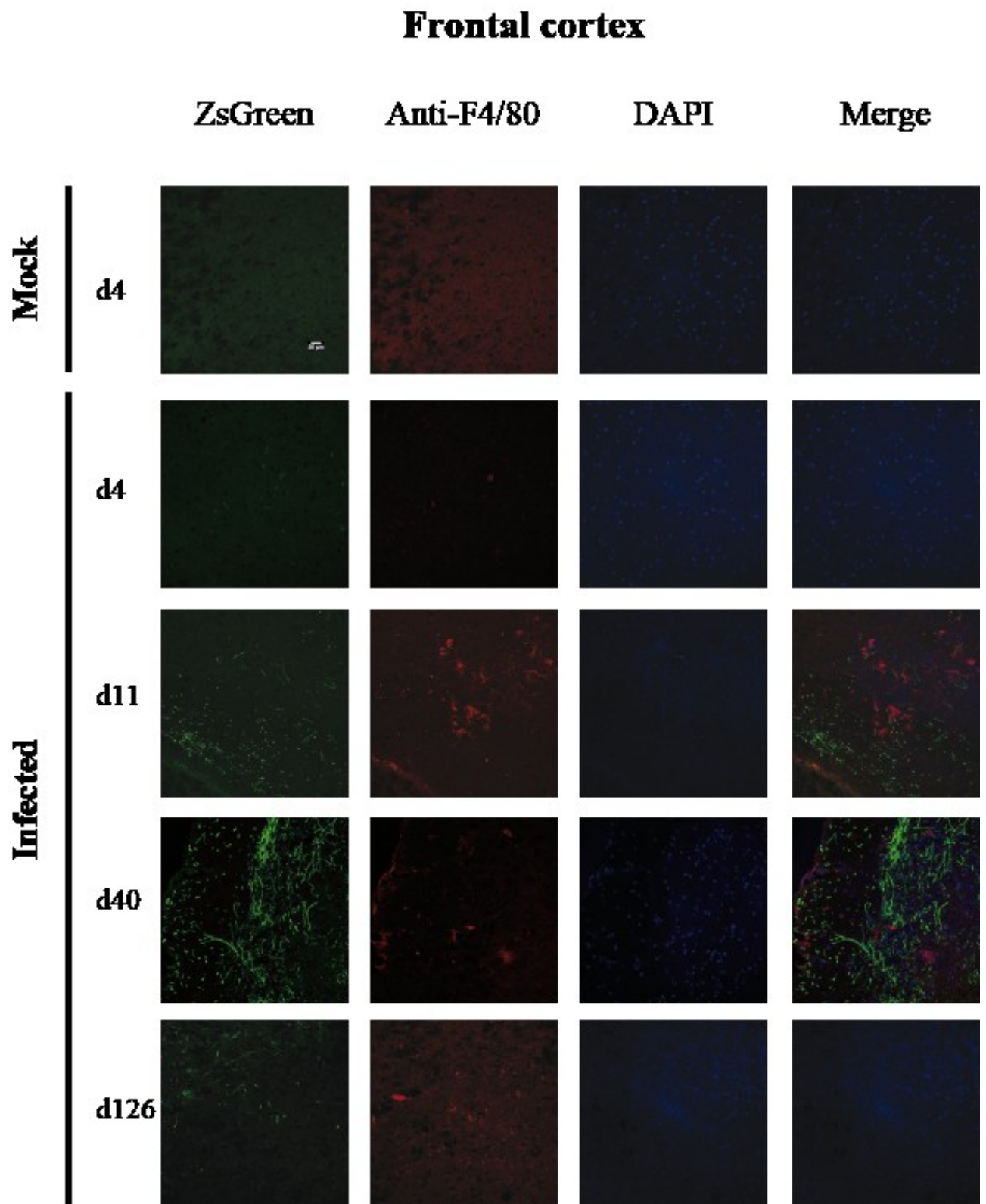


Fig. 5.8. Detection of activated macrophages in brain frontal cortex. Activated macrophages were detected by an antibody directed against F4/80, a surface antigen expressed by these cells when activated. First column shows the ZsGreen signal, second F4/80, third Dapi staining of the nucleus and fourth the combination of these channels. The first row shows mock infected sample, while from the second to the last row there are shown infected samples ordered from the earliest to the latest time point as indicated in the figure.

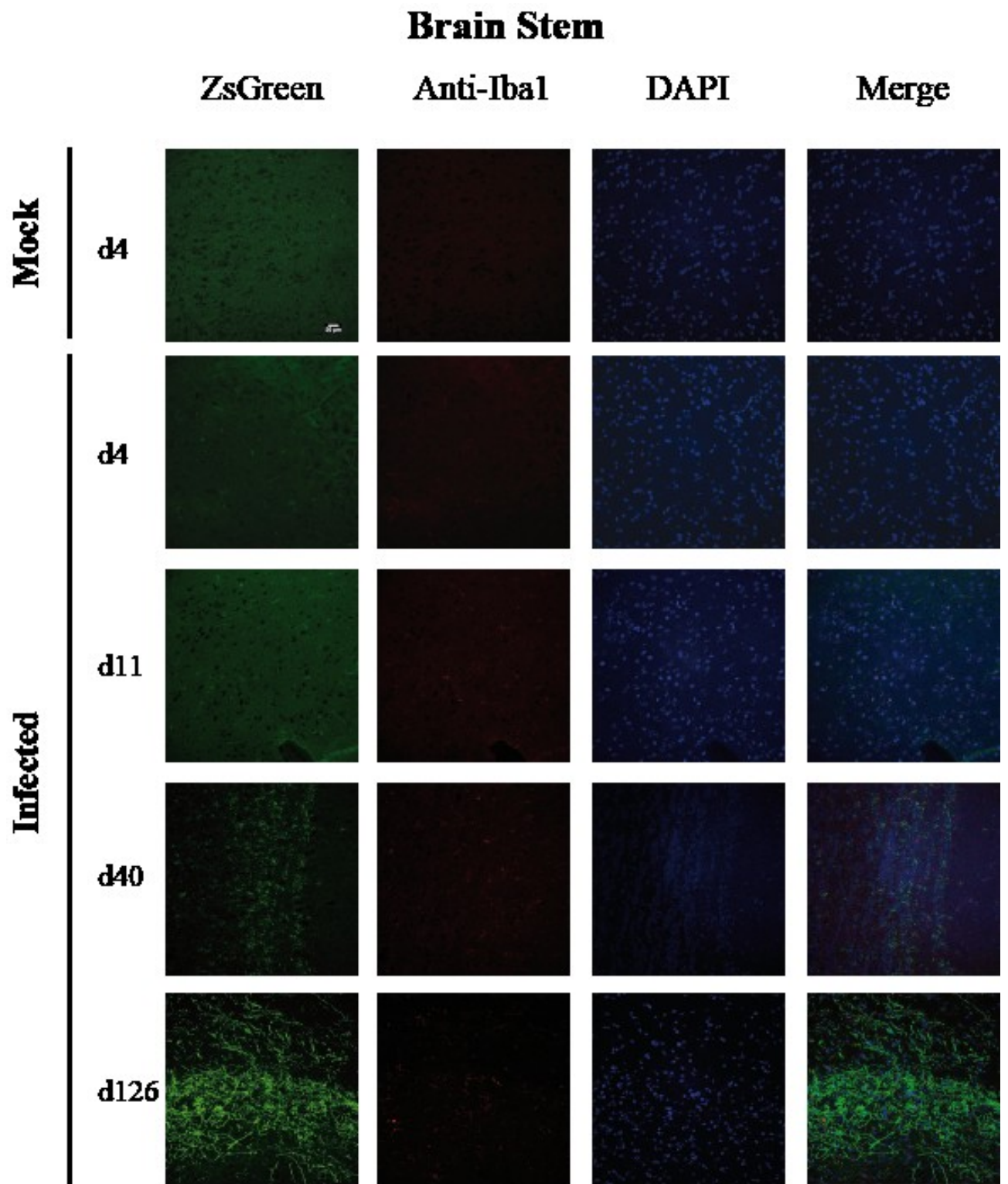


Fig. 5.9. Detection of activated microglial cells in brain stem. Activated microglia was detected by an antibody directed against Iba 1, a surface antigen expressed by these cells when activated. First column shows the ZsGreen signal, second Iba 1, third Dapi staining of the nucleus and fourth the combination of these channels. The first row shows mock infected sample, while from the second to the last row there are shown infected samples ordered from the earliest to the latest time point as indicated in the figure.

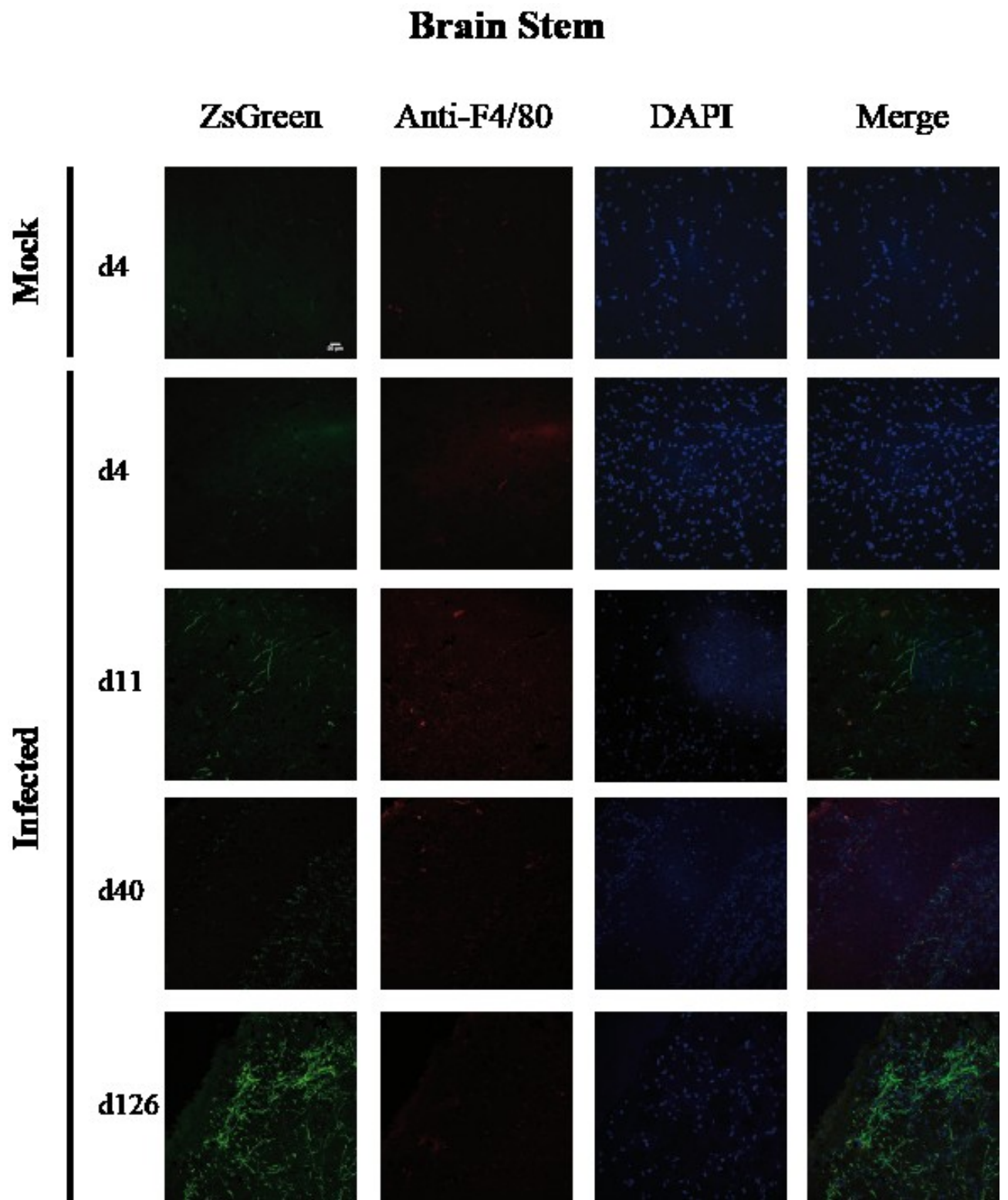


Fig. 5.10. Detection of activated macrophages in brain stem. Activated macrophages were detected by an antibody directed against F4/80, a surface antigen expressed by these cells when activated. First column shows the ZsGreen signal, second F4/80, third Dapi staining of the nucleus and fourth the combination of these channels. The first row shows mock infected sample, while from the second to the last row there are shown infected samples ordered from the earliest to the latest time point as indicated in the figure.

5.3.5 HSV-1 doesn't increase the amount of beta amyloid and phospho tau in Ai6 mice

It is known that extracellular A β deposits induce inflammation that may enhance tau upregulation, which, in turn, may promote intracellular tau aggregation in vulnerable neurons. As it has been reported above, using the Ai6 RosaZsGreen reporter mice model, inflammation occurs in the same CNS areas affected by AD and HSV-1 infection. In order to verify if the inflammatory process triggered by micro-reactivation episodes, following HSV infection and latency, can lead to the formation of A β and hyperphosphorylated tau deposits, coronal sections from TG, frontal cortex and brain stem, were stained with antibodies directed against phospho-tau and A β and analysed by immunofluorescence microscopy. The presence of NFT was analysed with an antibody raised against Tau phosphorylated on Serine 202. In TG, the staining for this antibody gave a weak signal, few cells were positive for this epitope both in infected and uninfected mice, and no aggregates were detected at any time point analysed (Fig. 5.11). In brains the same antibody stains almost every cells, both in infected and control samples, indicating that tau in CNS is constitutively phosphorylated at this epitope and again no tangles were visible (Fig. 5.12).

The staining with an antibody against aa 1-14 of beta amyloid revealed no signal either in TG or in brains. In conclusion in HSV-1 infected Ai6 mice, at the time points analysed and with the antibody used it wasn't possible to observe the formation of NFT and SP in nervous tissue.

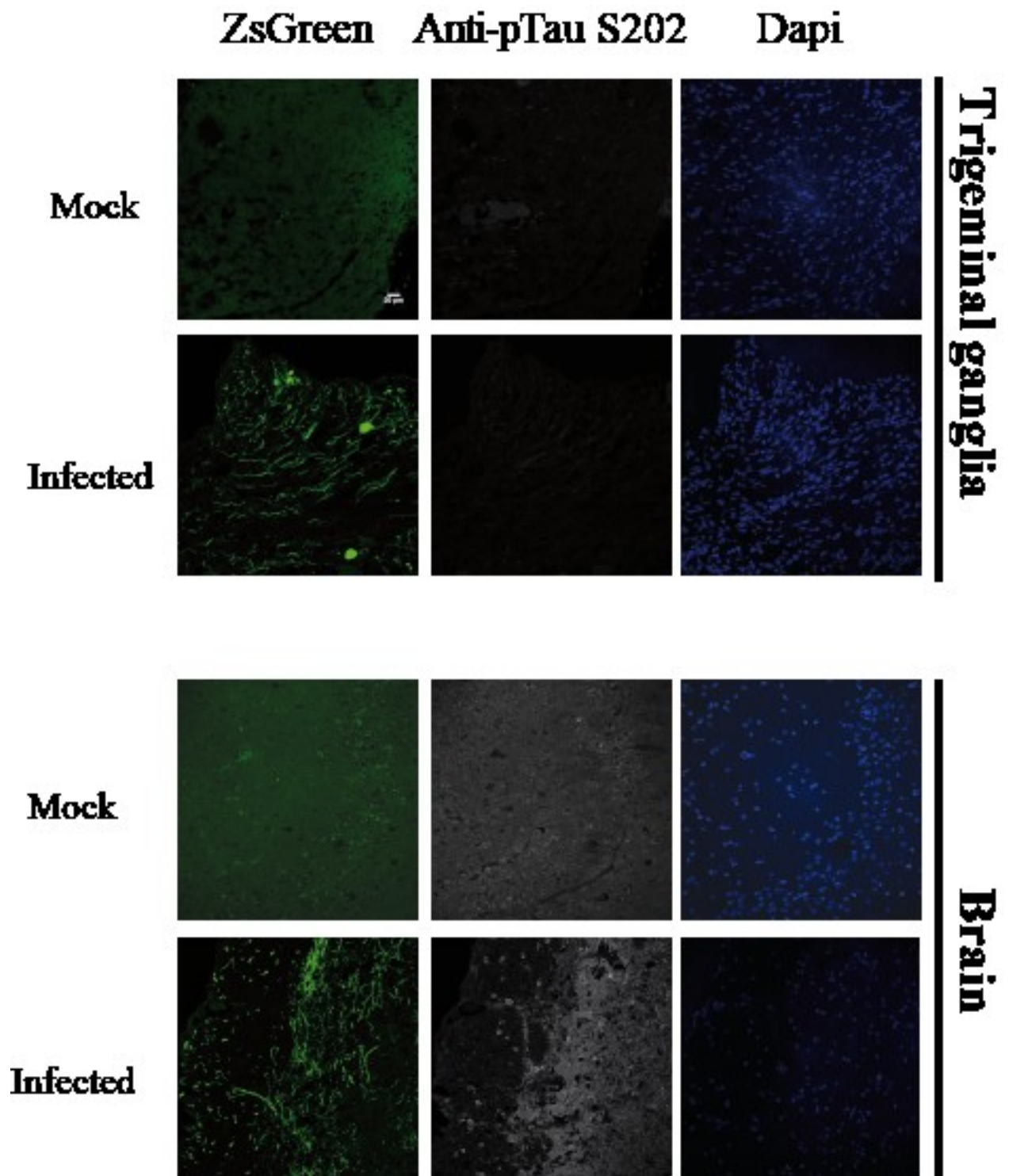


Fig. 5.11. Detection of NFTs. Neurofibrillary tangles were not detectable in every sample tested. This figure shows examples of TG (upper panel) and brains (lower panel) uninfected (first row of each panel) or infected (second row of each panel). In attempt to detect NFTs, slices were stained with an antibody against pTau S202 (second column). The secondary antibody used is an antibody goat anti-rabbit IgG conjugated to alexa fluor 633, reported by the microscope in gray. It is also shown ZsGreen signal (first column) and dapi signal (third column).

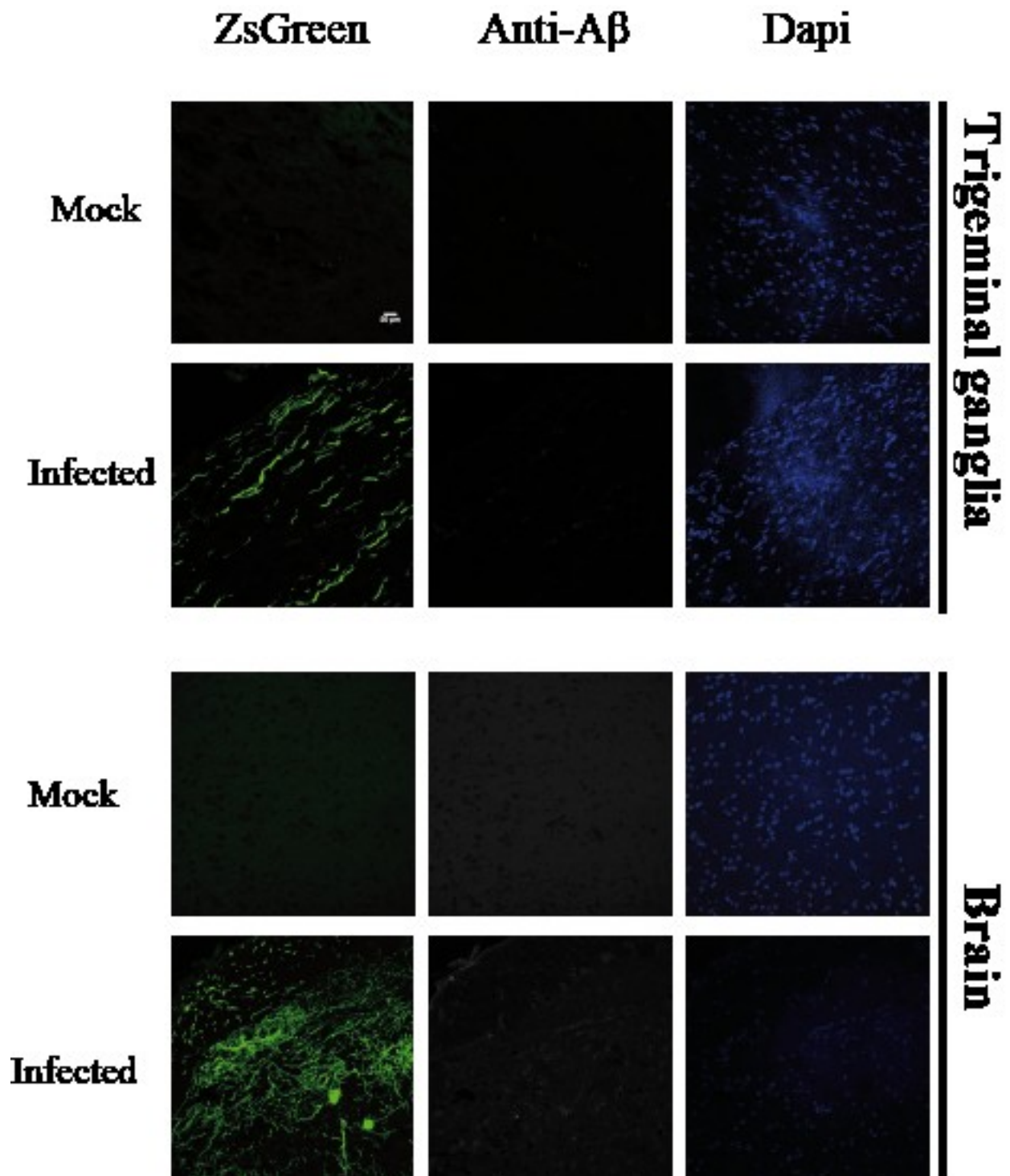


Fig. 5.12. Detection of SPs. Senile plaques were not detectable in every sample tested. This figure shows examples of TG (upper panel) and brains (lower panel) uninfected (first row of each panel) or infected (second row of each panel). In attempt to detect SPs, slices were stained with an antibody against A β (second column). The secondary antibody used is a goat anti-rabbit IgG conjugated to alexa fluor 633, reported by the microscope in gray. It is also shown ZsGreen signal (first column) and dapi signal (third column).

5.4 Discussion

The reactivation rate on HSV-1 in the human brain is relatively unknown; however animal and human studies involving the CNS and the peripheral nervous system suggest that periodic sub-clinical reactivation, also called micro-reactivation, may occur with subsequent immune response and neurodegeneration. Using *in situ* hybridization and immunohistochemistry, Feldman et al. found that HSV-1 spontaneous reactivation occurred in one neuron per 10 HSV-1 latently infected mouse TG tested [16] accountable of an high-level of productive cycle viral genes in each ganglion every 10 days. These neurons were surrounded by focal white cell infiltrate, indicating an inflammatory response. Asymptomatic reactivation of HSV-1 occurs also *in vivo* in the CNS of mice and is associated with production of markers of neurodegeneration found in AD [17].

In this study our group aimed to evaluate if asymptomatic neuronal reactivation of HSV could occur in Ai6 RosaZsGreen mouse model of whisker pads inoculation and also if these reactivation episodes could be associated with neuroinflammation and activation of microglial cell and macrophages in CNS areas typical of AD.

It has been previously described that ROSA26 reported mouse model of HSV infection allows marking of neuron infection via the use of HSV-1 strain SC16 recombinants expressing Cre recombinase [13]. By using this system to investigate the route of the virus from the peripheral nervous system to the CNS, we have shown that the virus is detectable at day 4 in TG, during the acute phase of infection, while at day 11 it starts to be present in CNS frontal cortex, reaching at day 40 the dorsal part of the brain. HSV-1 infection in TG was confirmed by immunoblot using anti ICP0 and ICP4 antibodies and by immunofluorescence, whereas in CNS the presence of the virus can be revealed only by immunofluorescence, due to Cre recombinase expression. These difference in detecting viral replication could be due to the small number of neurons in CNS that are involved in sub-clinical reactivation and, therefore, to the low level of immediate early gene expression. The ROSA26R reporter mouse model, therefore, provides an amenable approach to allow direct measurement of the frequency of micro-reactivation from HSV latency, *in vivo*, and to study the inflammation processes following HSV infection of CNS.

Viral induced inflammation was analysed by staining for markers of activated microglia and macrophages, the first line of defence against pathogen or other kind of injury occurring in brain tissue [3]. Our results show that a strong infiltration of these cells appears at 11 days post infection, during the acute phase, decrease at day 40, up to be completely absent at day 126.

The unexpected disappearance of detectable virus from the frontal cortex, 126 days post infection, could be explained by the removal of infected neuronal cells due to microglia/macrophages activation. Preliminary data (not shown) evidenced also T cells infiltrating the CNS at day 11. This observation need to be analysed thoroughly, since several studies have shown that CD4⁺T-cells infiltrate the CNS in many neurodegenerative disorders and that their participation have a critical influence on the outcome of microglia activation and consequent neuronal damage [18]. From our data, it is possible to assume that the virus enter the CNS very early and persist predominantly in latency. Macrophages and microglia are recruited to the site of infection where they stay active in a sort of “alert state”, even for a long time, inducing the mobilization of the adaptive immune system. Once neuroinflammation resolves, microglia resumes its inactive state. It is known that microglia changes with aging, becoming more responsive to inflammatory stimulation [3], so in the brain of an old person even HSV micro-reactivations might induce a hyperactivation of microglia, resulting in neuronal loss.

Inflammation is a crucial factor for AD and it has been observed, both in experimental models and in clinical studies, that microglial activation precedes amyloid plaques and tangles formation [19-21]. It has been also observed the induction of early neurodegenerative markers, such as hyperphosphorylated and cleaved tau protein *in vitro* and *in vivo* model of HSV-1 neuronal infection [17, 22]. These post-translational modifications of tau are considered important neurodegenerative markers initially associated to AD. To support the hypothesis that recurrent HSV-1 reactivation episodes in the CNS could promote chronic inflammation that constitute a risk factor of degeneration processes, we analysed, in the ROSA26R reporter mouse model, the appearance of A β and phospho tau aggregations. At this regard, our data did not show the presence of aberrant proteins, or during the acute phase of infection or later, indicating that an *in vivo* model of HSV-1 infection is not sufficient to promote this phenomenon, at least at the time points analyzed. The ROSA26R mice, as reported in material and methods, were infected at the age of 8 weeks and sacrificed at 11, 40 and 126 days, whereas, in the various transgenic rodent model of AD, the aberrant aggregates start to be visible at 6 months, becoming more evident at 12-18 months [20, 23]. Therefore, it

is possible that in HSV-1 infected Ai6 mice, the formation of these pathological hallmarks occur in later stages than those evaluated in this work, or that it doesn't occur at all, because even if evidences for a correlation between HSV-1 and AD is strengthening progressively, not all AD patients show evidence of HSV-1 infection neither all HSV-1 infected people, that is around the 80-90% of the population, develop AD [6, 24].

What probably happen is that in old age, when the host immune system becomes weaker and less regulated, the virus can reach CNS where it can reactivate several times, thus promoting microglia activation that with ageing has altered in a more pro-inflammatory phenotype [3]. The consequent stress condition may lead to the formation of anomalous protein aggregates, but this might require the proper genetic background.

In conclusion the use of transgenic reporter mouse seems to be a good system to associate the presence of the virus in brain and the development of neurodegenerative disorders such as Alzheimer's Disease, suggesting that a cross between Ai6 and a mouse model with a genetic background that predispose to the development of AD could give more information on this topic.

5.5 References

1. Blasko, I., et al., *How chronic inflammation can affect the brain and support the development of Alzheimer's disease in old age: the role of microglia and astrocytes*. *Aging Cell*, 2004. 3(4): p. 169-76.
2. Sastre, M., T. Klockgether, and M.T. Heneka, *Contribution of inflammatory processes to Alzheimer's disease: molecular mechanisms*. *Int J Dev Neurosci*, 2006. 24(2-3): p. 167-76.
3. Solito, E. and M. Sastre, *Microglia function in Alzheimer's disease*. *Front Pharmacol*. 3: p. 14.
4. De Chiara, G., et al., *Infectious agents and neurodegeneration*. *Mol Neurobiol*. 46(3): p. 614-38.
5. Jamieson, G.A., et al., *Latent herpes simplex virus type 1 in normal and Alzheimer's disease brains*. *J Med Virol*, 1991. 33(4): p. 224-7.
6. Jamieson, G.A., et al., *Herpes simplex virus type 1 DNA is present in specific regions of brain from aged people with and without senile dementia of the Alzheimer type*. *J Pathol*, 1992. 167(4): p. 365-8.
7. Ball, M.J., *"Limbic predilection in Alzheimer dementia: is reactivated herpesvirus involved?"* *Can J Neurol Sci*, 1982. 9(3): p. 303-6.
8. Mori, I., et al., *PCR search for the herpes simplex virus type 1 genome in brain sections of patients with familial Alzheimer's disease*. *J Clin Microbiol*, 2004. 42(2): p. 936-7.
9. De Chiara, G., et al., *APP processing induced by herpes simplex virus type 1 (HSV-1) yields several APP fragments in human and rat neuronal cells*. *PLoS One*. 5(11): p. e13989.
10. Alvarez, G., et al., *Herpes simplex virus type 1 induces nuclear accumulation of hyperphosphorylated tau in neuronal cells*. *J Neurosci Res*. 90(5): p. 1020-9.
11. Santana, S., et al., *Herpes simplex virus type 1 induces the accumulation of intracellular beta-amyloid in autophagic compartments and the inhibition of the non-amyloidogenic pathway in human neuroblastoma cells*. *Neurobiol Aging*. 33(2): p. 430 e19-33.
12. Wozniak, M.A., A.L. Frost, and R.F. Itzhaki, *Alzheimer's disease-specific tau phosphorylation is induced by herpes simplex virus type 1*. *J Alzheimers Dis*, 2009. 16(2): p. 341-50.
13. Proenca, J.T., et al., *A historical analysis of herpes simplex virus promoter activation in vivo reveals distinct populations of latently infected neurones*. *J Gen Virol*, 2008. 89(Pt 12): p. 2965-74.
14. Madisen, L., et al., *A robust and high-throughput Cre reporting and characterization system for the whole mouse brain*. *Nat Neurosci*. 13(1): p. 133-40.
15. Arthur, J.L., et al., *Herpes simplex virus type 1 promoter activity during latency establishment, maintenance, and reactivation in primary dorsal root neurons in vitro*. *J Virol*, 2001. 75(8): p. 3885-95.
16. Feldman, L.T., et al., *Spontaneous molecular reactivation of herpes simplex virus type 1 latency in mice*. *Proc Natl Acad Sci U S A*, 2002. 99(2): p. 978-83.
17. Martin, C., et al., *Inflammatory and neurodegeneration markers during asymptomatic HSV-1 reactivation*. *J Alzheimers Dis*. 39(4): p. 849-59.
18. Gonzalez, H. and R. Pacheco, *T-cell-mediated regulation of neuroinflammation involved in neurodegenerative diseases*. *J Neuroinflammation*. 11: p. 201.
19. Heneka, M.T., et al., *Focal glial activation coincides with increased BACE1 activation and precedes amyloid plaque deposition in APP[V717I] transgenic mice*. *J Neuroinflammation*, 2005. 2: p. 22.
20. Yoshiyama, Y., et al., *Synapse loss and microglial activation precede tangles in a P301S tauopathy mouse model*. *Neuron*, 2007. 53(3): p. 337-51.
21. Griffin, W.S., *Inflammation and neurodegenerative diseases*. *Am J Clin Nutr*, 2006. 83(2): p. 470S-474S.
22. Lerchundi, R., et al., *Tau cleavage at D421 by caspase-3 is induced in neurons and astrocytes infected with herpes simplex virus type 1*. *J Alzheimers Dis*. 23(3): p. 513-20.
23. Oddo, S., et al., *Triple-transgenic model of Alzheimer's disease with plaques and tangles: intracellular Abeta and synaptic dysfunction*. *Neuron*, 2003. 39(3): p. 409-21.
24. Itzhaki, R.F., et al., *Herpes simplex virus type 1 in brain and risk of Alzheimer's disease*. *Lancet*, 1997. 349(9047): p. 241-4.

6. Conclusion

Alzheimer's disease is the most common form of dementia and one of the great challenges of our ageing society. It is a complex multifactorial disorder and despite great stride in research the etiology and pathogenesis of AD has not been fully elucidated.

The objective of this work was to provide some insight in the role of the neurotropic ubiquitous Herpes simplex virus type 1, that in the last two decades has been proposed as an important risk factor for AD, as discussed above.

Understanding if and how HSV-1 contributes to the development of AD, may help to target new therapeutic and preventive strategies. To this purpose, we evaluated a possible interference of the virus in cellular and systemic functions of the host and we found some evidence that may explain the involvement of the virus in AD.

First despite we didn't establish the phosphorylation status of tau after viral infection, we observed that the virus induce the accumulation of different isoforms of this protein in various cell lines, that may contribute to the formation of PHF and thus to NFT.

Second HSV-1 triggers a Ca^{2+} signalling that may be increased in the absence of the interaction of the envelope glycoprotein gB to heparansulfate proteoglycans, a situation that may potentially depend upon the competition with $A\beta$ for the binding to these surface molecules.

Third infection of the virus in the nervous system leads to the activation of inflammatory cells.

It is reasonable to suppose that all these observed alterations may resolve under physiological condition, but combined with other etiopathological factors, the most relevant of which is ageing, may become chronic and lead to the progressive neurodegeneration that characterize AD.

In conclusion, further studies are needed to elucidate these mechanisms, however our data clearly support the idea that HSV-1 is a relevant, albeit not essential, agent for developing AD and it may suggest that the aggressors such as HSV that contributes to AD should be target of alternative treatment options including new antivirals or vaccines to may limit the long term consequences of CNS neurodegeneration.

Acknowledgements

I wish to thank my advisor Prof. Peggy Marconi for the continuous support of my Ph.D study and related research, for her patience, motivation, and immense knowledge. Her guidance helped me in all the time of research and writing of this thesis.

Besides my advisor, I would like to thank Prof. Roberto Manservigi, for giving me the opportunity to work in his laboratory and for the support in writing this thesis, Prof. Alessandro Rimessi for his support and guidance in the analysis of Ca^{2+} , Prof. Luca Ferraro for providing 3xTG neurons and Dr. Maria Cristina Tomasini that perform the neuronal explantation and guided me in the design of the experiments in these cells and Dr. Barbara Pavan for providing HRPE cells.

My sincere thanks also goes to Prof. Stacey Efstathiou, Dr. Colin Crump and Dr. Michael Gill who provided me the opportunity to join their team as visiting scientist at the University of Cambridge. A special thanks goes to Prof. Efstathiou for his guidance in the development of the studies related to nervous system inflammation, and to Dr. Michael Gill, who helped me in a particular difficult moment of my work, without its precious support it would not be possible to conduct this research.

Thanks to Maria, colleague and friend, who shared with me the difficulties of this work and moments of fun.

Finally I want to thank my parents, Vito and Annamaria, for their continuous support.

Last but absolutely not least, a big thank to Giulia, for her patience and support during these long three years, thanks for always standing by me.